letnik/volume **53** - št./no. **7-8/07** - str./pp. **423-522**
Ljubljana, jul.-avg./July-Aug. 2007, zvezek/issue **507**

STROJNIŠKI VESTNIK

JOURNAL OF MECHANICAL ENGINEERING

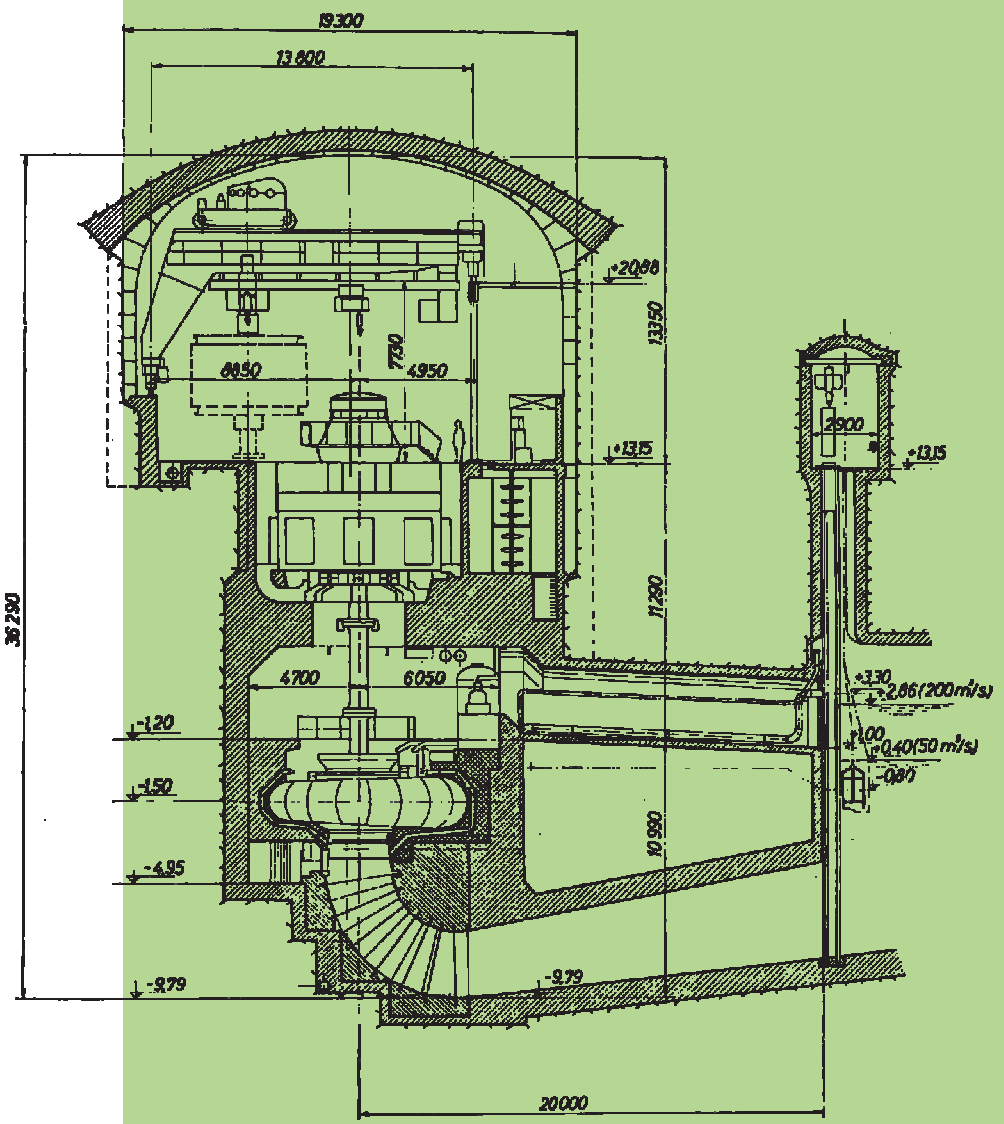

cena 3,34 EUR

ISSN 0039-2480

Vsebina - Contents

Strojniški vestnik - Journal of Mechanical Engineering
letnik - volume 53, (2007), številka - number 7-8
Ljubljana, julij/avgust - July/August 2007
ISSN 0039-2480

Izhaja mesečno - Published monthly

Strojniški vestnik - Journal of Mechanical Engineering 53(2007)7-8, 424-428
Uvodnik - Editorial

Uvodnik - Editorial

Računalniški postopki reševanja ključnih inženirskih problemov - Computational Approaches to Critical Engineering Problems

Znani fizik James Maxwell je nekoč izjavil: "Nič ni bolj praktičnega od dobre teorije." V tem duhu pričujoča tematska številka predstavlja napredne teoretično zasnovane računalniške rešitve nekaterih inženirskih problemov. Avtorji objavljenih prispevkov so za reševanje praktičnih inženirskih problemov uporabljali računalniške modele, ki vsebujejo veliko znanja. Obravnavana vprašanja segajo od konstruiranja strojev prek materialov in snovanja izdelkov do obdelave podatkov v razvojnem postopku. Predlagane rešitve imajo skupno to, da (i) so inženirske probleme odkrili avtorji, (ii) da so jih analizirali in se z njimi ukvarjali in (iii) da so na podlagi grobih teoretičnih osnov prišli do uporabnih računalniških rešitev za praktično delo. Končni nameni uporabe se med seboj zelo razlikujejo, prav tako tudi uporabljeni računalniška načela, ki so se prvotno pojavila na drugih področjih, to so denimo obdelava naravnega jezika, umetna inteligenca in poznejše vrednotenje izdelkov. Prispevki, objavljeni v tej tematski številki, združujejo vse te računalniške rešitve na raven zgodnje faze konstruiranja izdelkov. To kaže na to, da se uporaba računalniških orodij postopoma giblje v smeri njihovega čedalje večjega pomena za zgodnjo fazo konstruiranja in razvoja izdelkov, v kateri prihaja do najpomembnejših odločitev. Prepričani smo, da je za raziskovalce na univerzah in različnih raziskovalnih ustanovah bistvenega pomena, da se seznanijo s predlaganimi računalniškimi metodami in orodji. Upamo, da se bodo izkazala za uporabne in dovolj zanimiva tudi pri končnih uporabnikih v industriji.

Prispevki so bili prvič predstavljeni na Šestem mednarodnem simpoziju o orodjih in metodah sočasnega inženiringa (TMCE 2006), ki je potekal v Ljubljani, glavnem mestu Slovenije. Na rednih simpozijih TMCE si prizadevamo za nadaljnji razvoj znanstvenega, tehnološkega in praktičnega znanja na področju sočasnega inženiringa. Simpoziji imajo že več ko desetletje ključno vlogo pri prenosu akademskega znanja v industrijo. Simpozij se je od prvih začetkov leta 1995 do danes razvil v zrelo in dobro organizirano jedro izmenjave znanja med znanostjo in industrijo. Leta 2006 je več ko 250 udeležencev dejavno sodelovalo v razpravah o

James Maxwell, the famous physicist, said: "There is nothing more practical than a good theory". In this spirit, this thematic issue presents advanced theory-based computational solutions to some engineering problems. The included papers use knowledge-intensive computational models to address practical engineering issues. These issues range from machine design, through materials and product engineering, to information processing in the development process. What is common in the proposed solutions is that (i) critical engineering problems have been identified by the authors (ii) they have been theoretically analysed and underpinned, and (iii) the robust theoretical basis has yielded useful computational solutions for the practice. The target applications cover a wide range, likewise the used computational principles that were initially proposed in other fields of knowledge, such as natural language processing, artificial intelligence, and downstream product validation. The papers included in this issue integrate these computational solutions into the early phase of product design. This tells us that the application of computational tools is gradually moving towards, and increasing in, the early stages of product design and development, where the most influential decisions are made. We believe that it is essential for researchers and developers at universities and research institutes to learn the proposed computer-oriented methods and tools, and we hope that they will prove to be useful and sufficiently intuitive for industrial end-users too.

Originally, the papers were presented at the Sixth International Symposium on Tools and Methods of Competitive Engineering (TMCE 2006), held in Ljubljana, the capital city of Slovenia. The series of TMCE Symposia pursues the further development of the scientific, technological, and practical knowledge of competitive engineering, and it has been acting as a catalyst for knowledge transfer between academia and industry for more than a decade. Since its inception in 1995, the Symposium has grown to a mature and well-established platform for the exchange of scientific and industrial knowledge. In 2006, over 250 participants were actively involved in discussing the state of the art in four

vrhunski tehnologiji na štirih specifičnih področjih konstruiranja in tehnološkega razvoja izdelkov, in sicer na področju konstruiranja, hkratnega razvoja izdelkov, napredne izvedbe izdelkov in delovanja virtualnih podjetij.

Za tematsko številko smo izmed vseh referatov, predstavljenih na TMCE leta 2006, izbrali najbolj dodelane, preverjene in tiste z največjim potencialom. Vse prispevke smo natančno pregledali in popravili, pri čemer je sodelovalo več ko 30 recenzentov. Spodaj na kratko povzemamo bistvo predlaganih postopkov in opozarjamo na pomen njihovih prispevkov.

Prvi referat z naslovom "Boljše izluščevanje informacij s pomočjo metode verjetnosti", avtorjev S. Kima, S. Ahmeda in K. Wallacea se ukvarja s pomanjkanjem pomenskosti pri navadnem besedilnem iskanju. Glavni prispevek tega prispevka je v priredbi nenazorne primerjalne metode, ki z uporabo naivne Bayesove teorije verjetnosti prepoznava zasnove, temelječe na podobnosti. S tem postopkom se poveča trdnost odkrivanja in pridobivanja ustreznih podatkov za tehnološki razvoj. Rešitev, ki jo predstavljajo avtorji, temelji na kombinaciji različnih algoritmov za obdelavo naravnega jezika, ki avtomatično prepoznajo lastna imena. Avtorjem je uspelo izboljšati pokritost prepoznavanja lastnih imen v besedilih o tehnološkem razvoju. Ena od pomanjkljivosti je ta, da njihova rešitev temelji na nadzorovanem učenju, ki terja natančno urjenje algoritma s človekovo pomočjo.

Drugi prispevek z naslovom "Konstruiranje izdelka s pomočjo tehnike optimizacije stika", avtorjev I. Páczelta, A. Bakse in T. Szaba se ukvarja z različnimi postopki v zvezi z mehanskimi stiki med strojnimi elementi, zlasti s porazdelitvami obremenitev, zaradi katerih se skrajšuje doba trajanja strojnih elementov. Znano dejstvo je, da so velike obremenitve odvisne od oblike, materiala in obremenitev teles, ki so med seboj v stiku. Vendar natančno računanje porazdelitve obremenitev na dotikalnih točkah je še vedno precejšen izziv. Omenjeni prispevek prinaša izboljšavo v dveh delih: kot prvo predlaga nadzorovan analitični model stika. Kot drugo, avtorji predstavljajo ta model v ločen računalniški model. Z izbiro ustreznih nadzornih funkcij nato ta model uporabijo kot metodo končnih elementov. V želji po enakomerni razporeditvi obremenitve med deli v stiku, se je takšna kombinacija postopkov izkazala za učinkovito rešitev pri konstruiranju stikov strojnih elementov.

specific fields of product design and engineering, namely, in industrial design engineering, competitive product development, advanced product realization, and operation in virtual enterprises.

From the pool of papers presented at TMCE 2006, we picked the most elaborated, validated, and potential ones for this issue. All the papers were intensively reviewed and revised, which involved more than 30 reviewers. Below, we briefly describe the essence of the proposed approaches and point out the significance of their contribution.

The first paper titled "Improving information extraction using a probability-based approach", co-authored by Kim, S., Ahmed, S. and Wallace, K., addresses the problem of the lack of semantics in regular text-based searches. The main contribution of this paper is the adaptation of an inexact matching method, which employs naïve Bayesian probability to recognize concepts based on similarity. This approach increases the robustness of identifying and retrieving appropriate engineering information. The authors base their solution on a combination of various Natural Language Processing algorithms to automatically identify so-called Named Entities in written texts. They have been able to improve the coverage of identifying Named Entities in engineering texts. One of the limitations is that their solution relies on supervised learning, which requires careful training of the algorithm by human interaction.

The second paper titled "Product design using contact optimisation technique", by Páczelt, I., Baksa, A. and Szabó, T., discusses various issues related to mechanical contact problems between machine elements, in particular, the issue of stress distribution that decreases the lifetime of mechanical parts. It is well known that high stresses arise, depending on the shape, the material, and the loads of the bodies in contact. However, the high-fidelity computation of contact-stress distributions is still rather challenging. The novelty of this contribution is twofold: first, it proposes a controllable analytical model of contact in typical situations (punches, rollers and air-springs), covering kinematics and pressure; second, it translates this model into a discrete computational model, and implements this computational model as a finite-element method, by choosing appropriate control functions. Striving after obtaining a smooth pressure distribution among the bodies in contact, this combination of the means has proved to be an efficient solution for designing the contacts of the components of products.

Prispevek avtorjev J. Matthewsa, B. Singha, G. Mullineuxa in A. J. Medlanda pod naslovom "Proučevanje konstruiranja proizvodnih strojev s postopkom, temelječem na modeliranju omejitev" govori o prostorskih mehanizmih postopkovnih strojev, ki jih najdemo na primer pri predelavi hrane, sestavljanju polizdelkov za avtomobile ali v industriji električnih naprav. Ta prispevek je zbudil našo pozornost zato, ker so avtorji za pojasnjevanje uporabili izpopolnjen model na temelju zvezanosti, ki izvira s področja umetne inteligence, in ga razširili z modeliranjem omejitev. Ta postopek ima že sam po sebi omejitve pri skladnosti z večjimi prostorskimi mehanizmi, pri katerih je težko obvladovati zapletenost modeliranja in število parametrov. Predlagana metoda združuje modeliranje mehanizmov, pojasnjevanje napak in različne načine vizualizacije za prikazovanje omejitev kinematičnega obnašanja.

Četrti prispevek z naslovom "Omejitve, ki vplivajo na konstrukcijo stebla z ramenom in uporaba natančne geometrije", ki so ga napisali G. Mullineux, C.J. McPherson, B.J. Hicks, C. Berry in A.J. Medland, uvaja nov, numerični model, ki nima nič več skupnega z običajnimi metodami proizvodnje embalaže. Bistveni sestavni del pokončne naprave za oblikovanje, polnjenje in zapiranje embalaže je steblo z nastavkom, ki embalažo prepogne in ji med polnjenjem daje oporo. Tehnološki problem predstavljata vodilo folije in uravnavanje napetosti, zaradi česar se bodisi mečkajo vrečke in prihaja do zastojev na stroju, bodisi se zaradi prevelike napetosti material trga. To lahko preizkusimo z izdelavo matematičnega modela, ki ga dodelamo tako, da določimo omejitve zaradi deformacije folije. Dobimo okvir za konstrukcijo stebla z nastavkom, ki upošteva tako geometrijsko obliko kot razlike med uporabljenimi materiali. Čeprav prispevek ne prispeva k boljšemu razumevanju tehnoloških metod na temelju zvezanosti, je iz njega razvidno, da so tudi neoptimalne rešitve lahko sprejemljive v vsakdanji praksi.

Prispevek C. L. Goussarda in A. H. Bassona z naslovom "Ocena tlaka v kalupu za stroškovni model obstojnosti stroja za batno brizganje" predstavlja metodo za hitro določanje tlaka v kalupu. Kot rešitev tega zapletenega vprašanja avtorji predstavljajo polanalitični model, ki lahko pripelje do grobih konstrukcijskih rešitev. Pri konstruiranju sistemov za batno brizganje,

Titled "A constraint-based limits modelling approach to investigate manufacturing machine modelling design", the paper of Matthews, J., Singh, B., Mullineux, G. and Medland, A. J., focuses on the spatial mechanisms of process machinery, which can, for example, be found in the food processing, automotive sub-component assembly, or electrical device industries. This paper has attracted our attention because it employs an elaborated constraint-based reasoning model, originating in the field of artificial intelligence, and expands it by a limits-modelling approach. The approach inherently bears restrictions in supporting larger spatial mechanisms, in which the complexity of the modelling and the number of parameters are difficult to handle. The proposed method encompasses mechanism modelling, failure-mode reasoning, and various means of visualization in order to illustrate the boundaries of kinematical behaviour.

The fourth paper, titled "Constraints influencing the design of forming shoulders and the use of exact geometry", written by Mullineux, G., McPherson, C.J., Hicks, B.J., Berry C. and Medland, A. J., introduces a novel numerically based model in order to break with conservative paradigms in packaging manufacturing. An essential part of a vertical form, fill, and seal machine is a forming shoulder, which folds and supports the package during the filling procedure. The engineering problems are film tracking and tension control, which can result in either malformed bags and machine jams, or excessive stretch and tear of the material. To investigate this, a mathematical model is created and is refined by defining sheet-deformation constraints. The results constitute a reasoning framework in designing forming shoulders, covering both the geometry and the use of different sheet materials. Although the paper does not contribute to increasing our understanding in constraint-based engineering methods, it demonstrates that even sub-optimal solutions may be acceptable in standard practice.

The paper of Goussard, C. L. and Basson, A. H., titled "Cavity pressure estimation for a piston moulding life cycle cost model", presents a method supporting the rapid assessment of cavity pressures during the piston moulding of thermoplastics. As a solution for this complex problem, the authors contribute a semi-analytical model that can lead to more robust design solutions. In designing such piston-moulding systems, also known as Lomolding, the injection pressure and the clamping forces are the

imenovanih tudi “Lomolding”, največjo težavo predstavljajo tlak na vbrizgu in pritrjevalne sile. Vendar znane simulacije zahtevajo veliko časa - tako določanje sistemskih parametrov kakor samo izvajanje simulacije. Predlagani polanalitični model predpostavlja polimerno čelo tečenja, pri katerem je vzvodni in nizvodni tok enak povprečni širini nadzorne prostornine. Model so večkrat uporabili in primerjali s “Cadmouldom”. Natančnost rezultatov zadošča za konstruiranje strojev tako dolgo, dokler je Graetzovo število dovolj veliko. S pomočjo polanalitičnega modela se čas računanja skrajša na najmanj, v primerjavi z običajnimi simulacijami pa je razmeroma majhna tudi količina podatkov. Ta poenostavljeni model upošteva samo peščico dejavnikov v zvezi s kakovostjo postopkov. Zato ima ta postopek določene omejitve, ki se jih pri uporabi modela moramo zavedati.

Zadnji prispevek z naslovom "Optimiranje debeline brizganih plastičnih delov na podlagi simulacije Moldflow", avtorjev Y.-M Denga. in D Zhenga govori o računskem optimiranju delne geometrijske oblike pri brizganju. Napori so usmerjeni v dopolnitev sedanjih postopkov in obsežnega znanja o optimiranju debeline komponent. Zanimanje avtorjev za optimiranje debeline brizganih plastičnih delov je upravičeno. V praksi so stene brizganih plastičnih delov bodisi brez potrebe debele, ali pa so pretanke. Zato med brizganjem zaradi pretankih sten običajno prihaja do poškodb, predebele stene pa pomenijo nepotrebno porabo materiala. Predlagan postopek za optimiranje debeline temelji na znanem simulacijskem sistemu brizganja plastike (Moldflow). S postopkom ponavljalno spreminjamo debelino sten določenih delov, izvajamo simulacijo brizganja “Moldflow”, ocenjujemo brizganje glede na navedene kriterije in določamo nadaljnje spremembe debeline. Čeprav predlagana metoda uporablja zapletene numerične tehnike, hkrati računa tudi na človekov razum, zlasti pri določanju pragov in mejnih vrednosti ter pri odločanju o skladnosti med rezultati numerične simulacije in rezultati, ki jih pričakujemo na podlagi zdravega razuma.

Verjamemo, da nam je s to izbiro prispevkov uspelo predstaviti dobre primere čedalje večjega števila računalniških postopkov, s katerimi lahko rešujemo ključna vprašanja razvojnega postopka v industriji. Poleg tega upamo, da nam je uspelo podati

main concerns. However, existing mould-flow simulations are time consuming - both in terms of defining the system parameters and of running the simulations. The proposed semi-analytical model assumes a polymer flow front in which upstream and downstream flow paths are equal to the average width of the control volume. The model is implemented and compared to Cadmould in a number of cases. The results are sufficiently accurate for machine design, as long as the Graetz number is sufficiently high. The semi-analytical model lends itself to almost negligible computation times, and, in comparison with traditional simulations, the amount of data is also relatively small. This simplified model takes into consideration only a few factors to reason about the quality of the processes. This in turn results in limitations, which should be taken into consideration during the use of the method.

The last paper, titled "Minimizing thicknesses of injection molded plastic parts based on Moldflow simulation", by Deng, Y.-M. and Zheng, D., considers computational optimization of part geometries in injection moulding. The efforts are towards complementing the existing approaches and the large body of knowledge supporting the thickness optimisation of structural components. The authors' concern about the thickness optimisation of moulded plastic parts is relevant: in practice, the walls of moulded plastic parts are either unnecessarily thick, or too thin to satisfy all the moulding requirements. Consequently, too thin walls usually cause defects during the moulding process, and thick walls simply mean excess material usage. The proposed minimizing procedure relies on an existing injection-moulding simulation system (Moldflow). The process changes the wall thickness of the selected part features iteratively, executes the simulation of the moulding process using Moldflow, assesses the moulding against the stated criteria, and determines the subsequent alteration of the thickness. Although the proposed method employs a sophisticated numerical technique, it also counts on human reasoning, in particular when setting the threshold and boundary values, and to decide on the compliance of the results of the numerical simulation with those expected based on common-sense reasoning.

We trust that with this collection of papers, we managed to provide good examples of emerging computational approaches that can be used to solve critical engineering problems in industry. Moreover, we hope that we were able give examples of the best

primere najboljših raziskovalnih praks za bodoče raziskovalce. Hvaležni smo vsem avtorjem za njihov prispevek k tej tematski številki ter cenimo njihove napore in prijazno sodelovanje. Zahvalo smo dolžni tudi našim kolegom recenzentom, ki so pripomogli k večji znanstveni in strokovni vrednosti prispevkov ter njihovi kakovosti. Prav tako so se potrudili gostujoči uredniki in izdelali kar najboljšo izbiro ter pripravili prispevke po navodilih. Po drugi strani pa vsi dobro poznajo izrek Henryja Louisa Menckena, da "za vsako težavo obstaja rešitev, ki je preprosta, popolna in napačna."

Prof. dr. Imre Horváth
Ir. Jouke Verlinden
Tehnološka univerza Delft
Fakulteta za razvoj industrijskega oblikovanja
Nizozemska

Prof. dr. Jože Duhovnik
Univerza v Ljubljani
Fakulteta za strojništvo
Slovenija

research practices for fellow researchers. We are grateful to all the authors for their contribution to this issue, and we do appreciate their efforts and excellent collaboration. We are indebted to our peer reviewers too, who helped increase the scientific/professional value and quality of the papers. The guest-editors also tried to arrive at the best selection for this issue and to arrange the papers in a tutorial manner. On the other hand, they are aware of Henry Louis Mencken's saying that "For every problem there is a solution which is simple, clean and wrong".

Prof. Dr. Imre Horváth
Ir. Jouke Verlinden
Delft University of Technology
Faculty of Industrial Design Engineering
The Netherlands

Prof. Dr. Jože Duhovnik
University of Ljubljana
Faculty of Mechanical Engineering
Slovenia

Strojniški vestnik - Journal of Mechanical Engineering 53(2007)7-8, 429-441
UDK - UDC 025.4.03
Izvirni znanstveni članek - Original scientific paper (1.01)

Boljše izluščevanje informacij s pomočjo metode verjetnosti

Improving Information Extraction Using a Probability-Based Approach

Sanghee Kim[1] - Saeema Ahmed[2] - Ken Wallace[1]
([1]University of Cambridge, United Kingdom; [2]Technical University of Denmark)

Informacije imajo ključen pomen v celotnem trajanju izdelka. Rezultati raziskav kažejo, da se inženirji pogosto posvetujejo med seboj, da pridobijo informacije, potrebne za reševanje težav. Zaradi prehajanja ključnih kadrov v druga podjetja in upokojitev postaja vse bolj pomembna zmožnost izluščiti manjkajoče informacije iz tehnične dokumentacije, seveda, če le-ta obstaja. Zanimanje za različne načine izluščevanja tovrstnih informacij tako postaja vse večje. Iskanje po ključnih besedah je ustaljen način, vendar raziskave kažejo, da je ta način mnogokrat nezadovoljiv. Iskanje je mogoče izboljšati s standardiziranim načinom poimenovanja elementov in njihovih povezav v posameznih domenah, vendar je zaradi obilice sedanje dokumentacije, ki uporablja različna poimenovanja, izkoristek iskanja slab. Tako uporaba učenja, ki temelji na verjetnostnem modelu, obeta boljši izkoristek iskanja informacij ob enaki natančnosti, kakor ga omogočajo vnaprej določena iskalna pravila. Prispevek predstavlja rezultate iskanja informacij, ki temeljijo na verjetnostnem postopku. Preizkusi kažejo, da opisan postopek poveča izkoristek iskanja informacij s 53 odstotkov na 80 odstotkov, ob primerljivi natančnosti.

(Ključne besede: izluščevanje informacij, identifikacija dokumentov, iskalne strategije, klasifikacija, verjetnostne metode)

Information plays a crucial role during the entire life-cycle of a product. It has been shown that engineers frequently consult colleagues to obtain the information they require to solve problems. However, the industrial world is now more transient and key personnel move to other companies or retire. It is becoming essential to retrieve vital information from archived product documents, if it is available. There is, therefore, great interest in ways of extracting relevant and sharable information from documents. A keyword-based search is commonly used, but studies have shown that these searches often prove unsuccessful. Searches can be improved if domain entities of interest, e.g., 'gas turbine', are explicitly associated with their types, i.e., gas turbine is a type of engine, thus reducing the ambiguity of referring to the entities using various different ways of expressing them. It would be helpful to compile a full list of entities associated with the relevant types before identifying them in texts. However, due to the various ways of referring entities in the texts, manually defined identification rules tend to produce high precision but with low recall. In order to increase the recall, while maintaining the high precision, a learning approach that makes identification decisions based on a probability model, rather than simply looking up the presence of the pre-defined variations, looks promising. This paper presents the results of developing such a probability-based entity-identification approach. Tests show that the proposed approach achieves improved recall, i.e., from 53% to 80%, with comparable precision.

(Keywords: information searches, name entity identification, natural language processing, taxonomy, probability methods)

0 INTRODUCTION

Engineers frequently seek the information they need from colleagues. However, the time spent on acquiring and providing such information detracts from the time available to carry out their main tasks. In addition, as these engineers retire or move to other jobs, they can no longer be consulted. Engineers have to rely increasingly on documents, which are the prevalent information resource in organizations. Approximately 90% of organizational memory exists in the form of text-

based documents [1]. A computer-based document-management system can improve access to information contained in documents. Therefore, organisations are placing great emphasis on identifying reusable information in documents in order to improve access.

It has been reported that 35% of users find it difficult to access information contained in documents and at least 60% of the information that is critical to these organizations is not accessible using typical search tools [2]. There are three reasons for this problem. Firstly, there is simply too much information. Secondly, the keywords used by those searching for information might not be the same as those used to index the information. Thirdly, due to the nature of unstructured texts, it is a challenge to automatically index the information.

To address this problem, there have been many attempts to convert unstructured texts into more accessible formats. Recent research suggests the use of corporate taxonomies. As a hierarchical classification of entities, e.g., engineering products, a taxonomy supports the indexing and retrieval of information by annotating the content of a document with taxonomy entities, and then mapping a user's query onto those entities. In this way it is feasible to share and refer to the entities with less ambiguity. However, manually annotating texts with taxonomy entities can lead to time-consuming and error-prone indexing. Automatic annotating is thus preferred and this is one of the goals of Information Extraction (IE), which is a sub-field of Natural Language Processing (NLP). IE aims to extract entities that have pre-defined types, i.e., Named Entities (NE), using shallow NLP techniques.

The application of IE to engineering design document needs to pay particular attention to the difficulty of identifying engineering NEs, i.e., product names, due to their compositional features. This contrasts with typical IE systems that focus on NEs, which are usually identified using lexicon-syntactic grammar rules, i.e., people's names, dates, times. No previous research on developing IE systems for engineering design documents has been identified.

This paper presents a probability-based approach that achieves a good balance between precision and recall by automatically identifying NEs in engineering documents. Such an approach improves on the performance of the NE identification rules that simply enumerate pre-fixed variations and identify variations. A software prototype has been developed to test the performance of the proposed approach.

The overall aim of our research group is to understand how to make more information available in a readily useable form to engineering designers. The specific aim of the research described in this paper is to improve the IE from documents using a probability-based approach that is able to identify entities whose variations are not pre-defined.

1 LITERATURE REVIEW

Observations of engineering designers found that approximately 24% of a designer's time is spent acquiring and providing information [3]. This study also reported that in the aerospace industry, approximately 40,000 documents are produced during the design of a single aero-engine. Time could be saved if designers were able to retrieve the information they need from these documents rather than asking colleagues. However, this is only possible if designers are aware that relevant documents exist and they can retrieve the information contained in them easily. A further problem was identified by an empirical study that analysed 633 queries directed by novice designers to more experienced designers, which found that the novice designers were aware of what they needed to know in only 35% of all queries, i.e., they asked a specific question to which they received a specific reply [4]. These findings suggest that novice designers require support in identifying what they need to know. Such support could be provided through an explicit indexing structure that prompts the relevant queries.

Two common approaches to support information sharing in organizations are *knowledge repository* and *collaborative filtering*. A knowledge repository is a centralized resource where knowledge is structured into easily accessible formats [5]. The repository aims to explicitly represent knowledge for better distribution. One example is an expert system, which attempts to emulate the problem-solving ability of a domain expert by generating automatic solutions for a specific task. Expert systems have been widely deployed and have led to some significant improvements in knowledge sharing among employees. However, experience of using expert systems highlights the fact that organizational

knowledge does not remain static, so a dynamic knowledge-acquisition process is needed [6].

The second approach is to use collaborative filtering, which relies on the interactions between users to identify common task experiences and to recommend useful information [7]. It is easier to reuse information from the knowledge repository, but effort is required from the users to enter the information. Sharing through collaborative filtering does not impose such a burden on the users, but they do need to have a greater understanding of the context in order to retrieve the information they require. Whereas both approaches focus on capturing information, IE is more concerned with the indexing and retrieval of information. An empirical study by Furnas et al. [8] confirmed the importance of explicitly associating entities with types for retrieving needed information. They revealed that two users choose the same keywords for a single entity less than 20% of the time. In addition, according to industry experience, four synonyms are required for each entity [9].

Traditional IE systems use pre-defined templates that specify which NEs are to be extracted ([10] and [11]). However, templates can be too rigid to accommodate new types of entities and the relationships between them, so ontology or taxonomy-based IE systems are becoming increasingly popular ([12] to [14]). Ontologies and taxonomies make possible an inference-based approach that IE systems can use when the level of ambiguity is high.

One of the barriers to developing IE systems is their reliance on language experts for creating dictionaries of NEs along with extraction rules. The exploitation of learning techniques to reduce the reliance on human experts has therefore become popular. One such learning technique is supervised learning, which derives rules from manually tagged examples, e.g., 'AutoSlog' [15] and 'LTG' [16]. In AutoSlog, each extraction rule is defined by a trigger, a condition and a constraint in order to reduce the level of ambiguity. For example, the following rule identifies 'aircraft engine' as the entity of the 'started' event in the sentence: 'The aircraft engine was started by the pilot':

Trigger: verb should be 'started'
Condition: voice of sentence should be 'passive'
Constraint: subject should be a type of physical entity

The constraints are generally based on the syntax, implying that if the entities appear in different syntaxes, i.e., either as a subject or as an object, then two distinct rules need to be created to cover both cases [17]. LTG first identifies those text fragments that can be determined easily and delays the identification of the remainder until more evidence has emerged. This evidence includes 'position in a sentence' and 'whether the fragment is in lower case in a text'. It then uses a machine-learning method to identify the remaining text fragments.

The approach described in this paper incrementally creates the extraction rules from a limited number of examples of NE variations. In addition, the approach exploits the hierarchical classifications of NEs in order to recognize the more complex ones.

2 UNDERLYING CONCEPTS

2.1 Example

The following three unlinked extracts from Rolls-Royce's website[1] are used as examples throughout this paper.

<Extract 1> Like the motor car engine, the gas turbine is an internal combustion engine. In both, air is compressed, fuel added, the mixture ignited, and the rapid expansion of the resultant hot gas produces the power. However, combustion in a motor car engine is intermittent and the expanding gas produces shaft power through a piston and crank, whereas in a jet engine combustion is continuous and its power results from expanding gas being forced out of the rear of the engine.
<Extract 2> The intermediate case is a fabricated, spoked structure housing the thrust bearings for all shafts, and forming the air path between the IP and HP compressors. Externally it carries the A-frame support arms which brace the fan case (Module 7), and its internal hollow struts provide access for services such as oil tubes, cooling air, and the radial drive-shaft to the accessory gearbox.
<Extract 3> Largest of the modules, this is an assembly of forward and rear cylindrical casings and the fan outlet guide vane (OGV) ring. It is often referred to as the fan case. The titanium rear casing carries the fancase-mounted accessories and also contains acoustic linings. At their inner ends, the

[1] http://www.rolls-royce.com/education/schools/how_things_work/gasturbine/gasturbines.pdf

fan OGVs are secured to the torsion ring which locates the IP compressor module, whilst the outer ends are bolted to the front mounting ring. This assembly is welded to the titanium rear casing and bolted to the front casing.

Finding information using a keyword-based search is not always successful. For example, it may not be easy to find answers to the question: 'What material is used for the fan rear case'. For example, Google returns approximately 325,000 hits when it searches using the keywords 'fan rear case'. The first-ranked return is about improving the cooling system in a PC by adding a 'rear fan case'. Extract 3 above contains the answer to the query and it is available online. However, Google is unable to identify Extract 3 as it does not recognise that 'fan rear case' is the name of a product and that one of its variations is 'rear casing'. The search could be improved if Extract 3 had been indexed with NEs that identify product names and materials. If this had been done, Titanium could then be identified as the answer. Figure 1 shows the identification of the relevant NEs.

2.2 IE and Named Entity Identification

Using shallow NLP techniques, e.g., Part-Of-Speech (POS), IE can process a large number of documents effectively. It has demonstrated a significant improvement in retrieving relevant information compared to keyword searches.

IE structures information into easily accessible formats by identifying NEs and the relationships between them. NEs are pre-defined lists of domain entities. Generally, NEs are the proper names of organizations, people and locations. However, in this paper, NEs are text fragments referring to product names. For example, in the sentence 'Like the motor car engine, the gas turbine is an internal combustion engine.', 'turbine', 'gas turbine', 'engine' and 'car engine' could all be defined as product names. Highlighted texts, such as the one shown in Figure 1, help users to visually scan a large number of documents.

The three major tasks of IE are *NE identification, co-reference resolution and scenario filling*. NE identification involves the recognition of defined NEs and their variations. Co-reference is the referent shared by different entities. Its scope is broad, ranging from people (e.g., Joan and she) to objects (e.g., engine and it). Scenario filling integrates the extracted individual NEs into stories or new facts. This paper only addresses NE identification.

NE identification usually relies on two resources: (1) a dictionary of pre-defined NEs; and (2) extraction rules. The extraction rules are based on linguistic grammars specifying conditions under which the NEs are identified. For example, the following rule:

<Product> *is an assembly of* <Product>

states that if the left entity is identified as a type of 'Product', and then the right entity should also be tagged as 'Product'.

IE systems adopt different approaches. Systems with a complete list of NEs are less dependent on extraction rules, whereas systems with pattern-learning techniques need fewer pre-defined NEs. When an application domain generates new NEs frequently, it is difficult to manually maintain the NE dictionary, so a machine-

Largest of the modules, this is an assembly of <Product NE type=Front Casing>forward</Product> and <Product NE type=Fan Rear Case>rear cylindrical casings</Product> and the <Product NE type= Outlet Guide Van Inner Ring>fan outlet guide vane (OGV) ring</Product>. It is often referred to as the <Product NE type=Fan Containment Casing>fan-case</Product>. The <Material Type= Titanium>titanium</Material> <Product NE type=Fan Rear Case> rear casing</Product> carries the <Product NE type=Fan Containment Casing>fancase</Product>-mounted accessories and also contains acoustic linings. At their inner ends, the <Product NE type= Outlet Guide Van Inner Ring>fan OGVs</Product> are secured to the torsion ring which locates the <Product NE type= IP Compressor>IP compressor</Product> module, whilst the outer ends are bolted to the front mounting ring. This assembly is welded to the <Material Type= Titanium>titanium</Material> <Product NE type=Fan Rear Case> rear casing</Product> and bolted to the <Product NE type=Front Casing>front casing</Product>.

Fig. 1. *Example of NE identification*

learning technique is required. However, it is important to take into account the potential risk of relying entirely on the dictionary due to the possibility of polysemy. Polysemy is when an entity can be used in different contexts to express two or more meanings. For example, the entity 'bearing' has multiple meanings, e.g., (1) the 'bearing' supporting a rotating shaft and (2) the 'bearing' a ship is sailing on.

In engineering domains, NEs focus mostly on product and material names. The names of products and their components are relatively fixed, but have a large number of variations. For example, 'Fan Outlet Guide Vane Ring', can be shortened to 'Fan OGV Ring', and if the Ring is only used for the 'Fan' component, then the 'Fan' can be dropped, i.e. OGV Ring. In order to reflect this compositional structure, it is convenient to organise the product names in a hierarchical structure.

2.3 Taxonomy – NE Dictionary

The taxonomy employed as part of this research is Engineering Design Integrated Taxonomy (EDIT) [18]. One of the motivations for developing EDIT was to provide a visible indexing structure to help users search for information. There are two main advantages in having such a structure. Firstly, it helps designers focus their queries by browsing or navigating using the index; secondly, it provides the opportunity for search engines to recognise the context of a query. However, even if a search engine was able to recognise the context of a query, its results could only be as good as the original query. EDIT was developed by conducting interviews in two aerospace companies and analysing the transcripts of designers describing their design processes. EDIT consists of four root concepts:

1. The *design process* itself, namely, the different tasks undertaken at each stage of the design process. For example, conceptual design, detail design, brainstorming.
2. The *function* that must be fulfilled by all or part of a particular component or assembly. For example, one of the main functions of a compressor in a gas turbine is to 'compress air'.
3. The *issue* that the designer must consider while carrying out a stage of the design process. For example, considering the unit cost or manufacturing requirements.
4. The *product* itself, namely, component, sub-assembly and assembly. For example, outlet guide vane ring, fan case.

In this paper, NE identification is centred on the 'Product' root concept of EDIT, which currently has 220 entities defined. The 'Product' NEs are defined by both the 'Part-of' relation, e.g., 'IP compressor' is a part of 'Engine'; and 'Type-of' relation, e.g., 'IP compressor' is a type of 'Compressor'. One of the authors examined the 'Product' root concept from the perspective of NE identification and observed that:

- The names of 'Product' NEs in EDIT were largely determined from interviews with practising engineers and were the names they tended to prefer. However, texts contain an even wider range of names and many variations.
- As sub-classes are not always extended with the names of super-classes in EDIT, it can be difficult to correctly identify all the names simply through the taxonomy.

3 A PROPOSED APPROACH TO NE IDENFITICATION

3.1 Analysis of Product NEs in a Text

It is important to base NE identification systems on solid empirical evidence. The datasets provided by the Message Understanding Conference (MUC) have commonly been used for evaluating new identification systems [19]. However, the datasets define only seven types of NEs, i.e., Organisation, Person, Location, Date, Time, Money, and Percent, and product names are not included. In addition, no hierarchy is used for defining the NEs. Therefore, it was necessary to collect a new dataset in order to evaluate our approach. To do this 137 sample documents were collected from the same company with which EDIT was developed. These are one-page problem reports that describe problems, suggestions or new requirements that arose during product development. Once a new report is filed, senior engineers determine what further action is required to solve the problem described. A list of acronyms with their full definitions was provided by the company. One of the authors manually read each report and divided it into paragraphs, each of which was separated into sentences. After this the text fragments that contained relevant NEs were

identified, e.g., 'Forward Casing'. Each NE was then compared with the associated NE in EDIT, i.e., 'Front Casing', in order to identify any differences and how these differences could be defined.

Table 1 shows the results of the comparisons, which are split into seven categories: (1) singular or plural, (2) acronym, (3) compounds, (4) syntactic variation, (5) synonym, (6) separate reusable suffix, and (7) separate reusable modifier. Identical matches were included in the singular/plural variation. A total of 54% of the text fragments in the sample documents were matched with EDIT's Product NEs using one or more of the seven variations in Table 1. These seven variations are referred to as Exact Rules in this paper.

The first and second variations were identified frequently, singular/plural 24% and Acronym 13%, respectively. For example, the fragment 'HP Compressors' is matched with EDIT's 'HP Compressor' NE by identifying the plural form of 'Compressor'. Acronyms, e.g., 'OGV' for 'Outlet Guide Vane' can easily be matched from a list of definitions.

Compounds, e.g., 'Fancase' for 'Fan Case', are easy to match and syntactic variations, e.g., 'Starter Duct' and 'Starter Ducting', can be matched using POS tagging. However, the identification of synonyms, e.g., 'Forward Casing' and 'Front Casing' is more difficult since it requires appropriate definitions of the meanings of words. Synonyms can be matched by querying the lexical database WordNet [20].

Single and multiple terms are used for the names of Product NEs and it is difficult to identify the variations of NEs with multiple terms. In general, a multiple-term NE consists of a headword, the categorical part that contains the basic meaning, and a modifier that restricts the meaning. In the example 'Fan Case', the headword, 'Case' defines that it is a case for the fan. It is common practice to place the headword as the last of the terms. A separate reusable suffix, e.g., 'System' in 'Casing Cooling System', is part of an NE that can be removed without changing the overall meaning. Separate reusable modifiers, e.g. 'Electrical' in 'Electrical Harness', are often omitted because their purpose is to emphasise the headword and their meaning can be inferred.

It is necessary to combine multiple variations in order to correctly identify some fragments. For example, the fragment 'Case Cooling' is matched with 'Casing Cooling System' by identifying that 'Case' and 'Casing' are synonyms and 'System' is a removable suffix.

First, the Exact Rules are applied to determine if a fragment matches only one of EDIT's NEs. If more than one NE is matched, then the matching is ambiguous and the fragment remains untagged.

The remaining 46% of the text fragments in the sample documents were not uniquely matched with any of EDIT's Product NEs using the Exact Rules. Therefore, matching was based on the engineering judgment of the author who manually identified the NEs in the sample documents. Some examples are shown in Table 2. These NEs are difficult to extract automatically and a probability-based approach is necessary. Such an approach is the focus of this paper and is referred to as the application of Inexact Rules.

Table 1. *Exact Rules*

Variations	Example		Occurrences (%)
	Text fragment	EDIT Product NE	
Singular/plural	HP Compressors	HP Compressor	24%
Acronym	OGV	Outlet Guide Vane	13%
Compounds	Rear Fancase	Rear Fan Case	5%
Syntactic variation	Starter Duct	Starter Ducting	4%
Synonym	Forward Casing	Front Casing	3%
Separate reusable suffix	Case Cooling	Casing Cooling System	3%
Separate reusable modifier	Harness	Electrical Harness	2%
		Total	54%

Table 2. *Examples of partial matching*

Text fragment	EDIT Product NEs
LP Compressor Titanium Containment Case	Fan Containment Casing
Combustor Outer Casings	Combustion Outer Case
Fan Case Containment	(1) Fan Containment Casing (2) Rear Fan Case

The first fragment in Table 2, 'LP Compressor Titanium Containment Case', is matched with EDIT's 'Fan Containment Casing' NE by recognising that the 'Fan Containment Casing' is a part of 'LP Compressor' according to the 'Product' root concept in EDIT.

The second fragment 'Combustor Outer Casings' is not easily matched with 'Combustion Outer Case' although 'Combustion' and 'Combustor' are defined as synonyms. This is because 'Combustor', which is a part of the fragment, is defined as a single NE in EDIT. In order to achieve a correct identification, longer-length fragments should be clustered and a match attempted before single-word fragments are matched.

The third fragment 'Fan Case Containment' is matched with EDIT's 'Fan Containment Casing' NE if the *number* of shared terms is considered. However, if the *sequence* of terms is considered to be more important, then EDIT's 'Rear Fan Case' NE would be identified.

When identifying the text fragments above, it was necessary to take into account hierarchical or compositional descriptions of the NEs in EDIT. NE identification, therefore, does not rely entirely on the information from the dictionary. Instead, it is essential to pay special attention to the fragments that are partially matched with multiple NEs in EDIT. In summary, the following three guidelines are used to determine which of EDIT's NEs should be selected for each of the examples above. Preference should be given to the NE:

1. whose hierarchical descriptions match
2. with a 'maximum-length' match
3. composing terms preserve the partial ordering.

3.2 A Probability-based NE Identification

The proposed approach uses both the Exact and Inexact Rules. The Exact Rules contain a total of 1160 variations of the 220 Product NEs in EDIT, i.e., approximately five variations for each NE.

The Inexact Rules are based on naïve Bayesian probability. They are based on a simplified theorem that assumes variables to be independent in each class. In order to take into account the compositional descriptions of the NEs in EDIT, each fragment is encoded with the following attributes: (1) the two adjacent words; (2) POS tags; (3) the NE assigned to the previous text fragment; (4) the headword; and (5) all possible partial orders of the composing words of the fragment, with their orders preserved. Some of these encodings are described in the literature [16] and [21].

Given a text fragment, e_i, represented as a set of attributes, $t = (t_1, t_2 \ldots t_n)$, extracted from a text, $P(c_j \mid e_i)$, that represents the probability that Product NE, c_j, will be the NE against which will be matched [22]. This probability is defined as:

$$P(c_j \mid e_i) = P(c_j) \prod_{n \in positions} P(t_n \mid c_j)$$

with:

$$P(t_n \mid c_j) = \frac{(k_n + 1)}{(N + |vocabulary|)}$$

where is the number of times the attribute occurs in the NE ; N is the total number of attributes in the NE ; *vocabulary* is the set of all the distinct attributes for all the NEs; |*vocabulary*| is the total number of distinct attributes for all the NEs; *positions* is the set of attributes that appear in both the text fragment and *vocabulary*; and with:

The naïve Bayesian approach compares the attributes of a new text fragment with those of every NE in EDIT and computes the probability for each. The NE highest probability is assumed to be the best match. In this research it is assumed that each text fragment is assigned exactly to one Product NE. is the conditional probability that a fragment belongs to a particular Product NE, given that the fragment has the attribute values . Since it is difficult to estimate precisely all the combinations of the

values of the attributes, the conditional probability of each attribute value, $P(t_n \mid c_j)$, is computed instead based on the 'independence' assumption. Specifically, this means that the occurrence of a particular value of a specific attribute is statistically independent of the occurrence of any other attribute when predicting the Product NE of the fragment. The final probability is the product of the probabilities of all the attribute values in $t = (t_1, t_2 \ldots t_n)$. This conditional probability, $P(c_j \mid e_i)$, called the posterior probability, is then used to predict the Product NE for the next text fragment.

3.3 Software Prototype

To demonstrate the proposed approach, a software prototype was developed. Figure 2 shows the overall architecture of the prototype. It consists of two components: (1) automatic identification; and (2) verification. The first component was programmed using the Perl programming language, and the second component was programmed in Java and Protégé API[2]. The Protégé API was used for loading and displaying the EDIT Product NEs, which are specified in RDFS format. Extract 3 in Section 3.1 is used as an example.

3.3.1 Automatic identification

Step 1: Text Processing

The Text Processing step analyses a text with the following shallow NLP techniques.

1.1 Pre-processing

One paragraph is identified in Extract 3, which is then decomposed into five sentences. The first sentence is:

Largest of the modules, this is an assembly of forward and rear cylindrical casings and the fan outlet guide vane (OGV) ring.

Terms are identified as words lying between two spaces including the full stop.

1.2 Syntactic parse

The Apple Pie Parser [23] is used for a syntactic parse that tags Parts of Speech (POS) and identifies phrases. The Apple Pie Parser refers to the grammars defined in the Penn Treebank to determine the POSs [24]. For example, the first word 'Largest' is tagged as JJS, i.e., a superlative adjective. The remaining POSs for the sentence above are shown below:

POS taggings: *Largest/JJS of/IN the/DT modules/NNS, this/DT is/VB an/DT assembly/NN of/IN forward/JJ and/CC rear/JJ cylindrical/JJ casings/NNS and/CC the/DT fan/NN outlet/NN guide/NN vane/NN (OGV)/NNPX ring/NN.*

Phrase identification groups words grammatically, e.g., into Noun Phrases (NPs) such as {Largest of the modules} and {an assembly of forward and rear cylindrical casings}.

1.3 Lexical look-up

Each POS-tagged word is compared with WordNet definitions to achieve term normalisation. Acronym identification extends an acronym found in a text fragment with its full definition. An example of term normalisation is:

modules → module, casings → casing

and of acronym identification is:

OGV → Outlet Guide Vane.

Step 2: NE Identification

The NE Identification step takes the text fragments processed by Step 1 as an input and applies the Exact and Inexact Rules in turn.

2.1 Exact Rules

If the text fragment is identified as having a pre-defined variation, then the NE is identified and the process for that fragment is complete.

An example of a Product NE identified by the Exact Rules is:

Forward Casings → Front Casing (NE).

2.2 Inexact Rules

A probabilistic matching is required for those fragments that are not covered by the variations and that have multiple occurrences in the variations.

An example of a product NE identified by the Inexact Rules is:

Fan outlet guide vane (OGV) ring
→ Outlet Guide Vane Inner Ring (NE)

[2] http://protege.stanford.edu/doc/pdk/kb-api.html

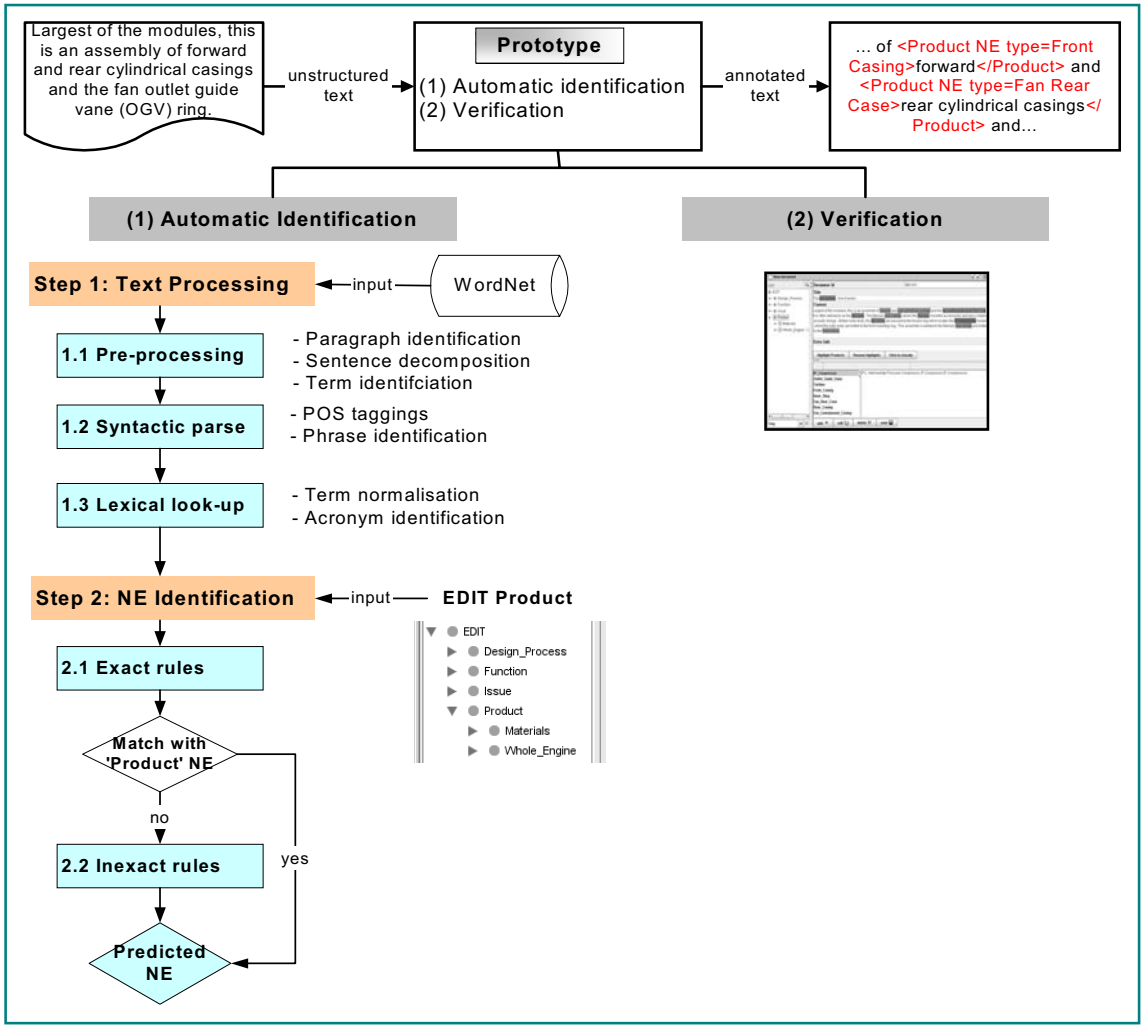

Fig. 2. *Architecture of the software prototype*

The full lists of identified Product NEs for Extract 3 given in Section 3.1 are shown in Figure 1 above.

3.3.2 Verification

A graphical interface has been developed for the prototype software with two specific objectives: (1) to assist the manual annotation process; and (2) to help visualize the results of automatic NE identification. Figure 3 is a screenshot of the interface showing Extract 3 as a sample text.

A user can click the 'Highlight Products' button, and all the text fragments that have been matched with Product NEs, shown as tree view in the left-hand frame, are highlighted in the text frame. Fragments that have the same NEs are shown in the same colour. A lower frame shows a list of the Product NEs that have been identified in the text. By clicking one of these NEs, its position in the tree view is highlighted. The corresponding variations are also shown in the adjacent frame. For NEs that have been incorrectly identified, the user can click the 'edit' button and make corrections. Similarly, missing NEs can be added by pressing the 'add' button. Each time the user presses the 'save' button, the text is identified as a new example and used by the naïve Bayesian approach for training.

4 TESTING THE PROTOTYPE

The prototype was tested to determine if using the probability-based Inexact Rules improved

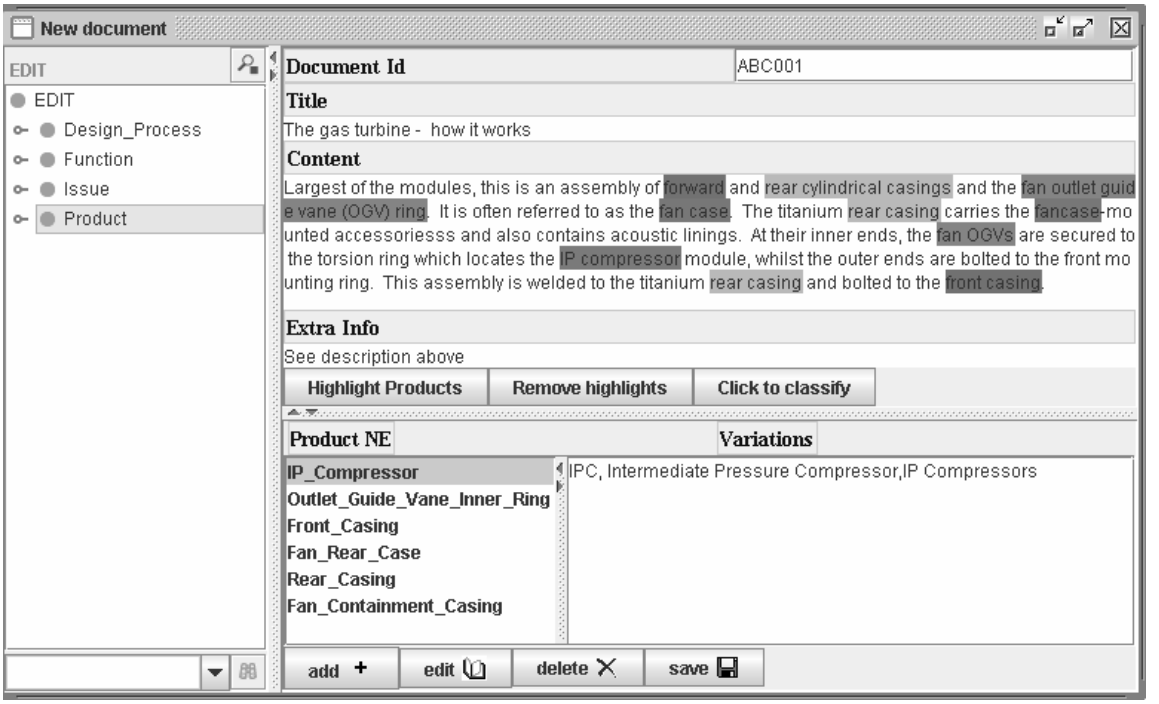

Fig. 3. *An example screenshot of the prototype*

the Product NE extraction over and above that achieved by the Exact Rules. A total of 267 problem reports, including the 137 reports used in Section 4.1, were used for the testing. A total of 977 text fragments were identified with 977 EDIT NEs. EDIT has 220 Product NEs and in the 267 reports 101 of them appeared, i.e., 119 NEs from EDIT did not appear in any of the reports.

From the 977 fragments and their assigned NEs, 50% were randomly selected for training the prototype and the remaining fragments were used for the testing. Precision and recall were used for measuring the prototype's performance. In this paper, recall is defined as the percentage of the test fragments that were matched with EDIT's NEs, whether these were correct or not. Precision is defined as the percentage of the recalled fragments that were correctly matched. Table 3 shows the results of the evaluation.

Overall, the prototype, using both the Exact and Inexact Rules, achieved a good balance of recall and precision, i.e., 80% recall and 81% precision. Using the Exact Rules on their own, the recall was 53% and the precision was 85%. The addition of the Inexact Rules therefore significantly increased the recall while maintaining the precision. The Exact Rules also failed to identify 20 of the 101 EDIT NEs that appeared in the reports. However, it is surprising that the precision achieved by the Exact Rules was not closer to 100%. This means that some of the Exact Rules are, in fact, not 'exact'. The reason is that the empirical evidence, from which the rules were derived, did not cover all the possible variations in EDIT and examples of ambiguity remained. For example, the Exact Rules included 'Stubshaft' as a variation of EDIT's 'Stub Shaft' NE, which is a part of 'Turbine'. However, the 'Stub Shaft' component is also a part of 'Compressor' and this variation was not included in the rules.

Ideally the Inexact Rules should be trained with the minimum number of examples. The effect of changing the number of fragments used for training is shown in Figure 4, where accuracy is defined by the number of correct NE identifications divided by the total number of NEs identified. The 977 fragments were divided into ten equal-sized clusters, each of which was used to estimate the accuracy at that point. For example, when tested with only 100 fragments, the accuracy was observed to be 42%. The maximum accuracy achieved was 84%. It was noticeable for this relatively small total sample size of 977 fragments that the accuracy was relatively constant at around 70% for between 400 and 800 training samples.

Table 3. *NE identification results*

NE Identification	Recall	Precision
Exact Rules only	53%	85%
Exact + Inexact Rules	80%	81%
Change	+27%	–4%

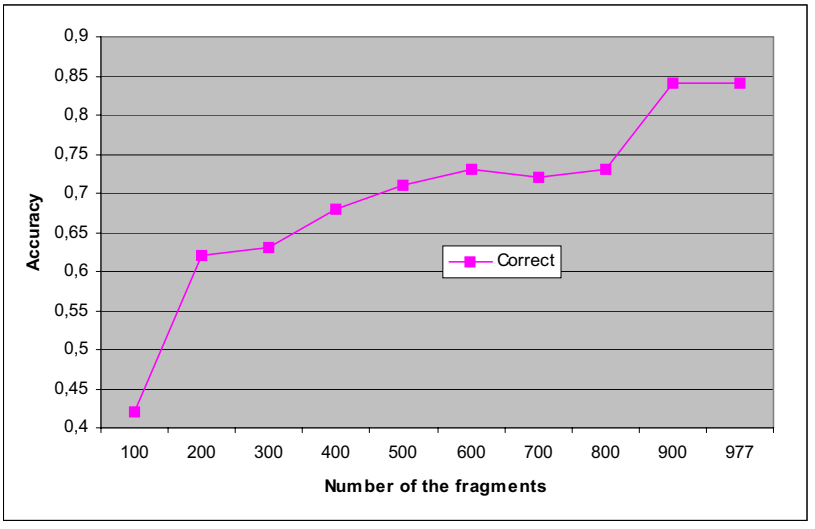

Fig. 4. *Naïve Bayesian predictions estimated for different numbers of NEs*

5 CONCLUSIONS AND FUTURE WORK

It is well established that when engineers need information they tend to ask colleagues in the first instance. However, the industrial world is now more transient and key personnel are retiring and frequently moving, either within their own organisations or to other organisations. It is becoming necessary to retrieve more information from archived documents. There is, therefore, great interest in ways of extracting such information. Information contained in a document is easier to retrieve if domain entities are explicitly tagged with their types so they can be more easily identified using keyword searches.

However, it is particularly difficult to automatically identify engineering entities, i.e., Product NEs, due to the hierarchical and compositional nature of their descriptions. Two IE approaches for achieving this are described in this paper: Exact Rules and Inexact Rules, the latter being based on naïve Bayesian probability. When using the Exact Rules on their own the recall was 53% and the precision was 85%. By adding the Inexact Rules the recall increased significantly to 80% and the precision remained good at 81%. State-of-the-art IE systems are known to demonstrate comparable recall and precision to the proposed approach. However, those systems have mainly been applied to limited types of NEs that do not use a hierarchy to classify them. This research has focused on a wider range of engineering Product NEs that use a hierarchical taxonomy to classify them.

The main contributions of this research are: (1) the observation that Product NEs are more complex than other types of NE; and (2) the development of a probability-based NE identification approach to identify correctly these complex NEs in texts. The improved recall achieved, i.e., from 53% to 80%, is believed to be due to the reliable and robust probability estimates based on how the various combinations of the attributes in a given fragment are related to the correct Product NE.

One of the shortcomings of using a supervised learning approach, e.g., naïve Bayesian probability, is that because it needs examples from which the probability distributions are derived, no predictions can be made for a given NE if that NE

has not appeared in any examples. In current practice, the identification is made incrementally, i.e., with each example the probability distribution is computed and revised, so that the existence of a new example is only recognised manually after the identification is evaluated incorrectly. Since the probability model might need a certain number of examples in order to learn a correct probability distribution, it might take some time to predict a Product NE correctly. This can be improved on by first clustering similar examples into groups without considering the potential NEs. In this way, it is easy to identify the list of Product NEs that might need further examples.

When the hierarchy of the *Product* root concept in EDIT changes, i.e., a new concept is added or an existing one is deleted, the existing probability model has to be revised. In doing so, it is necessary to check whether this change affects the existing model. Currently, the probability model is re-computed when such a change occurs. This can be improved by revising only the part of model where the change needs to be reflected.

Acknowledgements

This research was funded by the University Technology Partnership for Design, which is a collaboration between Rolls-Royce, BAE SYSTEMS and the Universities of Cambridge, Sheffield and Southampton.

6 REFERENCES

[1] Rosner, D., Grote, B., Hartman, K., and Hofling, B., (1998), From natural language documents to sharable product knowledge: a knowledge engineering approach, In Information Technology for Knowledge Management, 8, *Springer*, New York., pp.151-182.

[2] 80-20 software., (2003), 80-20 retriever enterprise edition, http://www.80-20.com/brochures/Personal Email Search Solution.pdf

[3] Marsh, J.R., and Wallace, K., (1997), Observations on the role of design experience, *WDK Annual Workshop*, Switzerland.

[4] Ahmed, S., and Wallace, K. M., (2004), Understanding the knowledge needs of novice designers in the aerospace industry, *Design Studies*, Vol. 25, No. 2, pp. 155-173.

[5] Donnellan, B., and Fitzgerald, B., (2003), A KMS application to support knowledge sharing in a design engineering community, *Proceedings of the Eleventh European Conference on Information Systems*, Italy.

[6] Otto, K., and Abecker, A., (1998), Corporate memories for knowledge management in industrial practice: prospects and challenges, In Information Technology for Knowledge Management, 8, *Springer*, New York, pp. 183-206.

[7] Herlocker, J. L., Konstan, J. A., Borchers, A., and Riedl, J., (1999), An algorithmic framework for performing collaborative filtering, *Proceedings of the 22nd Conference on Research and Development in Information Retrieval*, U.S.A., pp.230-237.

[8] Furnas, G., Landauer, T., Gomez, L., and Dumais, T., (1986), Statistical semantics: analysis of the potential performance of keyword information systems, Bell System, *Technical Journal*, Vol. 62, No. 6, pp.1753-1806.

[9] Gilchrist, A, (2001), Taxonomies for business: knowledge representation, *Proceedings of the 11th Nordic Conference on Information and Documentation*, Iceland

[10] Collier, R., (1996), Automatic template creation for information extraction, an overview, PhD thesis, *University of Sheffield*.

[11] Grishman, R., (1997), Information extraction: techniques and challenges, In *Lecture Notes in Artificial Intelligence*, Vol. 1299.

[12] Kim, S., Lewis, P., Martinez, K., and Goodall, S., (2004), Question answering towards automatic augmentations of ontology instances, *Proceedings of the first European Semantic Web Symposium*, pp. 152-166.

[13] Maedche, A., Neumann, G., and Staab. S., (2002), Bootstrapping an ontology-based information extraction system, *Intelligent Exploration of the Web*, editor (J. Kacprzyk).

[14] Staab, S. Maedche, A., and Handschuh, S., (2003), Creating metadata for the semantic web, an annotation environment and the human factor, *Computer Networks*, Vol. 42, pp.579-598.
[15] Riloff, E., (1993), Automatically constructing a dictionary for information extraction tasks. *Proceedings of the 11th National Conference on Artificial Intelligenc*e (AAAI-93), pp. 811–816.
[16] Mikheev, A., Grover, C., and Moens, M., (1998), Description of the LTG system used for MUC-7, *Proceedings of the Seventh Message Understanding Conference*, Virginia.
[17] Muslea, I., (1999), Extraction patterns for information extraction tasks: a survey, *Proceedings of the AAAI Workshop on Machine Learning for Information Extraction*, Florida.
[18] Ahmed, S., (2005), Encouraging reuse of design knowledge: a method to index knowledge, *Design Studies*, Vol. 26, No. 6, pp.565-592.
[19] Marsh, E., and Perzanowski, D., (1997), MUC-7 evaluation of IE technology: overview of results, *Proceedings of the Seventh Message Understanding Conference*.
[20] Miller, G.A., Beckwith, R.W., Fellbaum, C., Gross, D., and Miller, K., (1993), Introduction to wordnet: An on-line lexical database, *International Journal of Lexicography*, Vol. 3, No. 4, pp.235-312.
[21] Paliouras, G., Karkaletsis, V., Petasis, G., and Spyropoulos, (2004), Learning decision trees for named-entity recognition and classification, *Proceedings on the Workshop on Machine Learning for Information Extraction*, ECAI, Germany.
[22] Mitchell, T., (1997) Machine learning, McGraw Hill.
[23] Sekine, S., and Grishman, R., (2001), A corpus-based probabilistic grammar with only two non-terminals, *Proceedings of the 1st International Workshop on Multimedia annotation*.
[24] Macus, M.P., B. Santorini, M., and Marcinkiewicz, A. M.. (1994) Building a large annotated corpus of English: the penn treebank. *Computational Linguistics* 19 (2), 313-330.

Authors' Addresses:
Dr. Sanghee Kim
Prof. Dr. Ken Wallace
University of Cambridge
Department of Engineering
Trumpington Street
Cambridge, CB2 1PZ, U.K.
shk32@eng.cam.ac.uk
kmw@eng.cam.ac.uk

Prof. Dr. Saeema Ahmed
Technical University of Denmark
Department of Mechanical Engineering
Building 404
DK-2800 Lyngby, Denmark
sah@mek.dtu.dk

Prejeto: 2.5.2007
Received:
Sprejeto: 27.6.2007
Accepted:
Odprto za diskusijo: 1 leto
Open for discussion: 1 year

Strojniški vestnik - Journal of Mechanical Engineering 53(2007)7-8, 442-461
UDK - UDC 658.512.2
Izvirni znanstveni članek - Original scientific paper (1.01)

Konstruiranje izdelka s pomočjo tehnike optimizacije stika

Product Design Using a Contact-Optimization Technique

István Páczelt - Attila Baksa - Tamás Szabó
(University of Miskolc, Hungary)

Znano je, da v inženirski praksi nastajajo velike napetosti zaradi oblik in obremenitev teles v stiku. Porazdelitev napetosti običajno ni enakomerna, singularnosti pa skrajšujejo dobo trajanja strojnih elementov. Zato je pomembno z ustreznim oblikovanjem stikov odpraviti omenjene singularnosti. Eden od ciljev prispevka je predstavitev metode, ki rešuje problem singularnosti v stikih. Z nadzorom dotikalnega tlaka lahko dosežemo enakomerno porazdelitev dotikalnega tlaka. Postopek optimizacije upošteva mejne napetosti materiala. V prispevku obravnavamo dva tipa dotikalnih problemov. Najprej analiziramo dotikalne probleme s predpostavko o linearni elastičnosti in majhnih deformacijah ter ustaljeno obrabo. Dva numerična primera pojasnjujeta ta postopek. Obravnavani so tudi parametri nadzorne funkcije, ki omogoča največjo nosilnost, kar je uporabno za konstruiranje zavor in ležajev. V drugem delu prispevka obravnavamo rešitev dotikalnih problemov za velike pomike in deformacije. Za primer je zračna vzmet, pri kateri primerjamo računske vrednosti krivulje nelinearnega pomika z rezultati meritev.

(Ključne besede: metode končnih elementov, konstriranje izdelkov, optimiranje stika, iteracije)

It is well known that in engineering practice high stresses occur and that these stresses depend on the shapes and the loads of the bodies in unilateral contact. The stress distribution is often not smooth and has some singularities, thereby decreasing the lifetime of the machine elements. It is an important objective to obtain a smooth stress distribution when optimizing the shape of the elements. One of the goals of this paper is to present a method that resolves the above problem. By controlling the contact pressure a prescribed, smooth contact-pressure distribution can be achieved. The optimization problems take into account the limit stress constraints of the material. In the present paper two types of contact problems are investigated. Firstly, contact optimization problems are analyzed assuming linear elasticity and small displacements, including steady-state wear process. Two numerical examples are presented on this topic for a rolling machine element: a punch optimization and a shape optimization. We also investigated which parameter values of the controlling function result in the maximum loadability. This can be useful in the design of brakes or bearings. In the second part of the paper the solution of the contact problem for large displacements and deformations is investigated where an air-spring is analyzed by calculating the nonlinear load-displacement curve and comparing it with measurements.

(Keywords: finite element methods, product design, mechanical contacts, contact optimization, iterative methods)

0 INTRODUCTION

In engineering practice, connections between machine elements are frequently modeled as unilateral contact problems. Comparatively few studies can be found in the literature for contact optimization [1]. Nevertheless, a thorough mathematical investigation of the subject can be found in [2], and in [3] the contact problems of wearing processes are investigated in an analytical way.

The elimination of stress singularities is an important engineering task. In order to overcome this problem, the application of contact-pressure control is recommended, since this ensures a smooth contact-pressure distribution as well as a zero value on the part of the border of the contact zone.

The papers [4] to [6] provide solutions for 2D and 3D problems in which the contact-pressure distribution is partially controlled by minimizing the maximum contact pressure. The authors of [6]

took into account the stress limit in the case of solving contact-optimization problems for axially symmetrical bodies. The equivalent von Mises stress σ_e must be under a prescribed limit (σ_u). The present paper extends the load cases for the examined numerical examples; in addition to the external force load here the kinematical loads can also be applied on the contacting particles. Discretization of the domain with *p*-version finite elements is advantageous [7], since it results in rapid convergence, and high-order mapping ensures an accurate geometry for the shape optimization.

The lifetime of a roller bearing is influenced by many parameters, e.g., the type and the shape of the rollers, the number of rows, the shapes of the tracks of the bearing rings, the bearing dimensions, the materials and their treatment, the quality of manufacturing, etc. A number of papers, e.g., [8] to [13] are devoted to the issue of the roller's rounding-off. In these papers, except the last one, the radius of the rounding-off that results in a generally non-smooth contact pressure distribution is given.

Different rounding-off techniques, e.g., cylindrical or conical rollers, have rounding-off with a given radius at the ends, but it is also possible to make rounding-off a logarithmic function of radius, as published in [14] and [15]. The problem of rounding-off is also analyzed in case of elastohydrodynamic lubrication in [16] and [17]. The question of rounding-off is examined in references [4] and [6] for roller bearings without restrictions for the stress limit. The constraint for the equivalent stress limit is not taken into account in the papers referenced above, but due to the loadability it is required.

In the present paper the equivalent stress limit is considered through the optimization process as a constraint. The optimal shape is achieved by an iteration-based algorithm (see [18]). A numerical example is presented in Section 2.6.

Sub-section 2.3 of this paper deals with the wear problem of the relative sliding of two contacting bodies. The transmittable torque with a clutch and frictional power loss in the case of brakes are important quantities during the design process, and due to wear the shapes of the bodies are changing. There are numerous algorithms to describe the transient wear process ([19] to [21]). These algorithms have huge processing-time requirements. There is also the question of how we can determine the shape of the bodies and the contact pressure distribution in the case of steady-state wear without using the algorithms for a time-dependent wear process. One investigation [18] suggests a technique for the previous problem. The present paper gives a formulation for calculating the wear of disk brakes in steady-state based on the modified Archard law.

Recently, the classical springs used in vehicles for suspension have been replaced by air-springs. The advantage of an air-spring compared to a classical spring is its nonlinear behavior, which can be controlled by the inflation pressure. In addition to the force displacements of the diagram, the designer is interested in determining the stresses and strains in the reinforcing fibers. Accurate results can be obtained by a *p*-extension of the finite-element method, but its application for problems with large displacements requires much more work. Therefore, a simplification is performed, i.e., the contacting element sides are kept in a straight line, which made it possible to use the algorithm given by Crisfield [22] for the *h*-extension elements. A numerical example is presented in Section 4 to demonstrate the working process of an air-spring.

1 TREATMENT OF THE CONTACT

Without the restriction of generality let us consider the contact problem of two elastic bodies ($\alpha = 1, 2$). The surfaces of the bodies are separated into three regions: S_u^α denotes the part of the body where displacements $\boldsymbol{u}_0$ are given, in S_t^α the traction $\boldsymbol{t}_0$ is applied, while S_c^α represents the part of the bodies where the contact is expected. The S_c^α part of the body is called the proposed zone of the contact. The bodies are loaded with the body force $\boldsymbol{b}^\alpha$. We are interested in finding the displacement vector field $\boldsymbol{u}^\alpha$, the strain $\mathbf{A}^\alpha$ and stress $\mathbf{T}^\alpha$ tensor fields.

1.1 Contact kinematics

The contacting surfaces are described in parametric form (see [23]): The contacting surface of the body labeled $\alpha = 1$ (or $\alpha = 2$) is written in terms of the parameters ($\xi = (\xi^1, \xi^2)$) (or $\eta = (\eta_1, \eta_2)$). In the implementation the parameters will be associated with the element surfaces using optimal approximations based on the Babuška points.

Let $\mathbf{X}^1(\xi)$ and $\mathbf{X}^2(\xi)$ represent the possible contact points of bodies 1 and 2, respectively, in

the reference coordinate system. The position vectors of these points at time t can be written in terms of the displacement $\mathbf{u}^1(\xi,t)$ for body 1:

$$\mathbf{x}^1 = \mathbf{x}^1(\xi,t) = \mathbf{X}^1(\xi) + \mathbf{u}^1(\xi,t) \qquad (1)$$

and similarly for body 2:

$$\mathbf{x}^2 = \mathbf{x}^2(\eta,t) = \mathbf{X}^2(\xi) + \mathbf{u}^2(\eta,t) \qquad (2),$$

where $\mathbf{u}^2(\eta,t)$ is the displacement function of body 2. Therefore, the gap between the two bodies is given by:

$$\left(\mathbf{x}^2 - \mathbf{x}^1\right)\cdot\mathbf{n}_c \geq 0 \qquad (3),$$

where $\mathbf{n}_c$ is normal to body 1 at point $\mathbf{x}^1$ and intersects body 2 at point $\mathbf{x}^2$. The minimum distance between a fixed point of body 2 corresponding to parameter η and body 1 is given by

$$\left|\mathbf{x}^2(\eta,t) - \mathbf{x}^1(\bar{\xi},t)\right| = \min_{\xi}\left|\mathbf{x}^2(\eta,t) - \mathbf{x}^1(\xi,t)\right| \quad (4).$$

The points corresponding to body 1 that satisfy Equation will be identified by an overbar in the following: $\bar{\mathbf{x}}^1 = \mathbf{x}^1(\bar{\xi},t)$ and the corresponding normal will be denoted by $\bar{\mathbf{n}}_c$, see Figure 1.

The inequality constraint of the non-penetration condition is defined as:

$$d = \left(\mathbf{x}^2 - \bar{\mathbf{x}}^1\right)\cdot\mathbf{n}_c \geq 0 \qquad (5)$$

and the penetration function for the penalty method is written as:

$$d^- = \begin{cases} \left(\mathbf{x}^2 - \bar{\mathbf{x}}^1\right)\cdot\mathbf{n}_c & \text{if } \left(\mathbf{x}^2 - \bar{\mathbf{x}}^1\right)\cdot\mathbf{n}_c < 0 \\ 0 & \text{otherwise} \end{cases} \qquad (6).$$

1.2 Contact conditions

The normal stress along the surface $S_c^\alpha = \Omega$ is $\sigma_n^\alpha = \mathbf{n}^\alpha \cdot \mathbf{T}^\alpha \cdot \mathbf{n}^\alpha$, where $\mathbf{n}^\alpha$ is the outer normal of the body α, $\mathbf{T}^\alpha$ is the stress tensor and ' · ' means the scalar product. For small displacements after the deformation the gap can be calculated as $d = u_n^2 - u_n^1 + g$, where $u_n^\alpha = \mathbf{u}^\alpha \cdot \mathbf{n}_c$ and g is the initial gap. By introducing the notation of contact pressure $p_n = -\sigma_n^1 = -\sigma_n^2$ there is contact if $d = 0, p_n \geq 0, \mathrm{x} \in \Omega_p$ and there is gap if $d > 0, p_n = 0, \mathrm{x} \in \Omega_0$, i.e. $p_n \cdot d = 0, \mathrm{x} \in \Omega = \Omega_p \cup \Omega_0$.

Coulomb dry-friction models are examined henceforth. The boundary value problem is solved by variational principles using a modified complementary energy and the total potential energy with an augmented Lagrangian technique ([4] and [23]).

1.2.1 Control of the contact pressure

The resulting contact stress distribution and, therefore, the contact pressure, are mainly influenced by the shape of the bodies that are in contact, and the initial distance between them. The aim is to ensure the contact of the bodies on a sub-

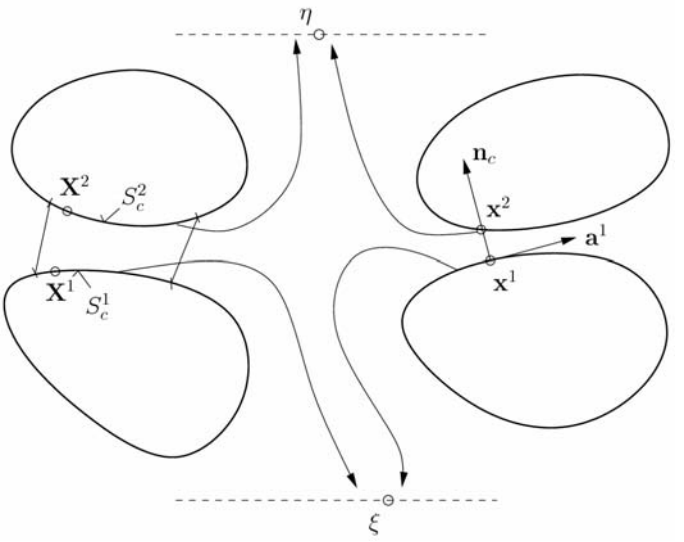

Fig. 1. *Notation*

domain, indicated by Ω_c (here is only a line), and on that contact surface the pressure varies as a prescribed function. This is achieved by the modification of the shape of the contacting parts. The rest of the supposed contact domain $S_c = \Omega$, which is Ω_{nc} where the pressure distribution is not known, but it must be less than a prescribed function.

In our optimization problems it is supposed that the bodies are in contact on the whole sub-domain Ω_c of the contact zone $S_c = \Omega$. The contact surface is modified in a way that the following function holds true for the contact pressure

$$p_n(\mathbf{x}) = v(\mathbf{x})\, p_{\max},\ \mathbf{x} \in \Omega_c = [s, t = 0] \quad (7),$$

where the chosen control function must satisfy the condition $0 \le v(\mathrm{x}) \le 1$, and

$$p_{\max} = \max p_n(\mathbf{x}),\ \mathbf{x} = [s,t] \qquad (8),$$

where s and t are surface coordinates in the region Ω_c. In the sub-domain $\Omega_{nc} = (\Omega = \Omega_c \cup \Omega_{nc})$ the fulfillment of the following inequality is required

$$\chi(\mathbf{x}) = v(\mathbf{x})\, p_{\max} - p_n(\mathbf{x}) \ge 0,\ \mathbf{x} \in \Omega_{nc} \quad (9).$$

The definition of the control function is arbitrary. In order to avoid the singularities in the stress distribution practically, it is defined in such a way that not only the value of the function must be zero at the end of the control zone but also the first derivative in a sort of direction as well.

Therefore, let us define a function $v(s)$ of class C^1 in the sub-region Ω_c (see Figure 1). The normal shape variation is assumed to be specified by a function $v(s)$ of class C^1 in the sub-region Ω_c We introduce the functions depending on the coordinate s:

$$V^*(s) = f_2 + (f_3 - f_2)\frac{s - L_2}{L_3 - L_2}$$
$$f_2 \ge 0,\ f_3 \ge 0 \qquad (10)$$

and

$$\begin{aligned}
&V(s) = 0, \\
&V(s) = V^*(s)\left\{3\left(\frac{s-L_1}{L_2-L_1}\right)^2 - 2\left(\frac{s-L_1}{L_2-L_1}\right)^3\right\}, \\
&V(s) = V^*(s), \\
&V(s) = V^*(s)\left\{1 - 3\left(\frac{s-L_3}{L_4-L_3}\right)^2 + 2\left(\frac{s-L_3}{L_4-L_3}\right)^3\right\} \\
&V(s) = 0,
\end{aligned} \qquad (11),$$

where some of the parameters f_2, f_3, L_i, $I = 1,\ldots,4$ are fixed, while the others are specified in the optimization process. For 2D problems it is assumed that $v(s) = V(s)$. Since $\left.\frac{\partial V(s)}{\partial s}\right|_{s=L_1,L_4} = 0$ holds true, at these points the pressure is zero and their derivatives also vanish, so there are no singular

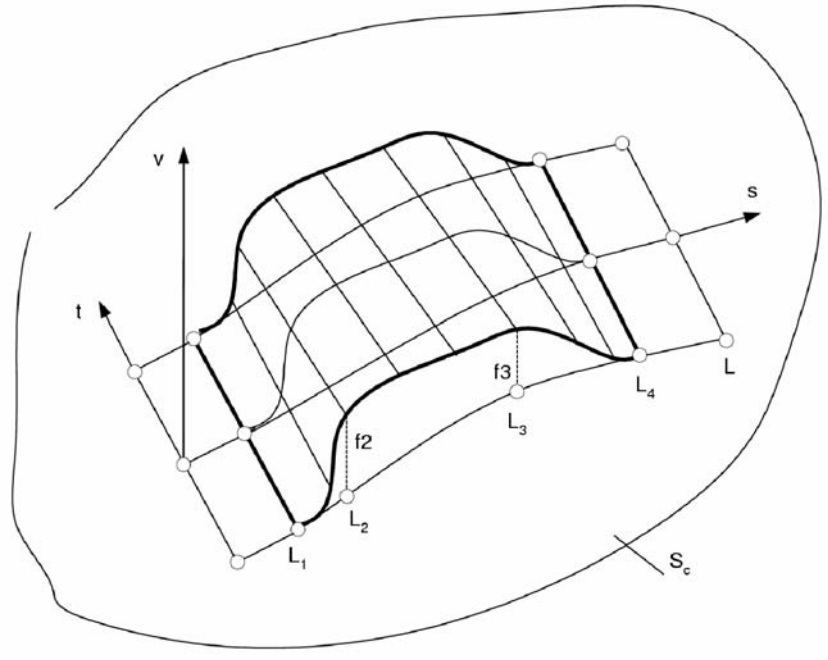

Fig. 2. *Control function*

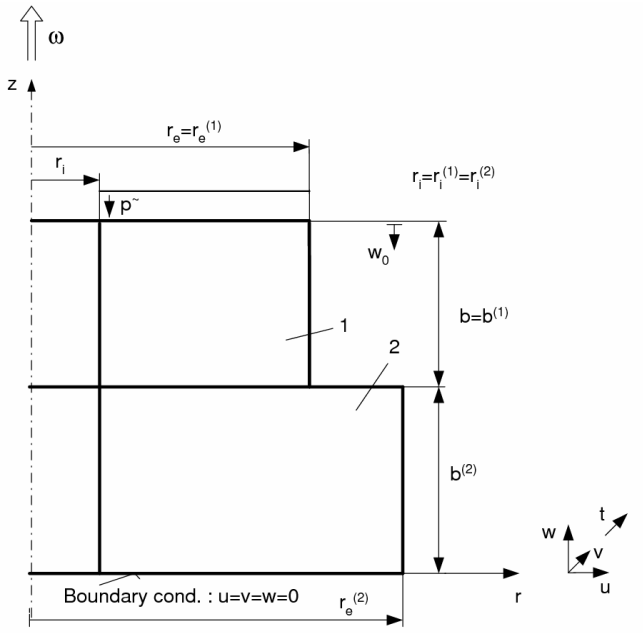

Fig. 3. *The geometry of the punch problems*

values in the stress distribution. In the 3D problems in paper [24] it is supposed that the upper body has a rigid translation and rotation, Ω_c is a line s, and the rotation vector is perpendicular to this line. The control function along direction t is $\tilde{v}(t) = 1$, i.e.

$$v(x) = V(s)\tilde{v}(t) \qquad (12).$$

2 SHAPE OPTIMIZATION FOR SMALL DISPLACEMENTS

2.1 Punch problems

Axially symmetrical machine elements are applied in many industrial constructions. The force distribution between the bodies gives a strong influence on the stress state of the construction. A designer always endeavors to avoid singularities within the contact region in order to keep stresses at a lower level. If the control pressure function is used, the contact stress can be easily achieved without a stress singularity.

In our investigation the same examples are given for different object functions with the control of the contact pressure distribution. The geometry of the punch construction is shown in Figure 3.

In [6] a couple of contact-optimization problems can be found for punches. Here, some new, additional optimization problems are formulated.

2.2 Additional optimization problems

In engineering practice rotating particles usually transmit torque. The torque is defined as:

$$M_T = \mu \int_{r_i}^{r_e} 2\pi r^2 p_n \, dr \qquad (13),$$

where μ is the coefficient of friction.

Let us denote the angular punch velocity by ω and specify the dissipation power due to frictional sliding at the contact surface by:

$$D_F = \int_{S_c} \boldsymbol{\tau}_n \cdot \dot{\mathbf{u}}_\tau = \omega\mu \int_{r_i}^{r_e} 2\pi r^2 p_n \, dr = M_T \omega \qquad (14).$$

Assume now that the punch rotates with respect to its axis with the angular velocity ω, and the uniform vertical displacement w_0 is prescribed on the top surface of the punch.

Consider the problem of torque maximization, assuming the parameters L_1 and L_2 are unspecified and L_3, L_4 and $L_2 - L_1$ are fixed. Maximize the torque M_T by determining the initial gap function $g = g(s)$, so that $g(s_*) = g_{\min} = 0$, where $s = r - r_i$ and r_i is the internal punch radius, thus the optimization problem is

PP1 :

$$\max_{g(s),L_1} \left\{ M_T \,\middle|\, p_n \geq 0,\ d = 0,\ g_{\min} = 0,\ \chi = \chi(s, p_n, L_1) = 0, \sigma_e \leq \sigma_u \right\} \qquad (15).$$

In order to minimize the dissipation power or torque, assume that $L_1 = 0$, $L_2 = 0$ and $L_4 - L_3$ are fixed; however, L_4 and L_3 may vary. The optimization problem is now formulated as follows **PP2** :

$$\min_{g(s),\, L_4} \left\{ D_F \,\middle|\, p_n \geq 0,\ d = 0,\, g_{\min} = 0,\ \chi = \chi(s, p_n, L_4) = 0,\ \sigma_e \leq \sigma_u \right\} \quad (16).$$

Using the optimization problems **PP1** and **PP2** different initial shapes of the punch surface are obtained.

2.3 Investigation of the wear process

Sliding particles that are in contact are continuously losing some material, i.e., wear occurs. Practically, it is important to know the rate of wear and the contact-pressure distribution during the wear process. When steady-state occurs during operation the information about the shape of the bodies and the stress distribution between them is significant.

Firstly, let us formulate the problem of the minimization of the wear volume rate at the contact interface. Assuming the specific wear rate $\dot{w}$ to be dependent on contact pressure, the relative slip velocity $v_r = \|\mathbf{u}_\tau\|$ and the contact shear stress $\tau_n = \|\boldsymbol{\tau}_n\|$, i.e. $\dot{w} = \dot{w}(p_n, \|\mathbf{u}_\tau\|, \|\boldsymbol{\tau}_n\|)$, the total wear volume rate is:

$$\dot{W} = \int_{S_c} \dot{w}\, dS \quad (17)$$

and the wear dissipation power at the contact surface S_c is equal to:

$$D_w = \int_{S_c} p_n \dot{w}\, dS \quad (18).$$

The optimization problem can now be formulated as follows. Assume that the punch rotates with respect to its axis with the angular velocity ω, and the uniform vertical traction $\sigma_z = -\tilde{p}$ is exerted on its top boundary with the resulting force $F_0 = \pi\left(r_e^2 - r_i^2\right)\tilde{p}$. Then the gap function must be determined in order to minimize $\dot{W}$ or D_w, thus

PP3 :

$$\min\left\{ \dot{W}, D_w \,\middle|\, \begin{array}{l} p_n \geq 0, \\ d = 0,\, F_p - F_0 = 0, \\ \chi = \chi(s, p_n, L_4) = 0,\, g_{\min} = 0 \end{array} \right\} \quad (19),$$

where $F_p = 2\pi \int_{r_i}^{r_e} p_n r\, dr$ is the contact force.

Assume that the wear rule satisfies the modified Archard law [25]:

$$\dot{w} = \beta\left(\mu\, p_n\right)^b v_r^a = \beta\, \mu^b\, p_n^b\, v_r^a = \tilde{\beta}\, p_n^b\, v_r^a \quad (20),$$

where a, b, β are the wear parameters, μ is the friction coefficient, p_n is the contact pressure, $\tilde{\beta} = \beta\mu^b$, and the relative velocity is $\|\mathbf{u}_\tau\| = v_r = r\omega$. The shearing stress in the contact surface τ_n calculated from the contact pressure by the Coulomb dry friction law is $\tau_n = \mu\, p_n$.

In [18] it is demonstrated that the wear dissipation power at the contact surface is minimal in the steady state of the wear process and corresponds to the uniform wear rate. However, the minimization of the wear volume rate and the friction dissipation power is not suitable for describing the steady-state wear process.

Using the minimum of the wear dissipation power the contact pressure is:

$$p_n = \frac{F_0}{I_{D_w}} r^{-\frac{a}{b}}, \text{ where } I_{D_w} = 2\pi \int_{r_i}^{r_e} r^{1-\frac{a}{b}}\, dr \quad (21).$$

The wear rate is uniform along the radius

$$\dot{w} = \left(\frac{F_0}{I_{D_w}}\right)^b \tilde{\beta}\, \omega^a = const \quad (22).$$

The wear volume rate is

$$\dot{W} = \int \dot{w}\, dS = 2\pi \int_{r_i}^{r_e} \tilde{\beta}\, \omega^a \left(\frac{F_0}{I_{D_w}}\right)^b r\, dr = \tilde{\beta}\, \omega^a \left(\frac{F_0}{I_{D_w}}\right)^b S_c = \dot{W}_{D_w} \quad (23).$$

When the upper body, e.g., a disc brake of a vehicle, is a segment of a rotationally symmetrical body with angle Φ, then Equations to remain valid, replacing I_{D_w} with $I_{D_w}^{(\Phi)}$:

$$I_{D_w}^{(\Phi)} = \Phi \int_{r_i}^{r_e} r^{1-\frac{a}{b}}\, dr \quad (24).$$

PP4 : Here the optimization problem is the following:

$$\min\left\{ D_w \,\middle|\, p_n \geq 0,\ d = 0,\, F_p - F_0 = 0,\ \chi = \chi(r, p_n) = \frac{F_0}{I_{D_w}^{(\Phi)}} r^{-\frac{a}{b}} - p_n = 0,\ g_{\min} = 0 \right\} \quad (25)$$

from which the shape of the bodies belonging to the steady state can be determined.

The importance of these results is that the shape of the contacting bodies and the contact pressure after wear are determined in the case of steady-state processes without solving the time-dependent wear problem.

2.4 Solution of the optimization problems PP1 – PP4

After the discretization of the optimization problem a non-linear programming problem evolves, which is solved by a special iteration process. We distinguish two types of iterations. In the first one, which was introduced in [4], the optimal shape is determined with the prescribed control parameters f_2, f_3, L_i, $i = 1,\ldots4$. The second type of iteration is an extension of the first one, with the stress constraint prescribed for the von Mises equivalent stress σ_e, $\sigma_e \le \sigma_u$, where σ_u is the ultimate stress [6].

When the stress constraint $\max \sigma_e \le \sigma_u$ is imposed at any Lobato integration points the values of the parameters assumed as fixed or specified in the first type iteration, should be updated in order to satisfy the stress constraint. Denote collectively the parameter that should be updated in the second type of iteration by f.

The "loading" process is characterized by the variable i_{step}. The value of f is calculated using the following formulae:

$$f = f_0 + \Delta f\,(istep + 1) \qquad (26),$$

where f_0 and Δf are chosen in advance. For instance, for the Problem **PP1** $f = L_1, f_0 = r_i$, and $\Delta f = 0.1\cdot(r_e - r_i)$. The optimization problem is solved by the first type of iteration at the fixed f. At each i_{step} a new shape is determined for the upper body.

The effective stress value σ_e is calculated at the Lobato integration points of the finite quadratic elements. We assume that for the value $f = f^*$ the effective stress is $\sigma_e^* < \sigma_u$ and at the next loading i_{step} the parameter $f = f^{**}$ and the effective stress exceeds the ultimate value $\sigma_e^{**} > \sigma_u$.

The optimal value of $f = f^{\text{opt}(i)}$ is searched for in the interval $f^* < f^{\text{opt}(i)} < f^{**}$ using the following linearization process:

$$f^{\text{opt}(i)} = f^* + \left(f^{**(i-1)} - f^*\right)\frac{\sigma_u - \sigma_e^*}{\sigma_e^{**(i-1)} - \sigma_e^*}, \qquad (27),$$

where $f^{**(0)} = f^{**}$, $\sigma_e^{**(0)} = \sigma_e^{**}$. At each step of the second type of iteration the contact shape is specified in the first iteration-based process. The second type of iteration proceeds until

$$\frac{\left|\sigma_u - \sigma_e^{**(i)}\right|}{\sigma_u} \le 0.01 \qquad (28).$$

2.5 Example for PP1

The following material parameters are assumed: Young's modulus $E = 2\cdot10^5$ MPa, Poisson's ratio $\nu = 0.3$, ultimate stress $\sigma_u = 250$ MPa and friction coefficient $\mu = 0.25$.

The geometrical parameters are defined as $r_i^{(1)} = r_i^{(2)} = r_i = 20\,mm$, $r_e^{(1)} = 120\,mm$, $r_e^{(2)} = 140\,mm$, $b^{(1)} = b^{(2)} = b = 50$ mm (see Figure 3). The boundary conditions are prescribed as follows: the cylindrical surfaces $r = r_i$ and $r = r_e^{(\alpha)}$ are traction free $\mathbf{t}_0^{(\alpha)} = \mathbf{0}$, the bottom surface $z = 0$ of the body B_2 is constrained, $u = v = w = 0$ and at the upper surface $z = 2b$ of punch B_1 is loaded by the axial displacement w_0 and is subjected to the rotational motion $v = r\omega t$.

The value of w_0, which is the prescribed displacement of the upper body, is determined in order to achieve the same specific strain in the cylindrical bodies with the height of $b^{(1)} + b^{(2)}$. It means that:

$$\frac{100\,w_0}{b^{(1)} + b^{(2)}} = 0.1\%.$$

If the radius of the cylindrical bodies is the same and the Young's modulus $E = 2\cdot10^5$ MPa then this specific strain will produce a 200 MPa compressive stress. Since the outer radius of the lower body is greater than the upper body's, i.e., $r_e^{(2)} = 140\,mm > r_e^{(1)}$, the stress distribution shows a singularity in the $(r_e^{(1)}, b^{(2)})$ position. The aim of the optimization is to avoid this singularity, which can be achieved by using the C^1 continuous control function defined by (10) to (12).

Using the iteration defined under Section 2.4 the problem **PP1** is solved and the results of these solutions are summarized in Table 1. The results are calculated for different values of $b = b^{(1)} = b^{(2)}$.

In order to obtain very accurate results a graded mesh in geometric progression is applied along the direction z with the common factor 0.15 [7]. In direction r, both sides of the contact bordering small elements are given with the size $L_2 - L_1$. Due to re-meshing, the oscillation of stresses does not occur. The polynomial order of the finite elements is $p = 8$.

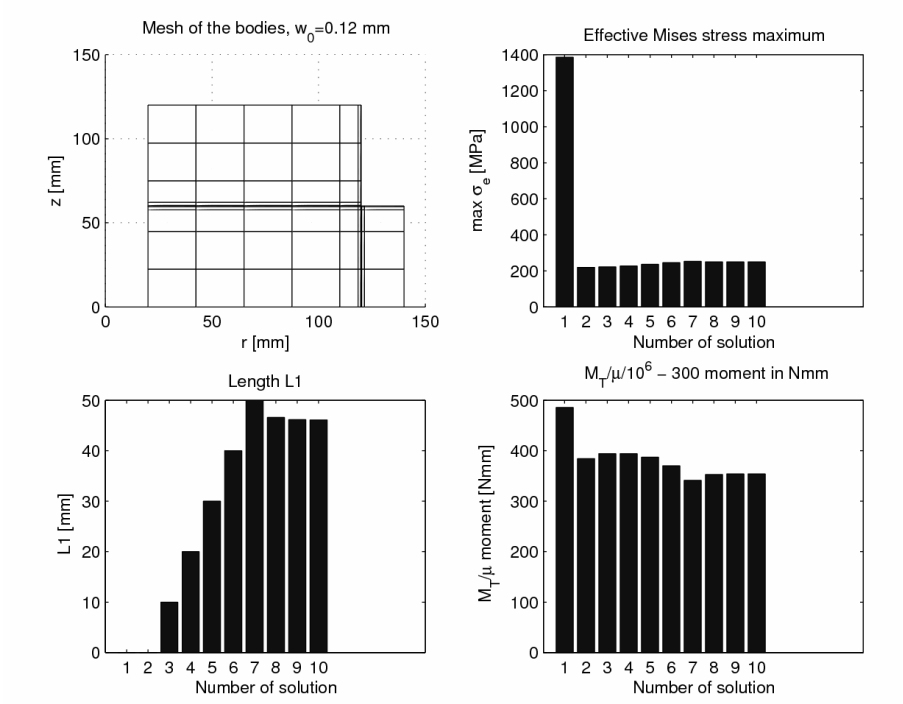

Fig. 4. *Numerical results of PP1 optimization with A geometry*

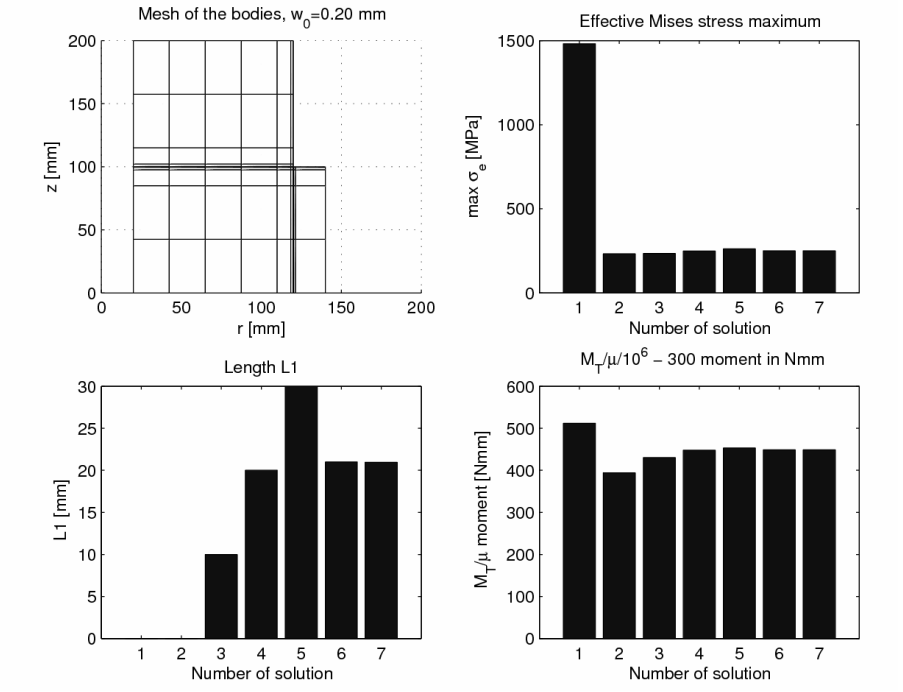

Fig. 5. *Numerical results of PP1 optimization with B geometry*

From Table 1 it is clear that for lower values of b and w_0 in case of max M_T the maximum of the equivalent stress is lower than the ultimate stress, i.e., $\sigma_{emax} < \sigma_u$ and the condition $\sigma_{emax} = \sigma_u$ is ensured only by increasing the distance L_1, but it results in a lower torque between the contacting bodies.

It is also obvious that for the original construction (without optimization) the σ_{emax} is substantially over the allowed value of σ_u, which means, in practice, the yielding of the material.

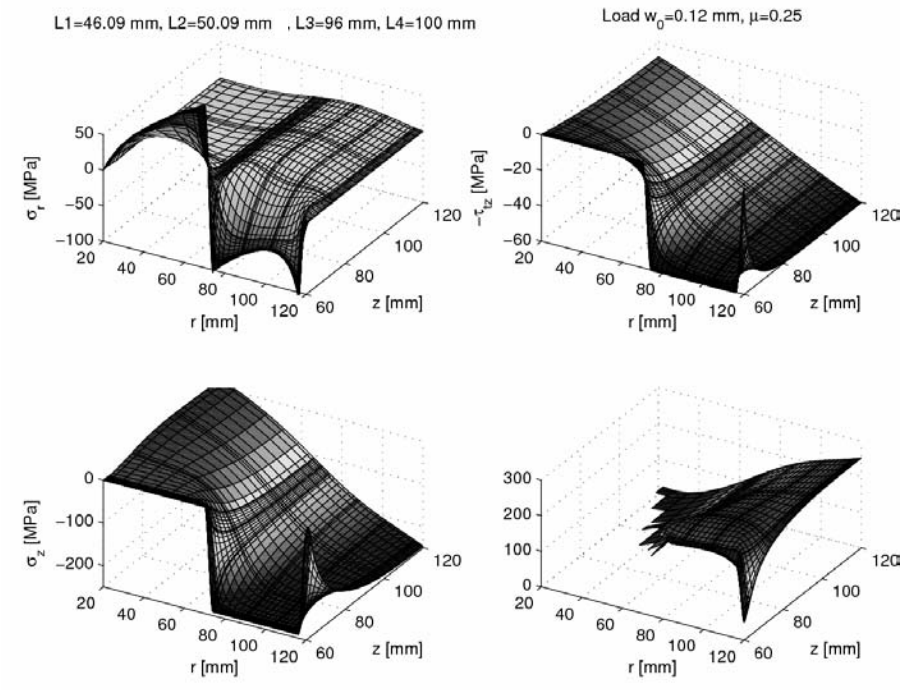

Fig. 6. *Stress distribution of PP1 optimization for the A geometry*

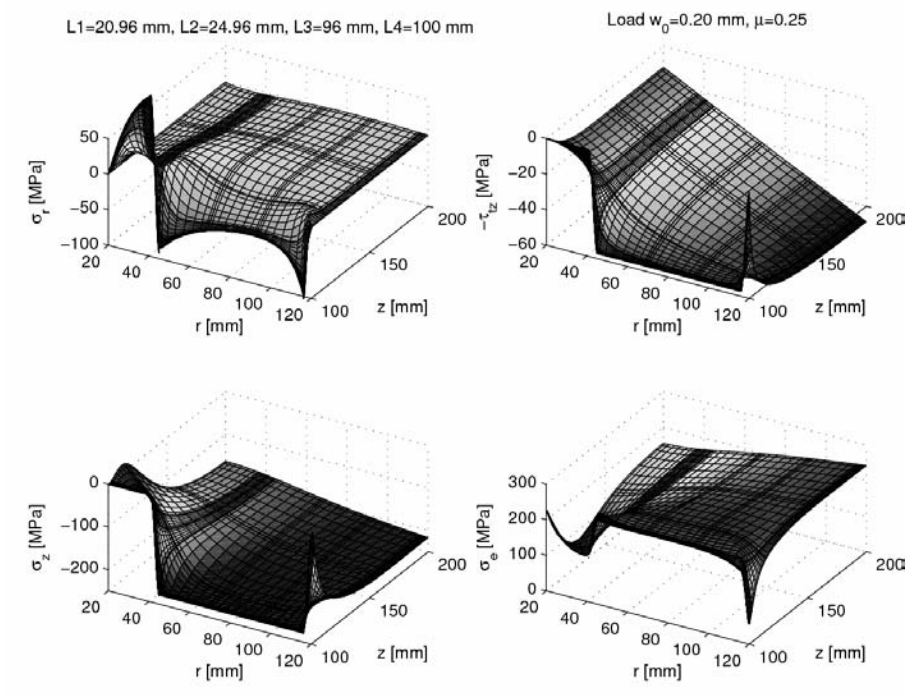

Fig. 7. *Stress distribution of PP1 optimization for the B geometry*

In Figures 4 and 5 the finite-element mesh and the values of L_1 and M_T/μ during the iteration are illustrated. The resulting stress states are shown in Figures 6 and 7, with σ_r as the radial stress; τ_{tz} as the tangential shear stress, σ_z as the normal stress and σ_e as the equivalent stress (Mises type). The tangential stress onto the lower surface of the upper body is defined as $|\tau_{tz}| = \mu |\sigma_z|$, according to Coulomb's law of dry friction. The top surface of the upper body has a rigid-body-like displacement.

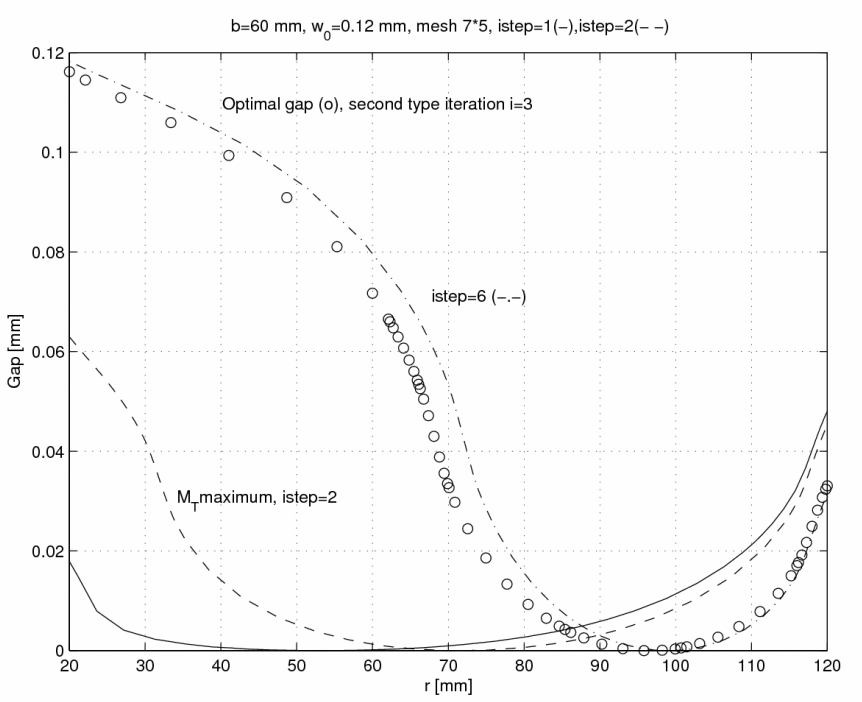

Fig. 8. *Gap (shape) evolution for the A geometry*

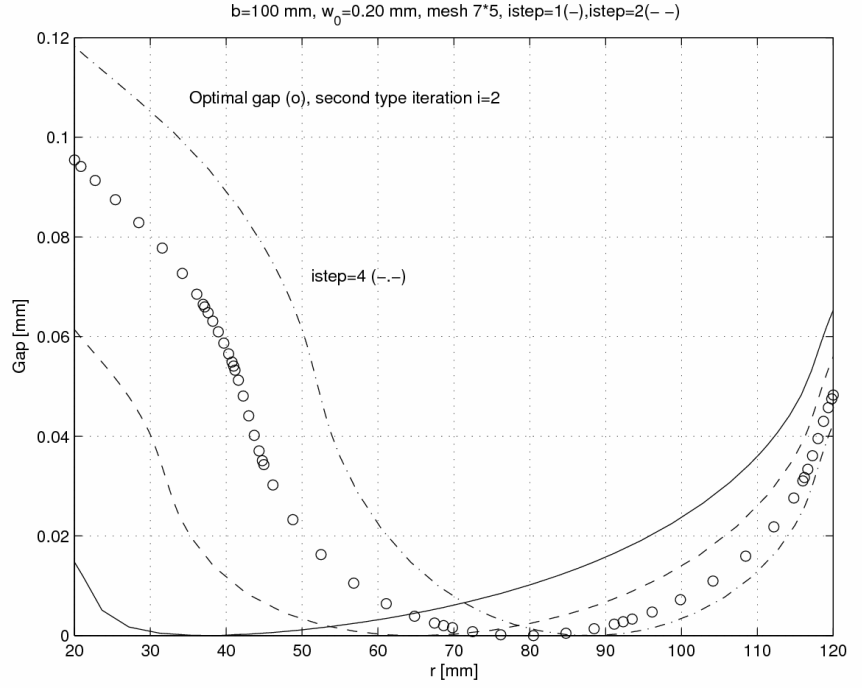

Fig. 9. *Gap (shape) evolution for the B geometry*

Increasing the value of *b* on the top surface, using St. Venant's theory, there is a linear distribution in the radial direction.

The optimal shapes of the lower edge of the upper body are drawn in Figures 8 and 9. This shape represents the initial gap function between the contacting bodies. The definition of `istep` = $i_{\texttt{step}}$ can be found in Section 2.4. The curve designated by *o* belongs to the solution that is fulfilled by the additional condition $\sigma_{e\max} = \sigma_u$. The labels `istep`

Table 1. *Numerical results of the optimization problem* **PP1**

		Original Const.	By Maximum M_T			$\sigma_{e\max} = \sigma_u = 250$ MPa	
b	w_0	$\sigma_{e\max}$ [MPa]	L_1 [mm]	M_T [mm]$\cdot 10^{-9}$	$\sigma_{e\max}$	L_1 [mm]	M_T [mm]$\cdot 10^{-9}$
50	0.10	1340.2	10	0.6941	222.27	56.82	0.5930
60	0.12	1386.3	10	0.7046	221.53	46.09	0.6629
70	0.14	1420.4	20	0.7209	234.76	38.74	0.7048
80	0.16	1446.3	20	0.7354	239.58	33.88	0.7317
90	0.18	1466.4	–	–	–	25.66	0.7510
100	0.20	1482.1	–	–	–	20.96	0.7599
120	0.24	1503.8	–	–	–	16.46	0.7707
140	0.28	1516.9	–	–	–	14.11	0.7791

= 6 and `istep` = 4 indicate that the stage in the iteration-based process belongs to $\sigma_e^{**} > \sigma_u$ (see Section 2.4). To resemble Figures 8 and 9 it is clear that a little change in the gap generates a notable difference in $\sigma_{e\max}$, which reminds one of the importance of accurate manufacturing.

2.6 Optimal shape design of the rollers

Rolling elements can be found in many types of engineering equipment. Their requirement for a long lifetime means keeping the stresses smooth and at a low value.

The roller is loaded by the force F_0, which gives a resultant vector couple: the resultant force F_0 and torque M_0. The geometry and the load of a roller can be found in Figure 10. On the surface of the half-space $z = 0$ and the rectangular contact region ($S_{ct} \times S_{cs}$) is divided into small rectangles ($D_t \times D_s$). Elements of the influence matrix are computed by applying the unit-intensity normal load or the tangential load in direction t in the sub-region ($D_t \times D_s$). The formulae can be found in [27]. In order to eliminate shearing stresses at the ends of the roller the mirror technique is taken into account.

For the case when the load is not applied to the center of the roller two types of problems were investigated in an earlier investigation [13].

In this study we analyzed the case when the stress constraint is taken into account in the optimization process.

Examples. The radius of the roller is R_0 = 60 mm. The roller is subjected to loads of $F_0 = 5000$ N in the middle. The proposed contact region (1 × 35 mm) is divided into $kt \cdot ks = 40 \times 100$ rectangular elements along the directions t and s. The parameters of the control function are $L_1 = 0$, $L_2 = 5$ mm, $L_4 - L_3 = 5$ mm, $L_4 = 35$ mm, $f_2 = f_3 = 0$.

The von Mises equivalent stress is calculated in the lower body at the coordinates $s = (is - 1)\cdot D_s$, $t = (it - 1)\cdot D_t$, $z = -(is - 1)\cdot D_z$, where $is = 1,\ldots,ks + 1$; $it = 1,\ldots,kt + 1$; $iz = 1,\ldots, 10$, $D_z = 0.025$ mm.

The following material parameters are assumed: Young's modulus $E = 2\cdot 10^5$ MPa, Poisson's ratio $\nu = 0.3$, ultimate stress $\sigma_u = 250$ MPa. The equations of the equilibrium related to the roller are:

$$\mathbf{f} = \mathbf{f}_0 - \int_\Omega \mathbf{p}\, dS = 0$$
$$\mathbf{m} = \mathbf{m}_0 - \int_\Omega \mathbf{r} \times \mathbf{p}\, dS = \mathbf{0} \qquad (29),$$

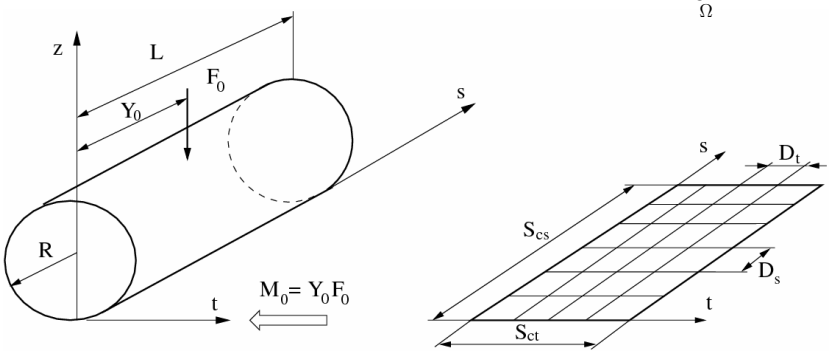

Fig. 10. *The roller's load and geometrical properties*

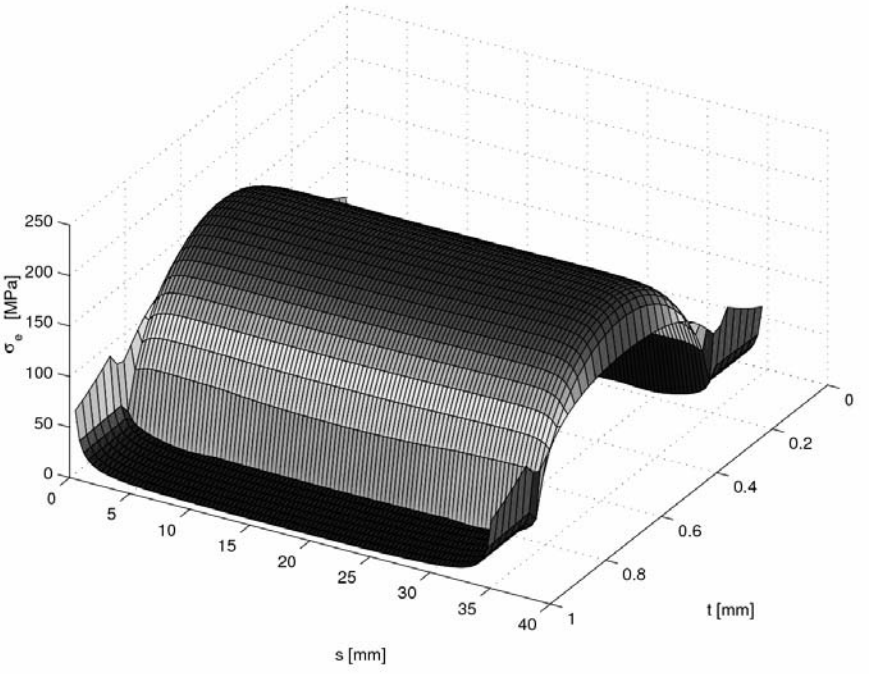

Fig. 11. *Equivalent stress distribution at z = 0 mm*

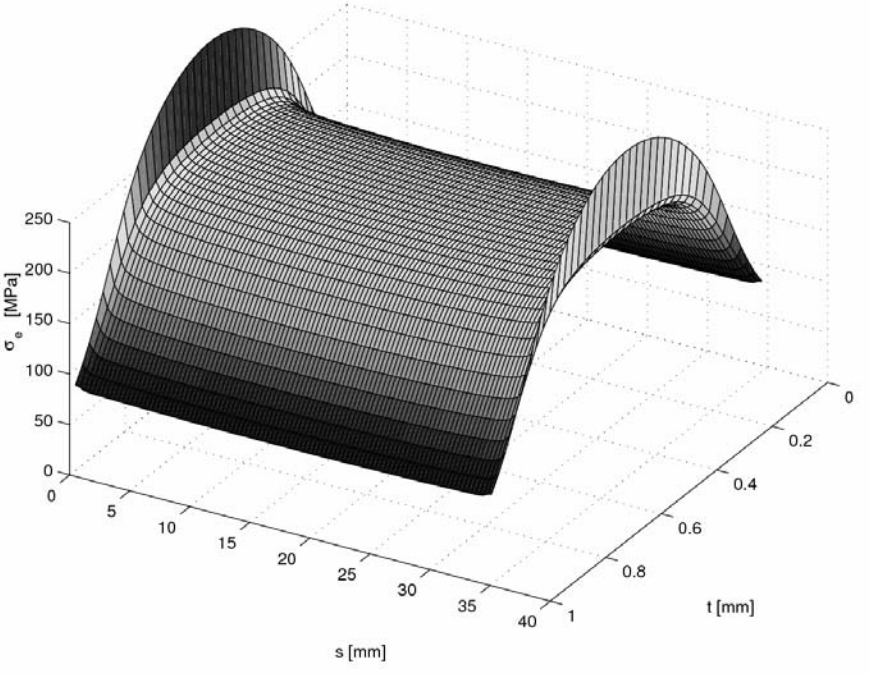

Fig. 12. *Equivalent stress distribution at z = 0.15 mm*

where **r** is the position vector, **p** is the vector of contact stress, $\mathbf{f}_0$ is the resultant force and $\mathbf{m}_0$ is the moment of the external load.

The distributions of the equivalent stress σ_e at $z = 0$ and its maximum value are found at $z = -0.15$ mm, as shown in Figures 11 and 12.

In the optimization process the lengths L_2 and L_3 are calculated because the control function is symmetrical, i.e., $\Delta L = L_2 - L_1 = L_4 - L_3$, and $L_1 = 0$, $L_4 = S_{cs} = 35$ mm. The control function is calculated using Equations (10) to (12).

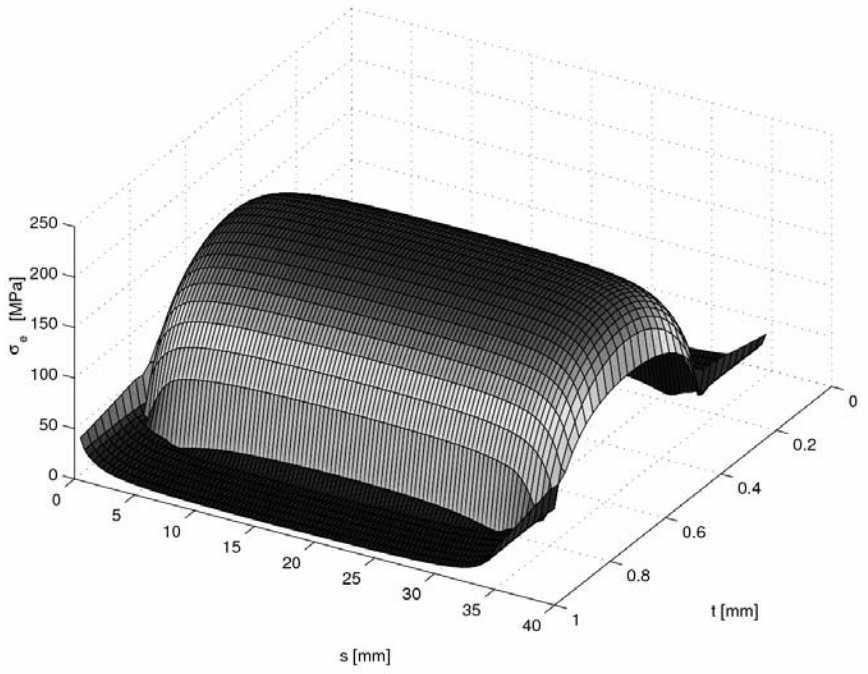

Fig. 13. *The equivalent stress distribution at z = 0 mm after optimization*

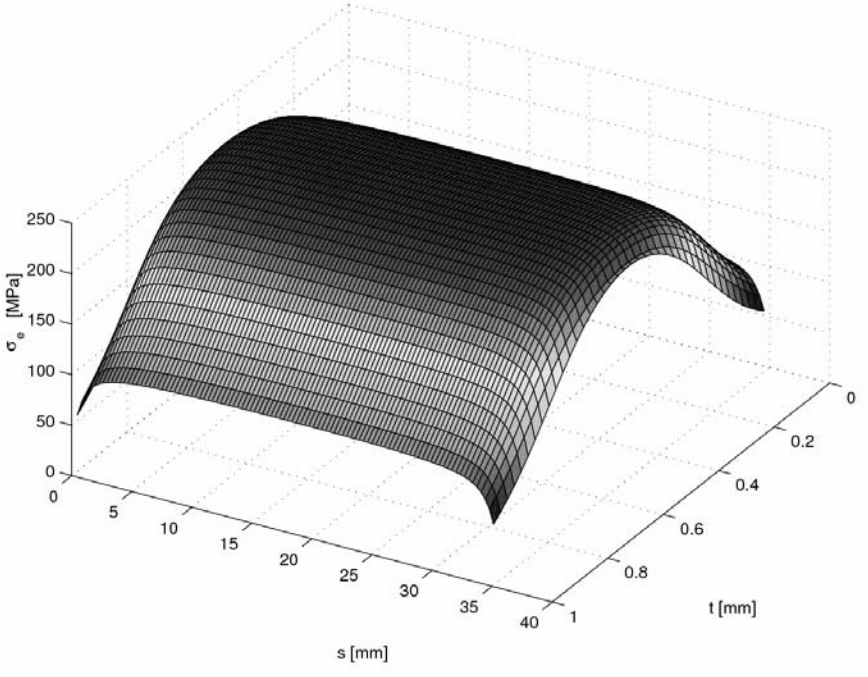

Fig. 14. *The equivalent stress distribution at z = –0.25 mm after optimization*

2.6.1 Optimization problem at a given load

The optimization problem at a given load is formulated as:

$$\min_{\Delta L}\left\{\sigma_{e_{\max}}\,\middle|\,\begin{matrix} p_n \geq 0,\, d \geq 0, \\ p_n\, d = 0,\, \chi \geq 0, \end{matrix}\; x \in \Omega, \quad \mathbf{f} = \mathbf{0}, \mathbf{m} = \mathbf{0}, \sigma_{e_{\max}} \leq \sigma_u\right\} \tag{30}$$

from which $\Delta L = 3.5$ mm is obtained.

Therefore, the solution is $L_2 = 3.5$ mm and $L_3 = 31.5$ mm. The minimization problem is solved by using the above-mentioned iteration process,

which is briefly described in Sub-section 2.4. The radius of the roller is $R = R(s)$, which is used to determine the initial gap $g(x) = g(s, t)$ between the bodies.

The distribution of the equivalent stress is demonstrated at $z = 0$ mm and $z = -0.25$ mm, as shown in Figures 13 and 14. Comparing the stresses in Figures 12 and 14, the influence of the optimization is obvious, i.e., $\sigma_{e\max}$ is significantly decreased.

2.6.2 Optimization problem for calculating the loadability

From the previous optimization problem the stress equality $\sigma_{\max} = \sigma_u$ can be achieved by different rounding-offs of the rollers at different loads, i.e., the rounding-off depends on the load. Since the control function is a uni-value, only a unique roller shape exists for a given load. Namely, after the numerical calculations the designer can select from the round-offs in order to achieve the maximum loadability.

The optimization problem can be written in the following form:

$$\max\left\{ F_0 \left| \begin{array}{ll} p_n \geq 0, d \geq 0, & \\ p_n\, d = 0, & \chi \geq 0\ x \in \Omega \\ \mathbf{f} = \mathbf{0}, \mathbf{m} = \mathbf{0}, \sigma_{e_{\max}} \leq \sigma_u & \end{array} \right. \right\} \quad (31).$$

For the different load levels the change in radius along the roller axis can be seen in Figure 15 and 16.

The load value for a different geometry (problem) is demonstrated in Figure 17. The calculation was made with different meshes (*kt*, *ks*). The modification of the mesh does not affect the results. In all cases $L_1 = 0$, $L_4 = 36$ mm and because of the symmetry $L_1 = L_4 - L_2$, the change in L_2 influences the loadability.

On the basis of the numerical results the round-off obtained for the third problem (see Fig. 17) provides the best performance for high loads.

The loadablity in the case of constant pressure along the meridian is approximately 4850 ≈ 4900 N (case No. 1), while in the case of problem No. 12, because of the 5.5-mm-long transition cubic section the loadability is only ≈ 4650 N.

3 CONTACT WITH A LARGE DISPLACEMENT AND DEFORMATION

In this section the air-spring shown in Figure 18 is analyzed. Air-springs are frequently used in heavy vehicles because of their favorable features, for example, the nonlinear spring characteristics can be controlled by the inflation pressure.

The designer is interested in having a computational tool that helps in analyzing an air-

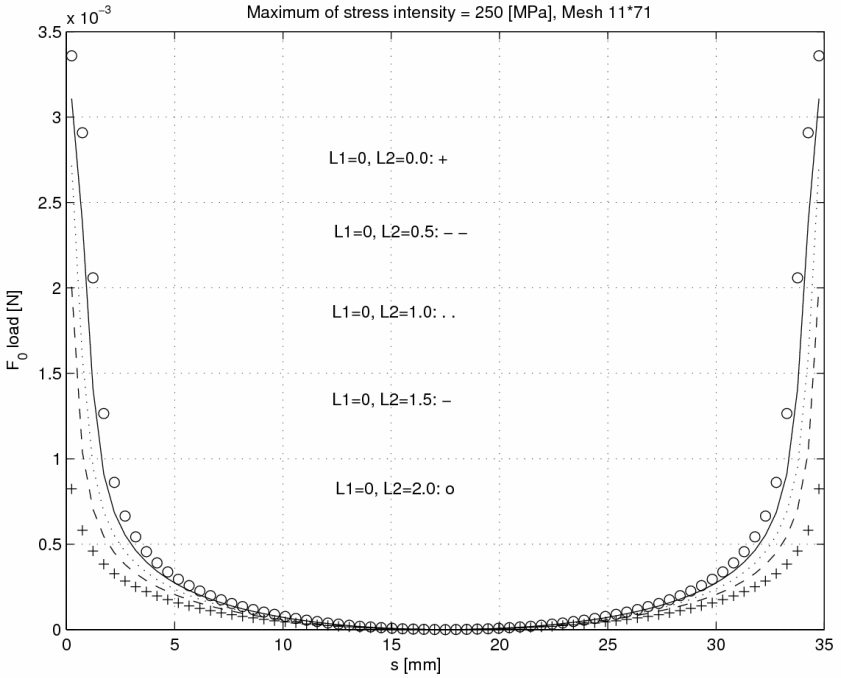

Fig. 15. *Gap along the roller axis at different round-offs*

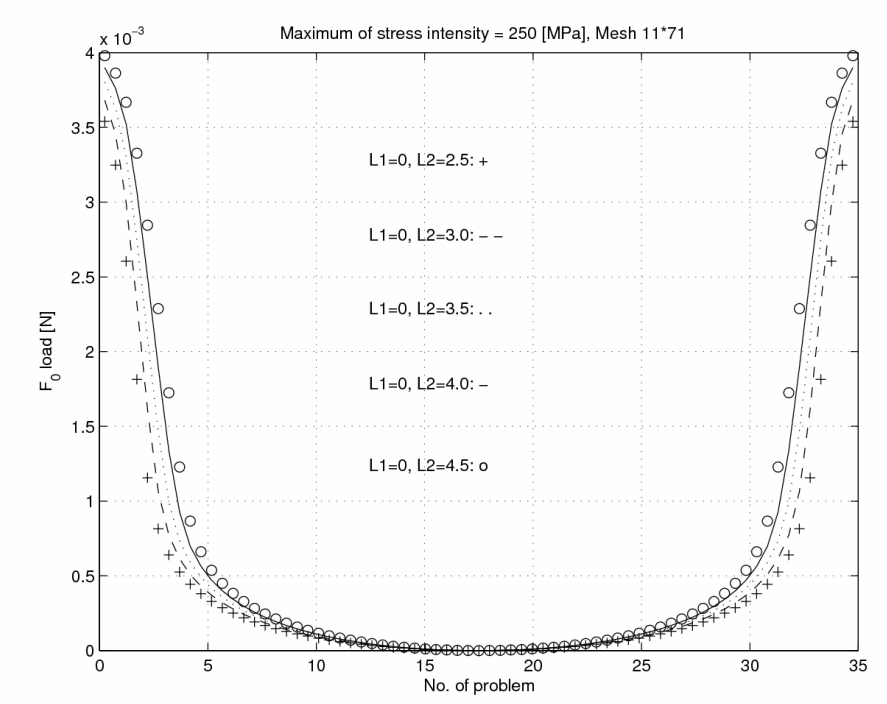

Fig. 16. *Gap along the roller axis at different round-offs*

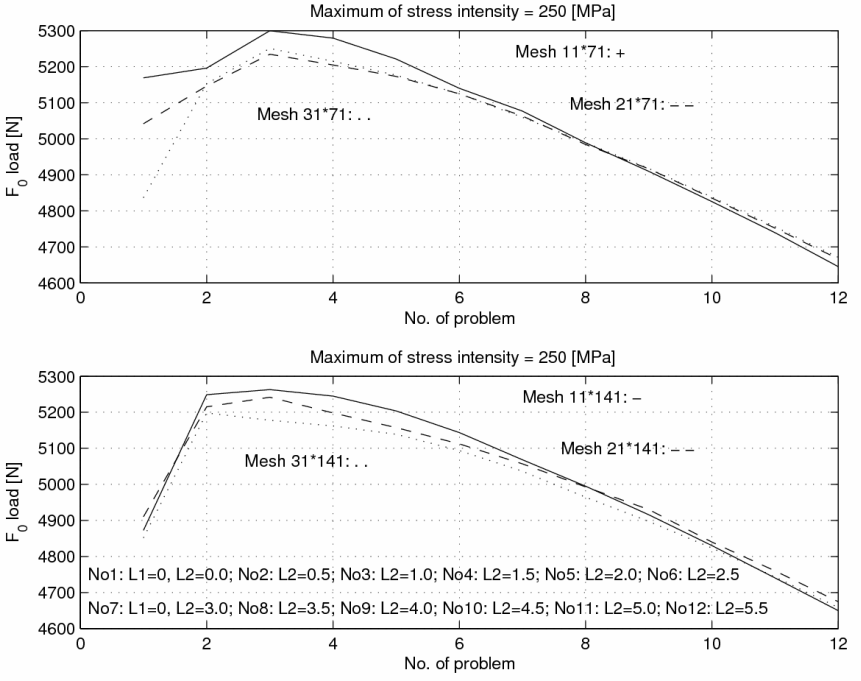

Fig. 17. *Load distribution versus different geometries*

spring before it is manufactured. One can determine its spring characteristics, the quantitative influences of the geometrical modifications, as well as the stresses and strains in the fiber-reinforced rubber composite. A finite-element program has been developed, which is based on the following theory.

The axially symmetrical problem is strongly nonlinear due to the contact problem, the large displacements and the incompressibility of the rubber.

Using the notation of Figure 1 the deformation gradient tensor is given as:

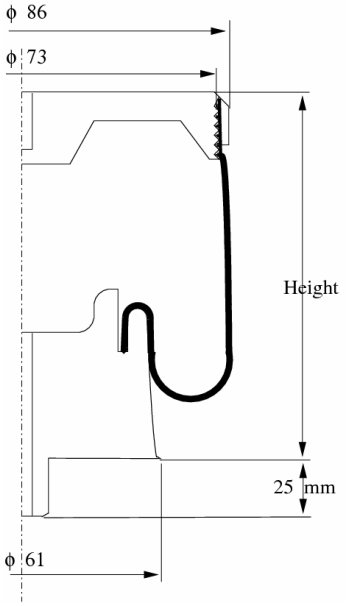

Fig. 18. *Cross-section of the air-spring*

$$\mathbf{F}^{\alpha} = \frac{\partial \mathbf{x}^{\alpha}}{\partial \mathbf{X}^{\alpha}} \tag{32},$$

where $\mathbf{X}^{\alpha}$ denotes the undeformed configuration, while $\mathbf{x}^{\alpha}$ belongs to the current configuration. In the examined problem the lower body is a rigid one; therefore, $^{\alpha}$ will be omitted in the following.

In order to treat the incompressibility condition we introduce the deformation gradient in a decomposed form:

$$\mathbf{F} = \mathbf{F}_{Vol}\hat{\mathbf{F}} \tag{33},$$

where the volumetric part of the deformation gradient is defined as:

$$\mathbf{F}_{Vol} = J^{1/3}\mathbf{I} \tag{34},$$

where $\mathbf{I}$ is the unit tensor. The deviatoric part of the deformation gradient is obtained as:

$$\hat{\mathbf{F}} = J^{-1/3}\mathbf{F} \tag{35},$$

and the volumetric change is:

$$J = \det \mathbf{F} \tag{36}.$$

The incompressibility condition is fulfilled when $J = 1$.

In our investigation the rubber ($\beta = 1$) is assumed to be a nearly incompressible material and it is modeled with the Hu-Washizu functional, see [26], and the fiber-reinforced layer ($\beta = 0$) is homogenized by the so-called Halpin-Tsai equations [28]:

$$\Pi_{HW}\left(\mathbf{u},\overline{J},\overline{p}\right) = \beta\left\{\begin{array}{l}\int\limits_V \widehat{W}(\mathbf{C})\,dV + \int\limits_V U\left(\overline{J}\right)dV \\ +\int\limits_V \overline{p}\left(J-\overline{J}\right)dV - \int\limits_{S_t}\mathbf{u}\cdot\mathbf{n}\tilde{p}\,dA\end{array}\right\} + \\ +(1-\beta)\frac{1}{2}\int\limits_V \mathbf{E}\cdot\cdot\mathbf{D}\cdot\cdot\mathbf{E}\,dV \tag{37},$$

where '$\cdot\cdot$' means the double dot product of two tensors, $\tilde{p}$ is the prescribed pressure and $\widehat{W}$ is the Mooney-Rivlin strain energy density:

$$\widehat{W}(\mathbf{C}) = \mu_{10}\left(\hat{I}_{1\hat{C}} - 3\right) + \mu_{01}\left(\hat{I}_{2\hat{C}} - 3\right). \tag{38}$$

in which μ_{01}, μ_{10} are the Mooney-Rivlin constants, invariants of the Cauchy-Green strain tensor:

$$\hat{I}_{1\hat{C}} = \hat{C}_{11} + \hat{C}_{22} + \hat{C}_{33} \tag{39}$$

$$\hat{I}_{2\hat{C}} = \frac{1}{2}\left(\hat{I}_{1\hat{C}} - \hat{\mathbf{C}}\cdot\cdot\,\hat{\mathbf{C}}\right) \tag{40}$$

and the Cauchy-Green strain tensors are defined by the different deformation tensors

$$\hat{\mathbf{C}} = \hat{\mathbf{F}}^{T}\hat{\mathbf{F}} \tag{41},$$

where ^{T} denotes the transpose of a tensor,

$$\mathbf{C} = \mathbf{F}^{T}\mathbf{F} \tag{42}.$$

The II. Piola-Kirchhoff stress tensor for the rubber is given by:

$$\mathbf{S} = 2\frac{\partial \widehat{W}}{\partial \mathbf{C}} + \overline{p}J\mathbf{C}^{-1}$$

and the fiber-reinforced layer is assumed to be linear

$$\mathbf{S} = \mathbf{D}\cdot\cdot\mathbf{E} \tag{43},$$

where $\mathbf{D}$ is the constitutive tensor and $\mathbf{E}$ is the Green-Lagrange strain tensor

$$\mathbf{E} = \frac{1}{2}(\mathbf{F}^{T}\mathbf{F} - \mathbf{I}) \tag{44}.$$

The incompressibility is enforced by a penalty function, as was proposed by [29]:

$$U\left(\overline{J}\right) = \frac{\kappa}{50}\left(\overline{J}^{5} + \overline{J}^{-5} - 2\right).$$

The finite-element computations were performed by *p*-extension elements. The

polynomial degrees of the displacements were chosen as p = 1,…, 4, while the independently approximated volumetric change $\overline{J}$ and the hydrostatic pressure $\overline{p}$ were approximated with an order of one degree lower than the displacement according to [30].

The contact problem is treated with a simplified approach. The contacting boundary is approximated by a polygon, i.e., the edge of the contacting element is forced to be a straight line, also when a high-order displacement approximation is used. In practice, three-node contact elements were implemented, as detailed in [22].

The fiber-reinforced rubber composite consists of four layers, i.e., a rubber inner liner, a rubber outer cover and two homogenized orthotropic fiber plies, which are oriented at angles of ±45°. The thicknesses of the rubber layers and the fiber plies are 1 mm and 0.5 mm, respectively. The inflation pressure is $\tilde{p} = 4\,bar$. The finite-element computations simulate the working process of the air-spring. Assuming a constant inflation pressure the deformations, stresses and resultant forces were determined in 19 positions.

Three deformed shapes, i.e., the 1st, 10th, 19th of the airspring are shown in Figure 19.

The vertical displacement versus the resultant force curve, i.e., the characteristic curve, is shown in Figure 20, together with the measured values (see [31]). It is also clear that on the working area, i.e., 15 – 45 mm the calculated and the measured values show good agreement, so validating the proposed method.

Numerical examples showed that accurate global results, like the force-displacement curve, can also be obtained for low-order displacement polynomial degrees p = 1, 2. When a high-order approximation is used, i.e., p = 2, 3, 4, stress peaks may arise at the corners of the polygon of the contact border. However, at the other side where the inflation pressure is exerted, the boundary condition is satisfied very accurately for the high-order displacement polynomial degrees p = 3, 4.

4 CONCLUSIONS

It is well known that the stress state of machine elements is highly sensitive to the geometry near the stress peaks. This is a requirement to avoid stress peaks. The second section of the article shows an effective method for accomplishing it. Namely, a smooth contact-pressure distribution can be achieved by using an appropriate *control function* on the controlled sub-domain.

Highly accurate results may be realized using p-extension finite elements for the solution of the contact problems, combined with a

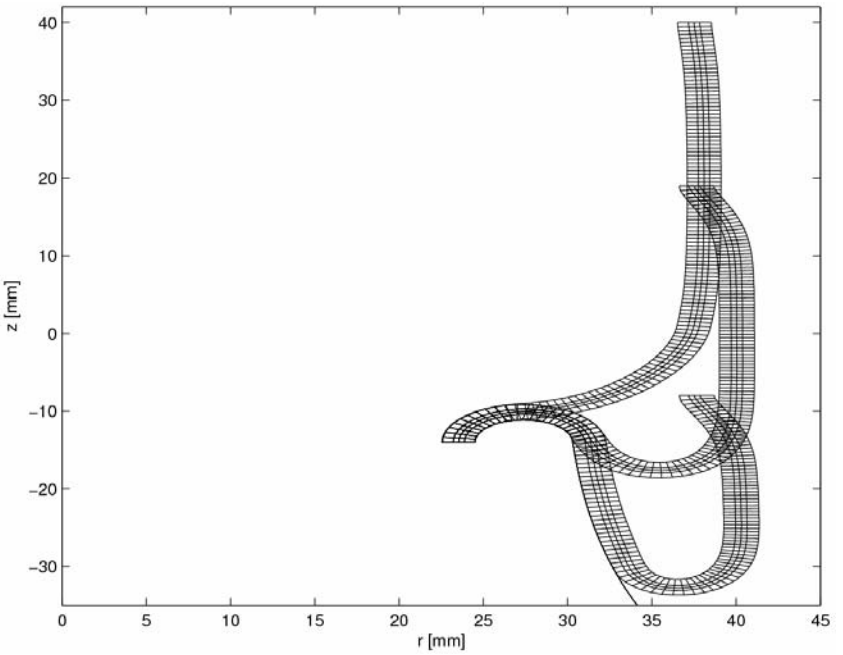

Fig. 19. *Deformed shapes in three positions*

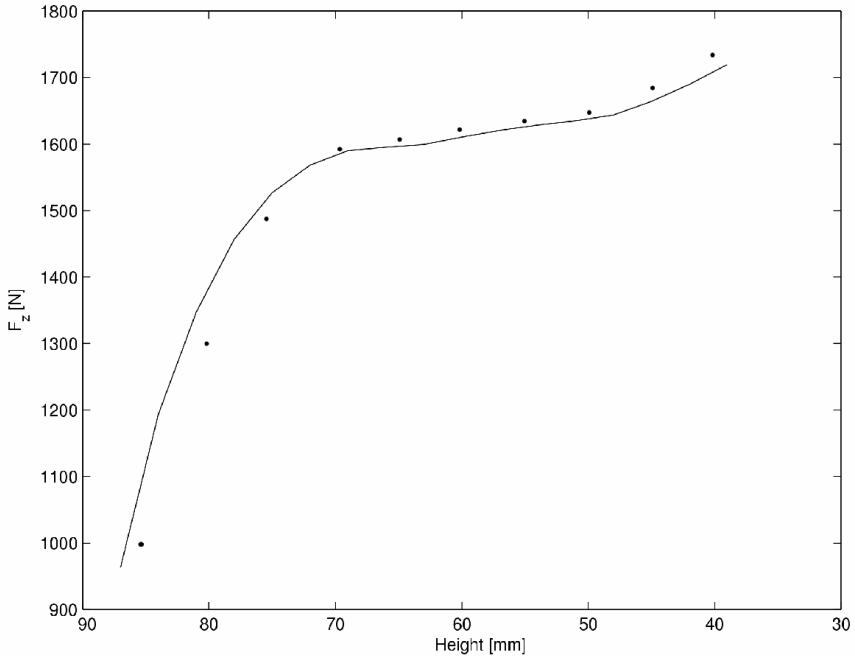

Fig. 20. *Characteristic curve of the air-spring; solid line: numerical results, dots: measurements*

positioning technique and *special re-meshing*.

The provided examples demonstrate the effectiveness of the proposed algorithms for the determination of the initial shape, i.e., the initial gap, by observing the stress constraint. The method is also applicable for designing a clutch to maximize the transmissible torque.

The applied optimization procedure is applicable for designing highly loaded rollers, which are characterized by a smooth contact-stress distribution along the contact surfaces. Two types of optimization problems were investigated. Firstly, the round-off (ΔL) is determined for a given force load (see Equation 30). Secondly, the force load is calculated for the prescribed round-off (see Equation 31). The maximum force load can also be determined with a modification of the round-off.

The *p*-extension finite elements are also very applicable for large-displacement problems when the contacting element's edge is kept as a straight line. The global results are accurate enough at a low order of approximations, i.e., the measured and calculated results show good agreement.

Acknowledgment

The research is partially supported by the Hungarian Research Fund (OTKA T037759).

5 REFERENCES

[1] Hilding, D., Klarbring, A. and Petterson, J. (1999) Optimization of structures in unilateral contact, *ASME, Appl. Mech. Rev.,* 52:(4) (1999), pp. 139-160.

[2] Haslinger, J. and Neittaanmaki, P. (1996) Finite element approximation for optimal shape design, *John Wiley & Sons Ltd*., London.

[3] Goryacheva, I.G. and Dobuchin, M.H. (1998), Contact problems in tribology, *Mashinostroenie*, Moscow.

[4] Páczelt, I. (2000) Iterative Methods for solution of contact optimization problems, *Arch. Mech*., 52:(4—5) (2000), pp. 685-711.

[5] Páczelt, I. and Szabó, T. (2002) Solution of contact optimization problems of cylindrical bodies using the hp-FEM, *International Journal for Numerical Methods in Engineering*, 53:(1) (2002), pp. 123-146.

[6] Páczelt, I. and Baksa, A. (2002) Examination of contact optimization and wearing problems, *Journal of Computational and Applied Mechanics*, 3 (2002), pp. 61-84.

[7] Szabó, B. and Babuška, I. (1991) Finite element analysis, *Wiley-Intersience*, New-York.
[8] Oh, K.P. and Trachmann, E.G. (1979) A numerical procedure for designing profiled rolling, *ASME, Journal of Lubrication Technology Series F*, 101(1979), pp. 105-109.
[9] Harnett, M.J. (1979) The analysis of contact stresses in rolling element bearings, *ASME, Journal of Lubrication Technology Series F,* 101(1979), pp. 105-109.
[10] Trostenfelt, B. and Fredriksson, B. (1984) Pressure distribution in crowned roller contacts, *Engineering Analysis*, 1:(1) (1984), pp. 32-39.
[11] de Mul, J.M., Kalker J.J. and Frederiksson, B. (1986) The contact between arbitrary curved bodies of finite dimension*, ASME, Journal of Tribology*, 108 (1986), pp. 140-148.
[12] Chiu, Y.P. and Harnett, M.J. (1987) A numerical solution for the contact problem involving bodies with cylindrical surface consireding cylindrical effect, *ASME, Journal of Tribology*, 109(1987), pp. 479-486.
[13] Páczelt, I. and Szabó, T. (1994) Optimal shape design for contact problems, *Structural Optimization*, 7(1994), pp. 66-75.
[14] Kania, L. (2006) Modelling of rollers in calculation of hewing bearing with the use of finite elements, *Mechanism and Machine Theory*, 41(2006), pp. 1359-1376.
[15] Krzeminski-Freda, H. and Warda, B. (1996) Correction of the roller generators in spherical roller bearings, *Wear*, 192(1996), pp. 29-39.
[16] Park, T.J. and Kim, K.W. (1998) Elasthogydrodynamic lubrication of a line contact, *Wear,* 223(1998), pp. 102-109.
[17] Lim, X. and Yang, P. (2002) Analysis of the thermal elastohydrodynamic lubrication of a finite line contact, *Tribology International*, 35(2002), pp. 137-144.
[18] Páczelt, I. and Mróz, Z. (2005), On optimal contact shapes generated by wear process, *International Journal for Numerical Methods in Engineering*, 63:(9) (2005), pp. 1250-1287.
[19] Wriggers, P. and Miehe, C. (1994) Contact constraints within thermo-mechanical analysis a finite element model, *Computer Methods in Applied Mechanics and Engineering*, 113(1994), pp. 301-319.
[20] Podra, P. and Anderson, S. (1999) Simulating sliding wear with finite element method, *Tribol. International*, 32(1999), pp. 71-81.
[21] Páczelt, I. and Pere, B. (1999) Investigation of contact wearing problems with hp-version of the finite element method, *Thremal Stress '99*, Skrzypek, J.J. and Hetnarski, R.B. (Eds), Crakow University of Technology, pp. 81-84.
[22] Crisfield, M.A. (1997) Non-linear finite element analysis of solids and structures, *John Wiley & Sons*, New York.
[23] Wriggers, P. (2002) Computational contact mechanics, *J. Wiley & Sons,* New York.
[24] Páczelt, I., Szabó, T. and Baksa, A. (2004) Product designing using finite element method and contact optimizations, *Proceedings of the TMCE2004*, Lausanne, Switzerland, Horváth & Xirouchakis (Eds), Millpress, Rotterdam, pp. 267-276.
[25] Archard, J.F. (1953) Contact and rubbing of flat surfaces*, Journal of Applied Physics*, 24(1953), pp. 981- 988.
[26] Bone, J. and Wood, R.D. (1997) Nonlinear continuum mechanics for finite element analysis, *Cambridge University Press*, Cambridge.
[27] Kalker, J.J. (1990) Three dimensional elastic bodies in rolling contact, *Academic Publisher*, Doordrecht.
[28] Halpin, J.C. and Tsai, S.W. (1969) Effect of environmental factors on composite materials, *AFML-TR*, 1969, pp. 67-423.
[29] Hartmann, S. and Neff, P. (2003) Polyconvexity of generalized polynomial-type hyper elastic strain energy functions for near-incompressibility, *International Journal for Solids and Structures*, 40(2003), pp. 2767-2791.
[30] Stenberg, R. and Suri, M. (1996) Mixed hp finite element methods for problems in elasticity and Stokes flow, *Numer. Math*., 72(1996), pp. 367-389.
[31] Firestone Industrial Products Company, Engineering Manual & Design Guide, 2006. Available online at: www.macsspring.com/website/catalogs/design.guide.pdf (accessed 05 July 2006)

Authors' Address:
Prof. Dr. István Páczelt
Dr. Attila Baksa
University of Miskolc
Department of Mechanics
H-3515 Miskolc-Egyetemvaros, Hungary

Dr. Tamás Szabó
Szechenyi Istvan University
Department of Applied Mechanics
Egyetem ter 1
H-9028 Gyor, Hungary

Prejeto: 2.5.2007
Received:
Sprejeto: 27.6.2007
Accepted:
Odprto za diskusijo: 1 leto
Open for discussion: 1 year

Strojniški vestnik - Journal of Mechanical Engineering 53(2007)7-8, 462-477
UDK - UDC 658.512.2
Izvirni znanstveni članek - Original scientific paper (1.01)

Proučevanje konstruiranja proizvodnih strojev s postopkom temelječim na modeliranju omejitev

A Constraint-Based Limits-Modelling Approach to Investigate Manufacturing-Machine Design Capability

Jason Matthews - Baljinder Singh - Glen Mullineux - Tony Medland
(University of Bath, United Kingdom)

Proizvajalci kupujejo proizvodne stroje, ki so zmožni obdelave nekega izdelka v določenem obdobju. Izdelki, ki se izdelujejo na teh strojih, pa se lahko zamenjajo v dobi trajanja stroja. Proizvajalci se pogosto obračajo na prvotnega proizvajalca opreme, da ocenijo zmožnost prilagoditve stroja na različico izdelka ali celo obdelavo povsem drugega izdelka. V Veliki Britaniji so proizvajalci take opreme majhna podjetja z največ 80 zaposlenimi. S tako omejenimi zmogljivstmi ni zadosti strokovnosti ne časa za izvajanje podrobne analize, kako izboljšati učinkovitost strojev. V preteklosti je bilo zato treba kupiti nove stroje, kar pa je pomenilo velik finančni zalogaj za podjetja, ki so želela predstaviti nove izdelke na že tako konkurenčnem tržišču. Ta prispevek predstavlja postopek raziskave proizvodne zmožnosti nekega stroja. Metodologija sloni na modeliranju omejitev in uporablja možnosti omejenega okolja za modeliranje variantnih oblik in omogoča primerjavo njihove odpornosti na neuspeh. Ta postopek omogoča izdelavo različnih grafičnih predstavitvenih tehnik, ki prikažejo in primerjajo omejitvene pogoje za vse stroje.

(Ključne besede: konstruiranje strojev, prilagajanje izdelkom, modeliranje omejitev, izboljšanje učinkovitosti)

Manufacturers purchase processing machinery, tailor made to handle a specific, limited product range. However, during the life span of the machines, these products are likely to change. The manufacturer often calls on the original equipment supplier to assess the ability of the machines to process either a variant of their existing range or even to consider the handling of a totally new product. In the UK such equipment manufacturers tend to be small concerns, employing 80 staff or less, and with such limited resources that there is not the expertise or time available to perform any in-depth analysis of how well the design operates or what constraints there are that may stop it reaching the new performance requirement. In the past this has led to the manufacturers purchasing new equipment, which puts a high financial burden on companies wishing to introduce new products into already highly competitive market sectors. This paper presents an approach to investigating the manufacturing capability of a machine. The methodology, based on limits modelling, utilizes the capability of a constraint environment to model multiple variations of a design and compare their performances against a range of failure modes. This process allows a variety of graphical visual representation techniques to be created to illustrate and compare the limiting conditions for all machines.

(Keywords: machine designs, product variations, modeling limits, constraints)

0 INTRODUCTION

All process machinery, whether from food processing, automotive sub-component assembly or electrical device sectors, is designed with an innate capability to handle slight variations in the product. This is initially achieved by simply providing tolerances to allow, for example, changes that occur in pack sizes to be accommodated, through user adjustments or complete sets of change parts. By the appropriate use of these approaches most normal variations in product setting can be handled. However, when extreme conditions of setting, major changes in product size and configuration are considered there is no guarantee that the existing machines will be able to cope. The

problem is even more difficult to predict when completely new product families are proposed for manufacture on an existing product line.

Such changes in product range are becoming more common as producers respond to demands for ever increasing customization and product differentiation. Within the process and packaging industries this is often achieved through changes in product-packaging formats, numbers in a pack and the types of presentation employed, particularly in supermarkets [1]. All result in the supplier being forced to make more and more frequent changes to the line with little to no guidance on how this can be achieved (or even if it is at all possible). The lack of knowledge about the capabilities of the machines being used forces the supplier to undertake a series of practical product trials. These, however, can only be undertaken once the product form has been decided and produced. There is then little opportunity to make changes that could greatly improve the potential output of the line and to reduce waste.

The production machines in question are generally constructed of multiple *spatial mechanisms* [2]. The machines are known to work but a full understanding of their design implications and capabilities are not available. This can mean that problems may occur if a customer wishes to purchase a machine to handle a product form that has not been encountered before. In the packaging sector this may be the case when a product with a size larger than normal needs to be wrapped. Often the response is to take a known machine and produce a variant design that can handle the new product. This means that the company is then committed to supporting that variant throughout its operating life. However, if a better understanding of the full range of machines was available, then an existing machine might be identified to handle the new product. Similarly, if that understanding was available, it would help to rationalize the existing range of machines so that the full spectrum of products could be catered for without significant duplication.

There is thus a need for a modelling approach that allows the effect of variation in products to be analyzed together with an understanding of the capability of the manufacturing machine. Only through their analysis and interaction can the capabilities be fully understood and refined to make production possible.

The remainder of the paper is structured as follows. Section one gives a critical overview of the related literature and technologies, and presents the rationale for the approach presented. Section two gives an overview of the constraint modelling environment. In section three the limits modelling approach is presented, along with a flowchart. The methodology is implemented in section four with a packaging-machine case study. A discussion of the approach is given in section five. The research is concluded in section six, including the limitations of the approach and future work.

1 BACKGROUND

1.1 Mechanism / machine analysis

This section provides a review of the relevant academic and commercial approaches that have been employed to investigate and analyse the functionality and performance of both machines and their constituent mechanisms. The limitations of these are discussed at the end of the section. The analysis of position and kinematics for mechanisms' limits has been well documented ([2] to [5]). Increased computational power now allows designers to model, analyze and simulate complex mechanisms. Simulation is widely reported [6] and [7], often utilizing standard packages for a design-through-simulation approach. These are generally used to evaluate the performance capabilities of a particular configuration during the machine's operation cycle. Commercial CAD packages ([8] and [9]) allow the designer to model and undertake motion analysis (both kinematic and dynamic), together with component interaction. Other packages such as ADAMS [10] allow the engineer to interactively undertake investigations of mechanical, pneumatics, hydraulics, electronics, systems as well as investigating other effects such as forces, noise, vibration, and harshness. In addition to these, higher-level CAE packages ([11] to [13]) offer the engineer the option to explore the design space by implementing parametric studies and provide sensitivity analyses to allow the engineer to compare the effects of several parameters on chosen responses. Such packages can give the engineer the option to optimize selected effects of parameter change by combining design-of-experiments methods. Hicks et al. [14] described a methodology using a constraint modelling

environment for supporting and analyzing the design of packaging machinery at the embodiment stage. This method showed the ability of the modelling package to analyze the design of a mechanism. Hicks et al. [15] extended this approach into optimal redesign of packaging machinery. In [16] Barton and Lee created a framework for the modelling, simulation and optimization of hybrid systems. Pusey et al. [17] developed a graphical interface, "BONK", to simplify the preparation and analysis of dynamic systems using Bond graphs. Their approach bounded the maximum and minimum kinematics properties for the given mechanism and optimized the mechanism to find the best solution.

The above methods analyze the design and its motions. Another area of research undertaken for the robotics industry forms the methods of understanding the limits of reach and motion for robots and manipulator mechanisms, in their configuration space (c-space) [18]. Through this an area, termed the workspace, can be defined, which represents the maximum limiting motion for the device. Research in [19] studied the design and workspace of a 6–6 cable-suspended parallel robot. This characterized the workspace volume as the set of points that the centroid of the moving platform can reach with tensions in all suspension cables at a constant orientation. An approach has also been developed that uses an algorithm to plot clouds of points to represent the workspace boundaries of a robot system [20]. These defined the cloud boundaries and are connected together to give the real workspace. Research in [21] devised a general method for workspace computation based on a geometric sweep of the spatial elements, representing partial workspaces. The geometric algorithms developed by Gosselin [22] define the geometric boundary edges of a dexterous robot together with the total orientation, maximal and fixed orientation workspaces by considering the limits of the actuators. The authors of [23] and [24] presented geometrical methods for the constant-orientation workspace of a hexa-slide manipulator, and developed an algorithm to reverse design a Gough platform from knowing the workspace.

1.2 Constraint-based approaches

It is evident from the research reviewed above that there are currently a variety of underlying methods for application assessment, analysis and problem solving, that could be applied to the issues discussed in this paper. The main reason for this stems from the fact that particular tools or techniques are frequently driven by the perspective of the particular problem and how it is to be solved rather than a generalized approach for reasoning about the problem. It is arguable that such variety makes the use, integration, exchange and unification of supportive tools, methods and processes (process elements) particularly difficult. This contributes to many of the research challenges now facing academia and industry [25]. In order to create a generalized approach for both modelling and reasoning a constraint-based approach was investigated. This has recently been applied to a range of different tasks associated with design and manufacture and forms the background to the approach adopted for the work presented in this paper.

Within the context of this research a constraint is defined as a rule that can be analyzed to determine its current 'truth'. This may take on many forms, which may, for example, determine a bound on a single design parameter, express the relationship between a set of design parameters or be any factor that limits the performance of a system. With a constraint-based approach the identified parameters and constraints for a problem can be specified and their consequences investigated [26]. Constraints take two forms: quantitative and qualitative. Quantitative constraints are perhaps the easiest to visualize. They are requirements that particular parameters must take specific numerical values at prescribed points or over prescribed regions. Qualitative constraints are requirements for the value of a parameter to be in an inequality relation with respect to a second parameter.

There are three distinct methods for working with constraints: satisfaction, optimization and checking [27]. With constraint satisfaction the aim is to find a configuration that satisfies all the imposed constraints as closely as possible. An extension to this is the constraint-optimization problem. Here constraints are used to find the optimum solution to a problem. Constraint optimization and satisfaction have become the dominant approaches for design ([27] and [28]), especially of mechanisms [29], machines [13] and [14] and for manufacturing problems, such as

computer-aided process planning ([30] and [31]) and scheduling [32]. For the optimization or satisfaction of constraints there are several techniques including, for example, numerical optimization [33], symbolic manipulation and re-ordering strategies [34], simulated annealing [35] and evolution strategies such as genetic algorithms [30].

The third approach, constraint-checking, is a passive technique that monitors whether a constraint has been violated. Previous research has employed this method for real-time modelling of industrial floor layouts. The authors considered the design rules and physical limitations as constraints. The Open SCheduling Architecture (TOSCA) developed by Beck [36] was used to addresses manufacturing scheduling problems from a constraint-based perspective. The constraints were monitored in terms of threats to their satisfaction and are opportunistically tackled through a process that iteratively refines the schedule by restricting the resourcing and start-time options. The authors of [37] use the constraint language SPARKS to check for constraint violation in constraint networks produced for concurrent engineering. A similar approach was employed by [38] for product life-cycle design. The constraint-checking approach has advantages over the other two methods, as it offers greater flexibility and requires less computational power. In a design scenario it also takes advantage of the engineer's knowledge and experience.

1.3 Background work discussion

The simulation and modelling approaches identified above perform well when describing the physical geometrical extremes and configuration space of the mechanism and/or the machine. They offer the user the ability to analyze motion and to explore the design space of a given system. If individual analysis tools and methods are employed for a detailed investigation of a particular machine or mechanism, then the ability to generate an optimum or best-performing design solution is severely frustrated [13]. With the tools and methods reviewed there are fundamental limitations, because:

- they allow no consideration of other modes of failure or limits,
- the user is constrained by the functions offered by the respective system for modelling and simulation attributes,
- even through the user has modelled the design, the tool many not allow complete access to the underlying constraints, which are fundamental to this approach.

With these factors in mind it is evident that there is currently no approach to answer the specific industrial question posed in this research. Further research into this area is required to establish a methodology where the whole performance of a system can be define and analyzed to assess its ability to handle change. A constraint-based system has been selected for this research because of the flexibility it allows: it offers parametric modelling, which is paramount to this approach, it allows motion and element interaction to be performed, its inbuilt functions give the option of a sensitivity analysis [39] and the constraint-based approach using hard and soft constraints [40] allows for optimization. The programming environment also permits the user to employ constraint checking while actuating models. To aid readability the term *system* is used in the remainder of the paper to describe both the machine and its constituent mechanisms.

2 MODELLING APPROACH

2.1 Constraint-modelling environment

This section gives an overview of the constraint-based approach used here and shows how systems can be modelled in the environment. In constraint-based modelling the identified constraints and parameters from a design can be specified and their consequences investigated. This holistic approach allows the representation of design knowledge and, more importantly, enables this knowledge to be expanded or modified at any stage during the design process. In this way changes in both the proposed solution and in the governing constraints of the particular design problem can be dealt with and investigated. The software has its own user language, which has been created to handle design variables of several types, including structured forms to represent, for example, geometric objects. The language supports user-defined functions. These are essentially collections of commands that can be invoked when required. Input variables can be passed into a function and the function itself can return a single value or a sequence of values. Functions are used to impose

constraints using an important in-built function, which is the "*rule*" command. Each rule command is associated with a constraint expression between some of the design parameters, which is zero (as a real number) when true. A non-zero value is a measure of the falseness of the constraint rule.

With satisfaction and optimization techniques, in order to investigate the effects of the constraints, they need to be resolved. There are several techniques for doing this ([28] and [34]), including, for example, symbolic manipulation and reordering strategies. The method used by the constraint modeller is based on optimization techniques. During the resolution the expression for each constraint rule (within a function) is evaluated and their sum of the squares is found. If this is already zero, then each constraint expression represents a true state. If the sum is non-zero, then resolution commences. This involves varying a subset of the design parameters specified by the user. The sum is regarded as a function of these variables and a numerical technique is applied to search for values of the parameters that minimize the sum. If a minimum of zero can be found, then the constraints are fully satisfied. If not, the minimum represents some form of best compromise for a set of constraints that are in conflict. It is possible at this stage to identify those constraints that are not satisfied and, where appropriate, investigate whether relaxing less important constraints can enable an overall solution to be determined. Constraint checking can be implemented when simulation or numerical models are being actuated. The constraints can be either equality or inequality in nature, with relationship functions being employed to check if these constraints are being violated.

For simulation-based models the software environment supports simple wire-frame graphics, such as line segments and circular arcs. These can be defined in a world space or associated with a 'model space' [41]. The model spaces can be embedded within each other. The modeller also has the capability to create solid objects. These can be embedded within model spaces [42] so that they can move with other geometries, including wire-frame entities. Solids have been incorporated into the environment by means of the ACIS library of procedures [43].

As an example, consider the representation of a four-bar linkage. This is shown schematically in Figure 1. In part (a) of the figure the two fixed pivot points are specified, and the line segments representing the three links are defined, each in a

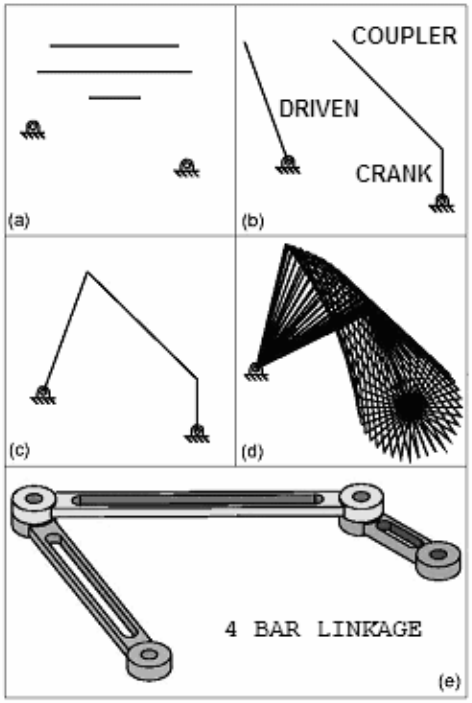

Fig. 1. *Modelled four-bar mechanism*

local model space. Here a model space is a group of entities with which a transform is associated. This transform dictates how the entities map, from their own local coordinates into world space or into another model space. In this way a hierarchy of model spaces can be set up and used to specify an initial assembly of some components of a design. In the example, the model space of the coupler link is "embedded" in the space of the crank, and the spaces for the crank and the driven links are embedded in world space. A partial assembly of the mechanism is achieved by applying the transformations to the links in each space. This is shown in part (b) of Figure 1. If the space of either the crank or the coupler is rotated, the hierarchy of their spaces ensures their ends remain attached. To complete the assembly, the ends of the coupler and driven link have to be brought together. This cannot be done by model space manipulation alone, as this would break the structure of the model space hierarchy. Instead a constraint rule is applied, whose value represents the distance between the ends of the lines. The user language has a binary function 'on', which returns the distance between its two geometric arguments. If *l1* and *l2* are the lines for the coupler and the driven links, then, in the user language, the constraint rule is expressed as follows:

```
rule ( l1:e2 on l2:e1 );
```

where the colon followed by e1 or e2 denotes either the first or second end-point of the line. In order to satisfy this constraint rule the system is allowed to alter the angle of rotation of the model spaces of the coupler and driven links. When the rule is applied the correct assembly is obtained as in part (c) of Figure 1. When the space of the crank link is rotated and the assembly of the other two links is performed at each stage, a step-wise simulation of the motion is obtained, as in part (d). If solid objects representing the link are constructed, these can also be included in the model spaces, as shown in part (e).

2.2 Mechanism system effects

To investigate the effects of product change, the factors which cause the system to fail need to be identified. For this purpose a study of the factors that cause such failures [44] was made and these are represented in the Ishikawa diagram, Figure 2. These factors represent the constraints of the system and are agreed with the designer/engineer, possibly informed by testing of the product.

In addition to these, the constraints which need to be employed for the constraint checking have to be established. Again, many of these can be identified by the designers and engineers of the manufacturing company. However, in addition to this, some modelling of the product is likely to be required, to establish its bounds to processing.

3 LIMITS MODELLING

The problem of investigating the inherent and potential manufacturing capability of a machine, defined in the introduction, requires an approach to find a solution. This paper presents a

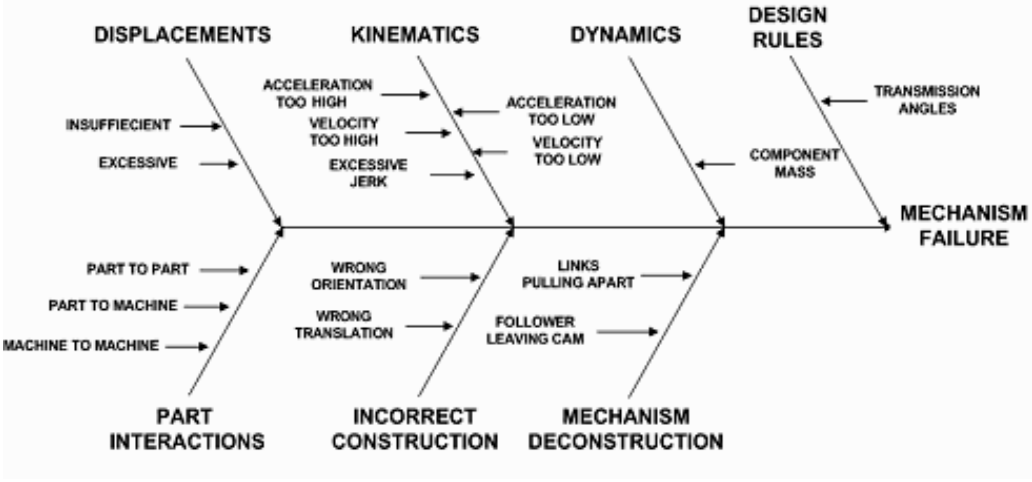

Fig. 2. *Ishikawa diagram of system failures*

technique called "limits modelling" as one possible alternative. The approach being adopted is, to work with a parametric model of a machine established within the constraint modelling environment [41]. The effects of variations within the machine can be investigated by adjusting suitably chosen parameters. Such variations can represent the effects of adjustments within the physical machine and the use of change parts.

3.1 The method

The system is parametrically modelled using an environment such as the constraint-modelling package, as described in Section 2. The dimensions for the modelling are taken from a part drawing (if they exist), manual measurements and high-speed video footage. Two inherent capabilities of the constraint-modelling package are employed to test the appropriateness of the model. Working with the designers or users of the actual machine, the possible failure modes are established.

- *Bounded search.* The search capability of the modeller is employed to establish whether the device is within the global limits set for the system. Examples of such limits can be the geometric footprint of the machine and cost factors. This gives a crude investigation, showing whether the system has functionality and is appropriate to undergo the limits-modelling process.
- *Sensitivity analysis.* This is the procedure of incrementing design parameters and examining the relative changes in the model's response. When small changes in a parameter of a system result in relatively large changes in the outcomes, the parameter is deemed sensitive. This information is then used to decide the important parameters to investigate during the limits-modelling approach.

With the models' appropriateness tested the next stage is establishing the constraints to be employed for the constraint checking. A variety of techniques can be employed within the modeller to check the violations of these constraints. For example, one failure mode may be the clashing of parts of the machine with each other or with the product. Here an interference check between solid objects within the model can be undertaken. An alternative is bounded boxes, where a box is a rectangular block that contains an object throughout its motion. When a change to the product necessitates a modification to a design and this modification causes the motion to exceed any of the walls of the box, then it can be concluded that this product cannot be processed using this system. Although this is crude, it is an approach that is sufficiently reliable for certain applications, such as an investigation of the extreme motions for a mechanism within a defined machine footprint. The next stage is to run the model repeatedly for different configurations (multiple instances), with each being tested for successful operation. This allows a matrix of functional points to be generated. When the model is being tested, performance characteristics can also be logged into the matrix. For this process two approaches can be employed.

- *Program modeller to disturb the dimensions of the model:* The variables within the model can be programmed to vary in dimensionality. A strategy for the disturbance has to be decided on prior to this step. This approach is only suitable for simplistic mechanisms with a small number of variables.
- *Set goal and make use of the modeller's optimizing function:* The internal optimizer with the constraint modeller can be used when a goal is set for the model. The modeller will iteratively optimize the model; all successfully functioning instances can be recorded to produce the functional matrix.

With the matrix defined, a crude method to test whether a new product configuration is such that it lies within the limits of the system is to search for the closest point to the new configuration. In this way the performance values can be used to find the best solution. If the values of the new configuration are greater than those recorded within the matrix then it can be assumed that the new product cannot be produced with this system/ machine

3.2 Results representation

The first representation of the functional points comes from the functional matrix, which can have the performance factor associated with them. It can also be useful to have the data from the matrix in a more graphical representation. The following are some of the options that have been employed for different limiting modelling design exploration situations.

- *Cloud Plot:* is a multi-dimensional scatter-gram. The 2D and 3D variants of this diagram are normally associated with statistical analyses and the presentation of data, for example, in the study of geophysical data [41]. However, recently scatter-grams have also been used as a tool for linking scientific and information visualizations. In this methodology, each successful entry in the matrix relates to a point plotted on the cloud map. The cloud map gives a visual representation of the function space of the system. The boundaries of the cloud map are the limit conditions for the system.
- *Convex Hull:* The convex hull for a set of data is the minimal convex shape containing the given data. It is simple to produce a convex hull from the data plotted from the cloud map in MATLAB; it also allows the volume and surface area of the hull to be computed. When a new configuration is required and the new point is plotted into the data set it can be compared with the original hull. If the volume or surface area has increased, then the new configuration lies outside the limits of the system. The use of the convex hull is suitable when the data set is large and closely grouped. Similar convex hulls have been successfully employed when representing the configuration space of the robot manipulators [21]. As with the cloud plot, the convex hull process can be extended to a range of machines for comparisons.
- *Failure-mode map (FMM):* This approach has been created from the limits-modelling approach. Effectively, the approach is used to perform an exhaustive search of the design area against a given setup, performance and function factors. The approach records points where the system functions correctly and where the constraints are violated. These violations are recorded and plotted. This offers the user the potential to see the given boundary for the system and the constraints that limit any other development (cf figure 3a).
- *Surface plot:* A multi-dimensional surface can be fitted to the categorized data variables. Surfaces for subsets of data determined by the selected categorization method can be arranged in one display to allow for comparisons between the subsets (cf. figure 3b).

This approach also opens up the possibility of redesigning the original machine so as to maximize its allowable space. Here, constraint-based techniques and optimization can again be used. Now, more of the fundamental design

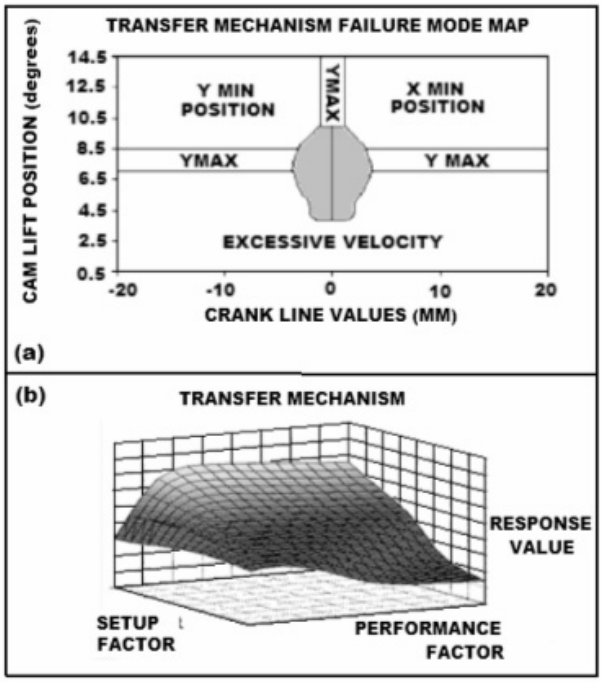

Fig. 3. *Results representation*

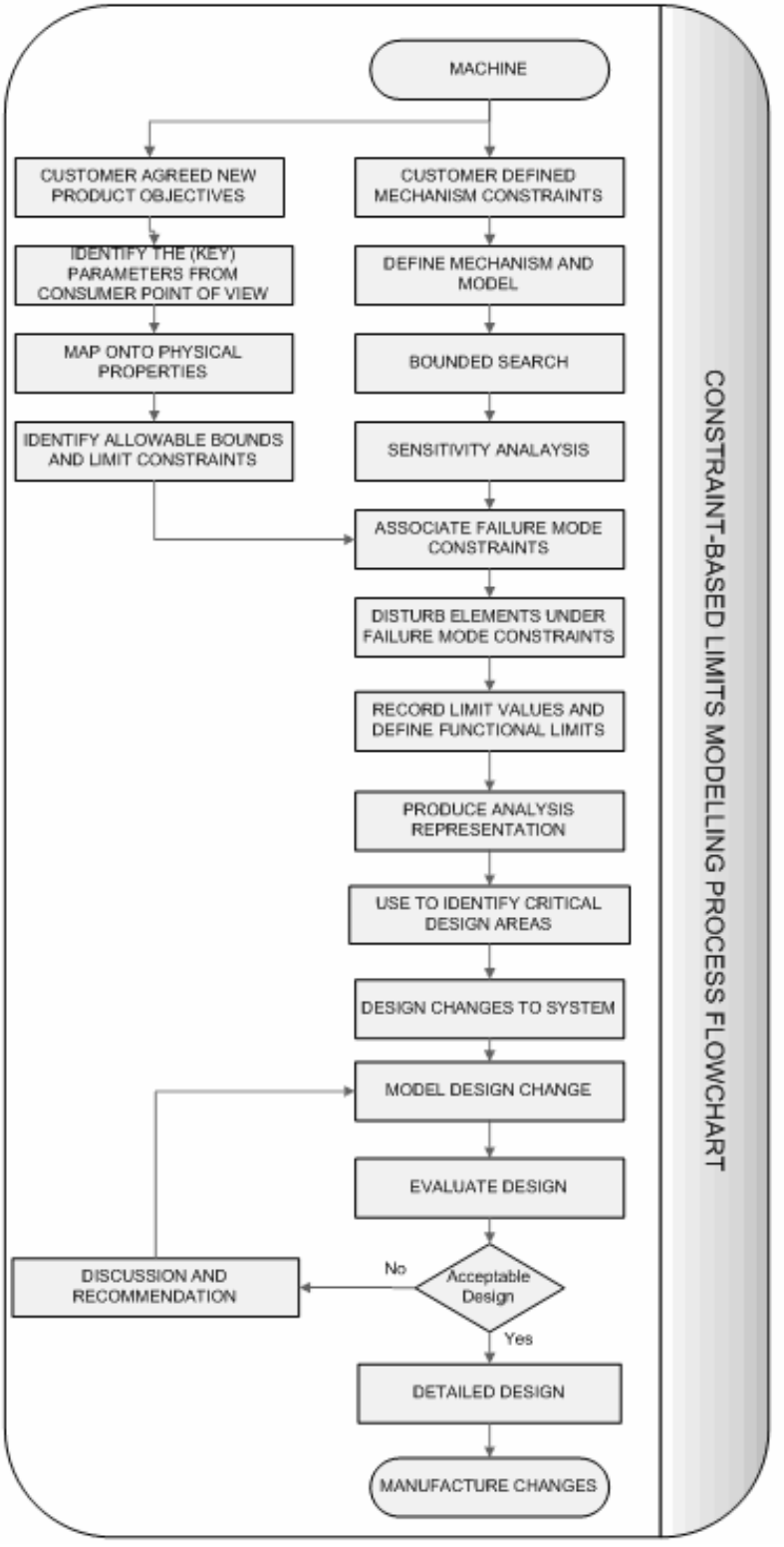

Fig. 4. *Methodology flowchart*

geometry is varied with the aim of increasing the volume of the allowable space obtained when the machine adjustments are varied. This then allows a more general-purpose machine to be designed and can permit the number of machines in a given family to be reduced. The complete approach is presented in the flowchart in Figure 4.

4 CASE-STUDY EXAMPLE

4.1 The system

The featured system is an ejection sub-assembly of a confectionary-wrapping machine (Figure 5). The confectionary is fed into the machine via a rotary table together with the film being fed by a de-reel unit. The confectionary and film are then lifted together into transfer gripper jaws. This operation also cuts the film to the correct length. The gripper jaws transfer the confectionary into the wrapping station. At this point two rotary-driven grippers clamp the film and twist, thus sealing the confectionary. From this station the gripper jaws transfer the wrapped confectionary to the ejection station. The function of this sub-mechanism is to push the wrapped confectionary from the transfer grippers onto a chute where the confection exits the machine.

4.2 Modelling and testing

In this study the physical measurements of the system were taken, and the operation was recorded with high-speed video footage. The system was then modelled using the constraint-modelling package. The resultant model was then compared with the high-speed video footage to verify the functionality. Figure 6 shows the ejection system modelled within the constraint modeller. The ejection system consists of a cam-driven four-bar chain with two fixed pivot points. The roughly circular form at the base of the model is the drive cam. The cranked arm attached to the fixed pivot point and resting on the drive cam is the cam follower. The upright line is the pushrod. The link is the line spanning the top of the pushrod and the top, fixed pivot point. The line descending from the top, fixed pivot point is the ejection arm.

4.3 Establish failure-mode constraints

With the model produced and tested the next stage was to define the factors that stop the model from functioning. The following failure modes were established for this example.

To identify when the limits (e) and (f) occur, hard limits are applied in the constraint-modelling program for the Cartesian position of the relative parts. The logic takes the form of a relationship statement. When this statement is true, the actions in the brackets are performed. This takes the form of writing a message to the screen, highlighting the mode of failure. It was also decided at this point to have a flagging system. When the system is functioning correctly each failure mode has a default value of one. When the failure-mode constraint value is reached this value is switched to zero. An overall flag value for the system was created as the product of all the individual failure modes. While the system is functioning correctly

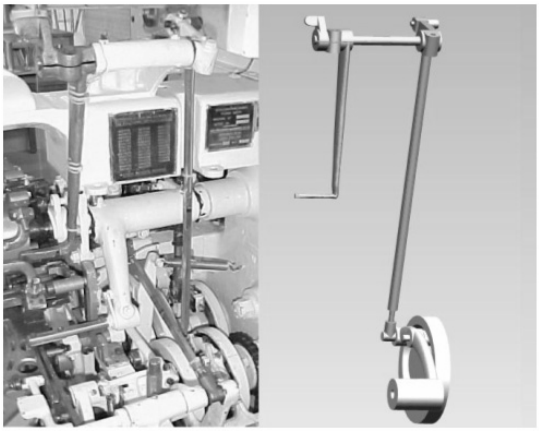

Fig. 5. *Ejection system*

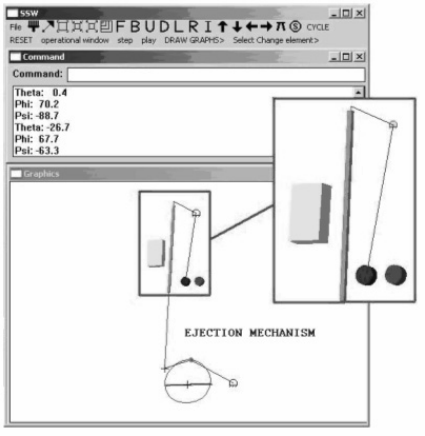

Fig. 6. *Constraint-based model of system*

Table 1. *Failure-mode constraints*

System-driven failure-mode Constraints	
MODE	**Description**
a	Ejection-arm movement is insufficient or incorrectly orientated to remove the confectionary
c	There is a breakage in the system
c	The pushrod interacts with the frame of the machine
d	The eject arm interacts with the pushrod of the system
e	The ejection-arm rest position is too far forward, causing a clash with other systems
f	Ejection-arm maximum position
Component-driven failure-mode constraints	
g	Excessive velocity

the default value is one. If any of the individual systems fail there its zero value will cause the overall system value to become zero. The constraint modeller performs assemblies by minimizing the error in constraint rules that represent the distance between parts. Its ability to do this can be used to access the success or failure of the assembly. The following function contains typical assembly rules. Once this *"assemble"* function has been invoked, the inbuilt function *"truth"* can determine its success (failure mode c). Cartesian positions recorded in model-simulation motion against time ratios are used to calculate the kinematics for the system, i.e., the failure mode (g). Solid elements are embedded into the model as a method for detecting the interaction of elements. Figure 6 shows the solid elements added to the ejection-system model. The four solid elements added to the model are the rectangular block to the left, which models the machine frame. The cylinder disc to the right of the model is the confectionary held in the machine jaws. The upright block on the pushrod is the body of the pushrod, and the cylinder disc at the end of the ejection arm is used to check the ejection-arm contact to the confectionary and the pushrod. The constraint modeller has the ability to identify the volumes of solid objects within a model using the *'volume'* function and this capability is utilized to detect element interaction. This method is also employed for failure mode (d), to identify the interaction of the ejection arm to the pushrod. As the construction of the ejection arm only requires a partial interaction with the confection to dislodge it from the transfer jaws onto the ejection chute, a limit value was set to look for an interaction of the solid disc modelled on the end of the ejection arm and the solid disc representing the confectionary. If a value, lower than this figure was achieved then the system was said to have failed under failure mode (a).

4.4 Parametric variations of system elements

With the modes for failure defined within the model the next stage is to configure multiple instances for the ejection system, then to check these instances against the failure-mode constraints. An individual element is selected by the user, and this element is then incrementally increased or decreased in size. The size of the other elements that make up the system were then increased and decreased in combination with the original elements until the model reaches one of the failure modes for the system noted in Section 3.3. This process was repeated until all possible configurations of element increase and decrease have been explored. The values from increasing and decreasing the elements are recorded individually to give a matrix of the functionality limits against the individual size of other elements. The maximum and minimum values recorded for these elements give us the functionality boundaries of the system. The values from running multiple instances of the system provide us with a matrix of functional points. As the functional points were recorded, it is also possible to run the model with specific failure modes active. This allows the user to retain information on which failure is active under which conditions and how the parametric variation affects individual elements.

4.5 The functional matrix

The matrix noted in Section 4.4 contains all the working points of the system. It can be seen from the partial matrix shown in Figure 7 that the working values can also have performance

ELEMENTS			PERFORMANCE		
n1	n2	n3	A1	J1	V1
385	-171	-165	1	-	1
385	-172	-165	1	-	1
385	-173	-165	2	-	1
385	-174	-165	2	-	1
385	-175	-165	2	-	1
385	-176	-165	2	-	1
385	-177	-165	2	-	1
385	-178	-165	2	-	1
385	-179	-165	2	-	1
385	-180	-165	2	-	1
385	-181	-165	2	-	1
385	-182	-165	2	-	1
385	-183	-165	2	-	1
397	-170	-165	2	-	1
398	-170	-165	2	-	1
399	-170	-165	2	-	1
400	-170	-165	2	-	1
401	-170	-165	2	-	1
402	-170	-165	2	-	1
403	-170	-165	2	-	1
385	-170	-162	1	-	1
385	-170	-161	1	-	1
385	-170	-160	1	-	1
385	-170	-159	1	-	0
385	-170	-158	1	-	0
385	-170	-157	1	-	0

Fig. 7. *Functional matrix*

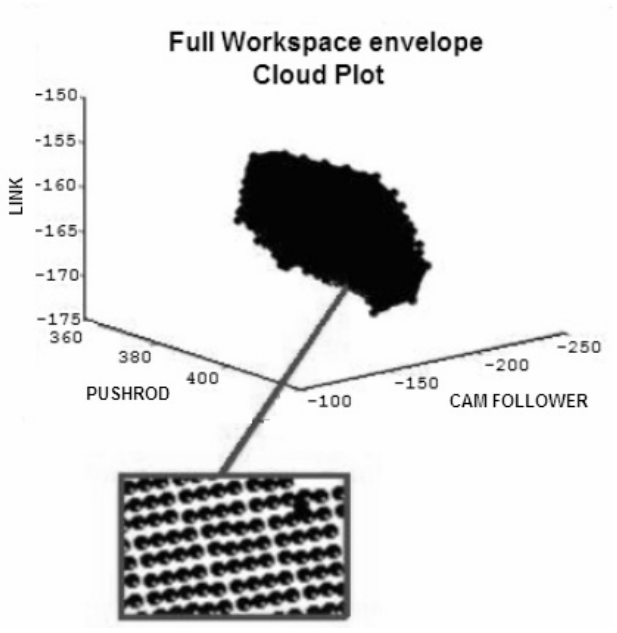

Fig. 8. *Cloud plot*

characteristics associated with them. These values could relate to accelerations, velocities or jerk (the third time-derivate of motion).

As mentioned in Section 2.1, by searching for the closest point to the new configuration, the matrix can be used to test whether a new product configuration is such that it lies within the limits of the system. The performance values can be used as an aid to find the best solution.

The production of a visual model describing the limits of the functional envelope can be very useful when you are evaluating the machine's ability to handle product variation and when optimizing performance. This section shows how two examples, the cloud map and the convex hull, can visually represent the results from the testing of the ejection system.

4.6 Cloud map plots

Figure 8 shows the cloud map plotted from the matrix in Figure 7. Each point plotted represents a line from the matrix. As noted previously, with the cloud map produced it becomes simple to test new configurations of the ejection system that may arise when new products need to be processed using the existing machine.

It is intended that future work with the methodology will centre on the usage of hyper-planes to dissect a modified cloud plot. This will give the option of using more than three elements for a change, while analyzing the system.

4.7 Convex hull

With the cloud map plotted a follow-on stage is to produce the convex hull. Figure 8 shows the convex hull for the ejection system generated using MATLAB®. The advantage of the convex hull is that it reduces the visual 'clutter' associated with the cloud map and gives a visual representation that is easy to understand and to interrogate.

4.8 Failure-mode plotting

It is also possible to run the model with the individual failure modes active. This allows the user to retain information on which failure is active under which conditions and how these effect the element variation.

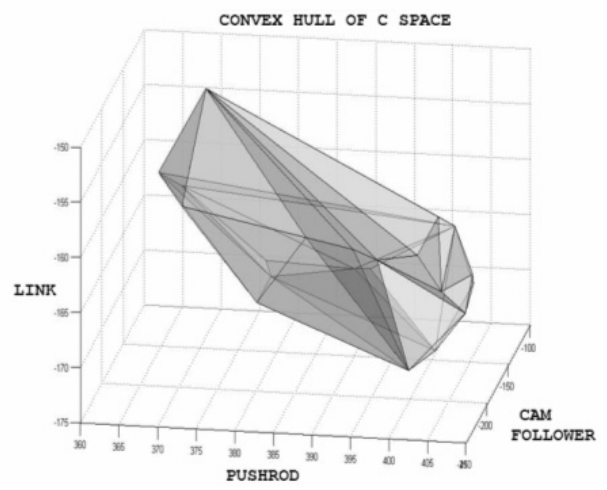

Fig. 9. *Convex hull*

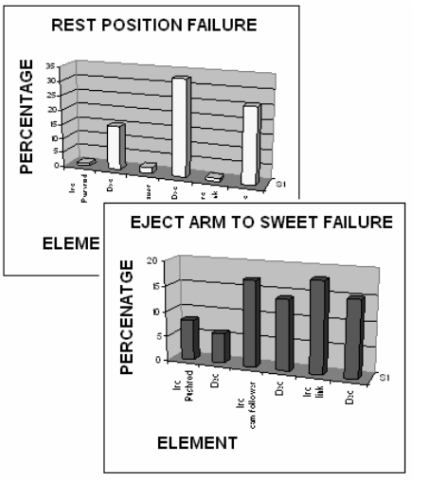

Fig. 10. *Failure-mode plots*

5 DISCUSSION

The case study has been described showing the use of the methodology for investigating the limits of an ejection system from a confectionary-wrapping machine. With the allowable space established and presented in visual forms, Figures 8 and 9, it becomes a straightforward process to test whether a given new product is such that it lies within the space and hence can be handled with that machine. In particular, it is clear that:

- In the original configuration the link dimension was close to its minimum limit. If a reduction adjustment to this link was required for a variant product change, it is likely that the cam follower and the pushrod will need modifying as well.
- It is highlighted that the link element was also the most sensitive to adjustment when investigating modifications, with the cam follower being the least sensitive.
- The best solution for any given system could be found by using either the matrix or the cloud plot diagram.

Figure 10 shows two of the six plotted failure-mode graphs. These are plotted to investigate the effects of the failure mode on the individual elements. From these graphs it was shown that from the original system configuration:

- the sweet contact mode allows for a large variation in configuration,
- for frame contact mode, only an element increase is permitted,
- for the maximum position and eject arm to frame the contact modes, only an elements decrease is permitted,
- the rest-position mode only allows small increases in element length, but it does allow large decreases.

With the graphical representations produced it became easy to understand the functional limits for the system. When modelling and recording the multiple instances of the system, it also became evident which elements were the most sensitive to change.

6 CONCLUSION

Generally, manufacturing machinery has been designed with the ability to process a range of products. Customer-focused manufacturing pressurizes manufacturers to produce ever-increasing families of products. So, what are the design implications, if the manufacturer has been asked to process a new or variant product? Does the machine have the inherent processing ability to manufacture the product? If not, what changes to the machine will give the ability to process the proposed product?

To address two questions, this paper has presented the limits of modelling methodology, where a constraint modelling environment is used within the environment, constraint optimization is employed for the structure and relationships of the system, and constraint checking is used to bound the model and its functionality against the given failure-mode constraints for the system and the processed product.

The specific outcomes of the methodology are as follows: It allows the opportunity for the engineer to investigate the redesign of a system to handle product variation. It offers the ability to represent failure-mode constraints into a constraint-based simulation/model. It permits a comprehensive sensitivity analysis to be performed on a design. It allows the functional envelope of a machine to be investigated and a range of visualization techniques can be employed to interrogate the analyzed design. The holistic constraint-based approach also offers the possibility for the engineer to optimize a design when resources are in conflict.

The current implementation has some limitations, i.e., at the construction stage the numerical techniques employed, and the struggle to handle large amounts of constraints and variables. At present the largest system modelled, a transmission system, had twenty-one variables and ten constraint rules. To overcome this, current work is concentrating on strategies for more complex systems. It is intended to employ the information gain from the initial sensitivity analysis to produce a network strategy for this purpose. Also, the selection of a visual representation is important. In the example, a convex hull was employed. Due to the convex nature of the representation it does have the weakness of overestimating the design area. Because of this, the surface plots and failure-mode maps present the greatest potential. The approach described in this paper is currently being employed to investigate the capability of UK food-processing equipment to handle product variation.

Acknowledgments

The research described in this paper has been carried out with the support of a Department of Environment, Food and Rural Affairs (DEFRA) research grant given as part of the Food Processing Faraday Knowledge Transfer Partnership (FPF-KTP). This support is gratefully acknowledged together with that of other collaborators.

7 REFERENCES

[1] Hanlon, J. F., Kelsey, R. J and Forcini, H. E.(1998) Handbook of package engineering. *Technomic Publishing Company*.

[2] Shigley, J. E and Uicker, J. J. (1995) Theory of machines and mechanisms. *McGraw-Hill International Editions*

[3] Freudenstein. F. (1956).On the maximum and minimum velocities and accelerations in the four-link mechanisms. *Transactions of the ASME* 1956,78, 779.

[4] Mable, H. H and Ocvirk, F. W(1965). Mechanisms and dynamic machinery. *J.Wiley and sons*. London.

[5] Dwivedy, S. K and Eberhard, P., Dynamic analysis of flexible manipulators, a literature review *Mechanism and Machine Theory*, 41(7),2006, 749-777

[6] Woolfson, M. M and Pert, G. J. (1999), Introduction to computer simulation, *Oxford University Press*.

[7] Gould, H. and Tobochnik, J.,(1996). An introduction to computer simulation methods: Applications to physical systems, *Addision-Wesley.*

[8] PTC Inc., 2005 Pro/ENGINEER Solutions. http://www.ptc.com/appserver/mkt/products/home.jsp?k=403

[9] Unigraphics NX3, http://www.ugs.com/products/nx/ (accessed December 2006)

[10] MSC Adam. http://www.mscsoftware.com/products/adams.cfm (accessed January 2007)

[11] BOSS Quattro. SAMTECH. http//www.samtech (accessed January 2007)

[12] NOESIS PLM. http://www.noesissolutions.com/index.php?col=/products&doc=PLMO (accessed January 2007)

[13] CATIA V5, Project engineering optimizer. http://www-306.ibm.com/software/applications/plm/catiav5/v5-latest.html . (accessed January 2007)

[14] Hicks. B.J., Medland.A.J., Mullineux.G. (2001) A constraint-based approach to the modelling and analysis of packaging machine. *Packaging technology and science* 14 (2001) 209-225.

[15] Hicks. B.J., Medland.A.J and Mullinux. G. (2003) A constraint-based approach for optimum redesign of a packing operation. *Packaging technology and science* 16 (2003) 135-148.

[16] Barton, P. I and Lee, C .K (2002) Modelling, simulation, sensitivity analysis and optimization of hybrid systems. *ACM Transactions on Modelling and Computer Simulation*, 12 (4) (2002), 256-289.
[17] Hussu, A (1999) Analysis of dynamic systems by Bond-graphs. *Strojniški Vestnik-Journal of Mechanical Engineering* 45 (1999). (7-8), 278-286.
[18] Pusey.J , Fattah.A , Agrawal.S and Messina.E (2003) Design and workspace analysis of a 6–6 cable-suspended parallel robot. *Procs IEEE/RSJ International Conference on Intelligent Robots and Systems*, Las Vegas, NV, 2003.
[19] Curto, B., Moreno, V and Blanco, F. J., A general method for c-space evaluation and its application to articulated robots. *IEEE Transactions on Robotics and Automation*, 18(1):24–31, 2002
[20] Kazerounian, S. M. K. and Gupta, K. C., (1982) Synthesis of position generating crank-rocker or drag-link mechanisms,' *Mechanism and Machine Theory*, 17: 243-247, 1982.
[21] Botturi,D., Fiorini,P and Martelli.S. (2003)A geometric method for robot workspace computation *Proceedings of ICAR03 - The 11th International Conference on Advanced Robotics* (2003).
[22] Gosselin, C. M., Lavoie. E and Toutant, *P ASME 22nd Biennial Mechanisms Conference*, 45, Scottsdale, 1992, 323–328
[23] Lin, V. C., Gossard, D. C. and Light, R. A. (1981), Variational geometry in computer-aided design, *Computer Graphics* 15(3), 171–177.
[24] Merlet, J. P. (1995)Designing a parallel robot for a specific workspace. *Rapport de Recherche* 2527, INRIA, 1995.
[25] Culley, S. J. (1999) Future issues for engineering design research. *UK Department of Trade and Industry (DTI) Workshop and Report*. Bath, 18,19th Feb 1999.
[26] Matthews, J., Singh, B., Mullineux, G., Medland, A.J., and Hicks,B.J. (2006). Constraint modelling as a means for understanding the limitations of a design and its performance. *Proc 6th International conference on Integrated design and Manufacturing in Mechanical Engineering.* (IDMME) 2006 Grenoble, France.
[27] Lin, L and Chen, L. C. (2002) Constraints modelling in product design. *Journal of Engineering Design*, 2002, 13(3) 205-214.
[28] O'Sullivan (2002) Constraint-aided conceptual design, *Professional Engineering Publication Limited*, London 2002.
[29] Sandgren, E (1990) A multi-objective design tree approach for optimisation of mechanisms. *Mech Mach Theory*, 25(3), 257-272, 1990
[30] Ding, L., Yue, Y., Ahmet, K., Jackson, M and Parkin, R. Global optimization of a feature-based sequence using GA and ANN techniques. *International Journal of Production Research*, 2005, 15(1) 3247-3272.
[31] Márkus, A., Váncza, J., Kovács, A., (2002), Constraint-based process planning in sheet metal bending, *Annals of the CIRP*, 51/1: 425-428
[32] Sadeh, M, and Fox, N,(1996) Variable and value ordering heuristics for job shop scheduling constraint satisfaction problem, *Artificial intelligence*, 86, 1-41 (1996)
[33] Mullineux.G. (2001)Constraint resolution using optimization techniques. *Computers & Graphics*, 25, Issue 3, June 2001, Pages 483-492.
[34] Anderl, R., and Mendgen, R., (1996). Modelling with constraints: theoretical foundations and application, *Computer-Aided Design* 28 (1996) 155-68.
[35] Li, W. D., Ong, S. K. and Nee, A. Y. C., (2002) Hybrid genetic algorithm and simulated annealing approach for the optimization of process plans for prismatic parts. *International Journal of Production Research*, 40, 1899
[36] Beck, H. A. (1992) Constraint monitoring in TOSCA. In *Working Papers of AAAI Spring Symposium: Practical Approaches in Planning and Scheduling*, Stanford, CA, March 1992.
[37] Young, R., Greef, A and Ogrady, P., (1992)An artificial intelligence-based constraint network system for concurrent engineering. *International Journal of Production Research*. 30(7), 1715-1735.
[38] Bowen, J and Bahler, D (1992) Frame, quantification, perspectives, and negotiation in constraint-networks for life-cycle engineering. *Artificial Intelligence in Engineering*, 7(4), 119-226.

[39] Frank, P. M (1978) Introduction to systems sensitivity theory. *Academic Press*. New York.
[40] Detcher, (2003) Constraint process, *Kaufmann Publishing*, USA
[41] Leigh R.D., Medland A.J., Mullineux.G. and Potts I.R.B Model spaces and their use in mechanism simulation. Proceedings of the I. Mech. E part B *J.Eng. Manufact*. 203 (1989):167-74.
[42] Gindy, N.N and Saad, S.S (1998) Flexibility and responsiveness of machining environments. *Integrated Manufacturing Systems*. (4) 218-227.
[43] Corney, J. (1997) 3D Modelling with the ACIS Kernel and Toolkit. *Wiley*: Chichester.
[44] Mullineux, G. (2006) Capability of food processing equipment to handle product variation. COFFEE Project report SID5 FT1106. *Department of Environment, Fisheries, and Rural Affairs (DEFRA)* July 2006.

Authors' Address:
Jason Matthews
Baljinder Singh
Prof. Dr. Glen Mullineux
Prof. Dr. Tony Medland
University of Bath
Department of Mechanical Engineering
Bath BA2 7AY, U. K.
j.matthews2@bath.ac.uk
b.singh@bath.ac.uk
g.mullineux@bath.ac.uk
a.j.medland@bath.ac.uk

Prejeto: 2.5.2007
Received:
Sprejeto: 27.6.2007
Accepted:
Odprto za diskusijo: 1 leto
Open for discussion: 1 year

Strojniški vestnik - Journal of Mechanical Engineering 53(2007)7-8, 478-490
UDK - UDC 677.057.78
Izvirni znanstveni članek - Original scientific paper (1.01)

Omejitve, ki vplivajo na konstrukcijo stebla z ramenom in uporaba natančne geometrije

Constraints Influencing the Design of Forming Shoulders and the Use of Exact Geometry

G. Mullineux - C. J. McPherson - B. J. Hicks - C. Berry - A. J. Medland
(University of Bath, United Kingdom)

Prispevek obravnava konstrukcijo stebla z rokavom pokončne naprave za oblikovanje, polnjenje in zapiranje embalaže. Kakor pri večini strojev za embaliranje, je tudi tu konstrukcija doživela vrsto popravkov in temelji na mnogih izkustvenih pravilih, ki jih je težko in drago uveljaviti naprej. Da bi zmanjšali ta vpliv, poskušamo s tem prispevkom raziskati medsebojna vpliva stroj - material in kako sama konstrukcija vpliva na to. Obravnavana in najbolj vplivna je geometrijska oblika ramena, katere zahtevna narava definiranja je v razpravi, skupaj s konstrukcijskimi izvedbami, ki vplivajo na učinkovitost stroja v pomenu napetosti folije in možnosti pravilnega vodenja. V industrijski praksi se raje spremeni geometrijsko obliko tako, da je vodenje boljše, čeprav se s tem poveča napetost v plašču. Eksperimentalne ugotovitve z natančnimi rameni so pokazale, da imajo boljše vodenje od običajnih in da lahko delujejo s širšim razponom materialov. Ugotovili smo tudi, da je mogoč drugačen način konstrukcije ramena, in sicer z začetno usmeritvijo na napetost plašča namesto na vodenje. Ker natančen rokav pokriva širši razpon materialov, je bilo ugotovljeno tudi, da je mogoče konstruirati stroje z manjšim številom delov.

(Ključne besede: CAD, modeliranje izdelkov, stroji za embaliranje, geometrijske oblike)

This paper considers the design of the forming shoulder, which is a crucial part of a vertical form, fill and seal machine used for packing small discrete items. As with other forms of packaging machine, the basic design has evolved over a number of years and is based on a number of empirical design rules, whose application can be time consuming and costly. To address this issue, the aim of this paper is to investigate the effects of machine-material interaction and the parameters of the design that influence these effects. In particular, the geometry of the shoulder is considered and means for defining its complex form discussed, together with the design issues related to the performance of the machine in terms of web tension and its ability to track correctly. In industrial practice, a modified form of the geometry is used to encourage better tracking, even though this increases web tension. An experimental investigation with exact shoulders has shown that they have better tracking properties than conventional ones and that they can deal successfully with a wider range of materials. It has also been found that a different approach to the design of the shoulder is possible, concentrating initially on web tension rather than tracking. As an exact shoulder can handle a wider range of materials, it is also found that it is possible to design machines in which fewer change parts are required.

(Keywords: computer aided design, product modeling, form-fill-seal machines, forming shoulders)

0 INTRODUCTION

The production of packaging machinery is a highly competitive global market driven by the ever-increasing demands of customers and legislation ([1] and [2]). In 2000, American exports of packaging machinery were valued at just under $5 billion [3]. Packaging manufacturers continue to try to improve the performance of their machines with the aim of increasing the production capabilities, improving reliability and reducing down time and production costs [1]. To do this

successfully it is important not only to improve the machines themselves, but also to understand the interaction between the packaging materials and the machines [2]. Recent legislation, such as the European Packaging Waste Directive, aims to reduce the amount of material being used in packaging. This means that the producers of Fast Moving Consumer Goods (FMCG) are trying to use thinner, lighter weight and recycled packaging materials to take their products to the consumer. The changing specification of materials and the need to meet new requirements puts additional pressure on machinery manufacturers to update their machines.

The underlying design principles of many packaging machines are the result of incremental improvements over the years [4]. In many sectors of the industry, designers lack the fundamental understanding of the process and, of increasing importance, is an understanding of the machine-material interface, which more often than not dictates the performance capabilities of the machine. In today's competitive environment mathematical modelling and simulation are the preferred choice for the design of processes and machine systems rather than the trial-and-error methods still used in some sectors of the industry.

This paper considers a particularly complex production process, i.e., the vertical form, fill and seal machine ([5] and [6]). An example is shown in Figure 1. This is used for the creation of bags or pouches from a reel of packaging material. Such a process is commonly used to package food items like confectionary, biscuits, and snacks ([7] to [9]), and disposable medical devices [10]. It is also possible to use the machines to packages liquids [11].

The material for a vertical form, fill and seal machine is usually supplied as a flat, pre-printed sheet of uniform width and stored on a roll. Figure 1 shows a vertical form, fill and seal machine, and Figure 2 shows a schematic view of the machine illustrating how the film or paper is taken from a roll and bags produced.

A single web of material is drawn from the roll and fed over a forming shoulder that guides the material from the flat into a cylindrical shape around the product feed tube. The action of forming the cylinder brings the edges of the film together. They are either over-lapped so that the opposite sides of the film meet producing a lap seal, or the internal sides of the film are brought together to form a fin seal. The seal itself is usually produced by applying heat and pressure.

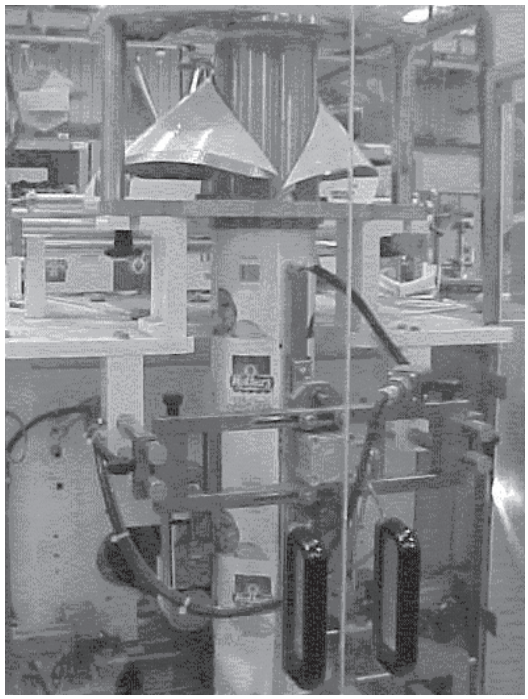

Fig. 1. *Vertical form, fill and seal machine*

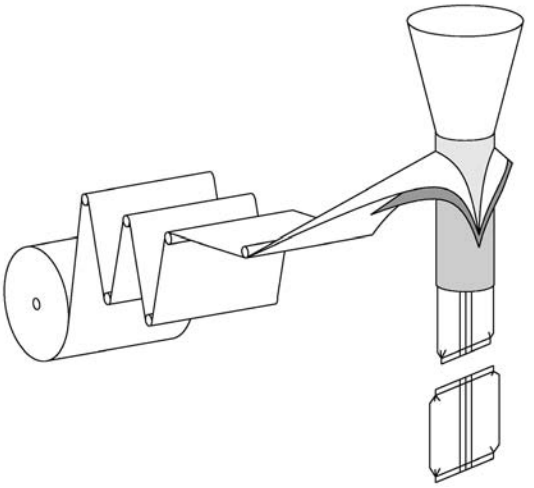

Fig. 2. *Schematic of the use of a forming shoulder*

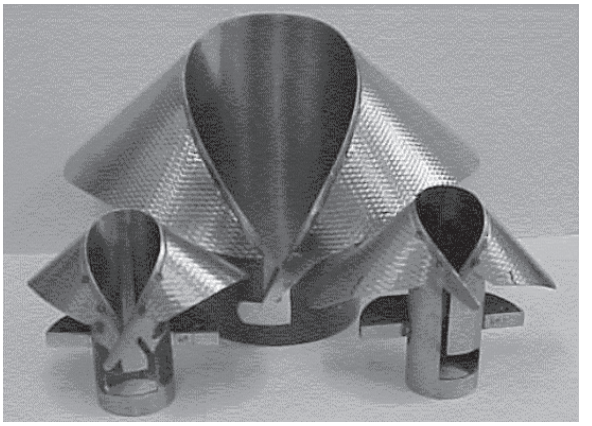

Fig. 3. *Examples of forming shoulders*

The process has now created a tube into which the product is dropped in measured quantities. The packaging material is then cross-sealed and cut to form the complete bag. The action of making this final seal also forms the bottom seal of the next bag. This approach can be adapted to produce a variety of different packs, including packs with flat bottoms and tetrahedral tea bags [1].

In the final stages of formation, the bag is formed around a tube. Often, this is of circular cross-section. Some attention has been given to the cases in which the cross-section takes other forms ([12] to [14]). However, little work has been undertaken which investigates the impact of changes in geometry on the performance of the shoulder and its interaction with a given material, although a historical overview of how materials have evolved over the last half century is available [15].

A number of problems are recognised with vertical form, fill and seal machines. The chief of these is concerned with tracking. This is the ability of the film to pass over the forming shoulder without moving off to one side (or oscillating). Poor tracking results in malformed bags and, in extreme cases, in the film jamming in the machine. It is usually thought that increasing the tension in the web of material improves the ability to track properly. However, excessive tension leads to another problem, which is stretch, or even tearing, of the material. The third problem is creasing or other distortion of the web as it passes over the shoulder.

The aim of this paper is to investigate the effects of machine-material interaction and the parameters of the design that influence these. There are three areas where the machine and material interact: the feed system where the film leaves the roll, the passages over the forming shoulder, and the traction system below the shoulder which pulls the material through. Each acts to increase the web tension. The one that seems to have the largest effect is the shoulder and it is the design of this that is considered in this paper. Some typical shoulders are shown in Figure 3.

A small number of authors ([16] to [18]) have attempted to represent the geometry of the forming shoulder. The details of such a representation are considered in Section 1. This leads to the parametric model for the geometry that is used here.

The model can be combined with search and bound techniques to investigate the feasible performance envelope for the full range of changes in the design variables of the forming shoulder. This is discussed in Section 2.

The results of this investigation are considered in conjunction with an experimental study into material flow over forming shoulders. The resulting design rules help to provide a more fundamental understanding of the relationships between the design parameters of the forming shoulder, its performance capabilities and the properties of the material.

Factors such as compliance, stiffness and surface friction are particularly important. These properties determine the force necessary to draw the material over the shoulder. If this known, it can be compared with the maximum loading that the material can accommodate before it distorts or fails.

In order to relate these factors to the theoretical investigation, it is necessary to understand the relationship between the shoulder design, tracking and loading. Through experimental studies, given in Section 3, it is shown that the force required to draw the material over the shoulder can increase by 100% for a corresponding decrease in height:radius ratio by a factor of two. Similarly, the ability to control the tracking improves as the height:radius ratio decreases. These practical findings can be combined with the results of the theoretical modelling to generate a set of design rules and a more robust design method for conventional shoulders. These design rules help to provide a more fundamental understanding of the relationships between the design parameters of the forming shoulder, its performance capabilities and the properties of the material.

In particular, what has been found is that the use of shoulders where the geometry is exactly that prescribed by the model tends to result in improved tracking properties. Section 4 gives details of this. What this means is that when a shoulder is designed for a new material there is less need to concentrate upon the tracking aspects. This is discussed in Section 5. The significance of this is that it suggests a different approach to the design of forming shoulders to handle given materials. It means that, initially, tracking can be ignored and instead attention can be focused on the issue of tension and keeping this as low as possible.

1 MODEL OF THE FORMING SHOULDER

Typical forming shoulders are shown in Figure 3, and Figure 4 shows the basic geometry. This comprises the tube (Figure 4(c)) and the collar (Figure 4(d)). The geometry is to a certain extent specified by that of the bag to be produced. For example, the tube of the forming shoulder must have a circumference equal to twice the width of the bag.

The main determining factor for the geometry of the shoulder is the bending curve. This forms the edge over which the film passes. The bending curve can be regarded as a planar curve of (roughly) parabolic shape, as shown in part (a) of Figure 4.

The vertical tube can be thought of as being formed by wrapping the part below the curve into a circular cylinder. Similarly, if the part above the planar bending curve is wrapped around, then it forms the collar surface. The assembly of these two pieces is shown in Figure 4(b).

With a vertical form, fill and seal machine the material is fed from a roll. This means that it starts as a plane and so there needs to be a smooth transition between the flat plane and the curved

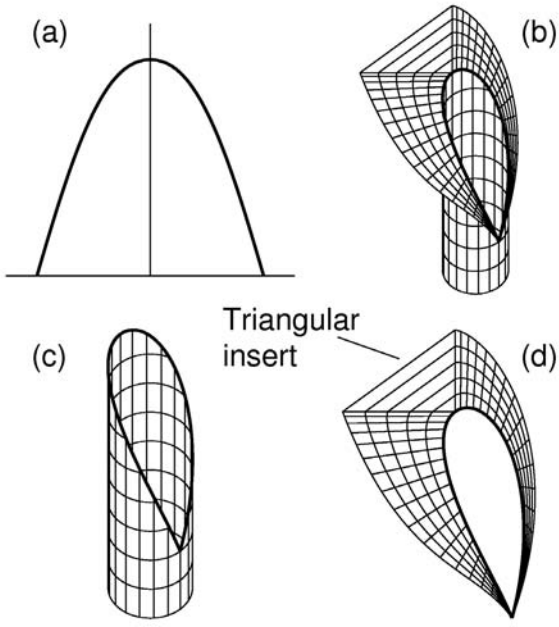

Fig. 4. *Bending curve and shoulder*

collar. To achieve this, a triangular planar surface is usually inserted into the collar surface at its highest point. This is shown in Figure 4(d).

The geometry of the collar surface is complex and there are many constraints upon it. It is important to be able to describe its shape by some form of geometric model.

A model based on two conic surfaces separated by a planar triangle can be used [18]. The bending curve can be taken as the intersection of the surface with a circular cylinder. In this way a collar surface containing a triangular planar insert at its highest point can be created directly.

Although this approach is workable, the resulting set of shoulders that can be used in practice is somewhat limited. There are more versatile approaches available that depend upon initially selecting suitable bending curves in their planar form ([16] and [17]). It is this latter approach that is discussed here.

It is clearly important that the material should not wrinkle, stretch or tear as it passes over the shoulder. This means that the collar surface must be isometric to a plane. Thus the collar needs to be a developable surface ([19] and [20]). Such a surface is formed from a collection of straight-line generators.

As noted in [16], it follows from a result in differential geometry [19], that for a given bending curve wrapped around a cylinder, there are two developable surfaces that contain the curve. One of these is the cylinder itself and the other can be used to define the collar.

Suppose that κ is the curvature of the bending curve when wrapped around the cylinder and that $\bar{\kappa}$ is the curvature of the corresponding planar curve. It is clear that $\bar{\kappa}$ is smaller than κ. Let θ denote the angle between the surface normal to the cylinder and the collar at a typical point on the bending curve. This is also the angle between the tangent planes to the two surfaces. Then, as in [16], this angle is related to the curvature as follows:

$$\cos\theta = 1 - 2(\bar{\kappa}/\kappa)^2$$

If $z(v)=0$ is the equation of the planar bending curve (for $-\pi R \le v \le \pi R$, where R is the radius of the tube), then the curvatures can be found [16] and the above relation can be expressed as follows:

$$\cos\theta = -(R^2 z_{vv} - z_v^2 - 1)/(R^2 + z_v^2 + 1) \quad (1),$$

where the subscript v denotes partial differentiation with respect to v.

If extended sufficiently, the collar surface has an edge of regression along which it turns back on itself. Such a singularity needs to be avoided on that portion of the surface used for the collar itself. It is normally arranged so that the edge of regression lies within the region occupied by the circular cylinder. From [16], the condition for this is the following:

$$R^3 z_{vvvv} + R z_v < 0 \quad (2).$$

Straight-line generators that emanate from the bending curve form the collar surface. Provided the curve is smooth, the generators emanate at smoothly varying angles and the surface is well formed and continuous. However, it turns out that if the curve has a discontinuity at its highest point, then the generators on either side are in different directions and a planar triangle can be inserted into the collar. Suppose that the bending curve $z(v)$ in its planar version is an even function so that $z(-v) = z(v)$ and the surface has symmetry. The required discontinuity is in the third derivative of z at v=0, the derivative being continuous everywhere else [16].

Suppose that β is the angle between the generators at the highest point of the bending curve. Then this is also the angle at the apex of the inserted triangle. The following expression determines β, where it is assumed that the sign convention and choice of bending curve is such that $z_{vvv}(0+)$ is negative:

$$\tan(\beta/2) = -(2R^2 z_{vvv}(0+)/(R^2 z_{vv}^2 + 1) \quad (3).$$

A purely parabolic bending curve does not allow sufficient freedom to obtain the required discontinuity. So a modified curve is used [16], which is as follows:

$$z = R f(\xi)$$

where:

$$\xi = v/R \text{ for } -\pi \le \xi \le \pi$$

and $f(\xi)$ is the even function given by:

$$f(\xi) = c_0 + c_2\xi^2 + c_3\xi^3 + c_4[\cos\xi - 1 + \xi^2/2] + c_5[\sin\xi - \xi + \xi^3/6] \text{ for } \xi \ge 0 \quad (4).$$
$$f(\xi) = f(-\xi) \text{ for } \xi < 0$$

Four main design parameters can be identified. These are shown in Figure 5, and are discussed below.

h / R is the ratio of the height h of the wrapped bending curve to the radius R of the cylindrical tube.

θ_0 is the back angle, which is the angle between the tangent plane of the shoulder surface and that of the cylinder at the highest point of the bending curve (equivalent to the angle between the normal to the surface and the normal to the tube).

θ_1 is the front angle, which is similar to the angle between the tangent planes of the surface and the tube at the lowest point of the bending curve.

β is the opening angle, which is the angle at the apex of the triangular insert.

There are restrictions on the choices for the coefficients in Equation (4). The first of these are the end conditions at $\xi = 0$ and $\xi = \pi$.

$$h/R = c_0 \tag{5}$$

$$0 = c_0 + c_2\pi^2 + c_3\pi^3 + c_4(-2 + \pi^2/2) + c_5(-\pi + \pi^3/6) \tag{6}.$$

If Equation (1) is applied to determine the back angle θ_0, then the following equation for coefficient c_2 results.

$$c_2 = - (1/2) \tan(\theta_0/2) \tag{7}.$$

Similarly, Equation (3) relates the coefficients to the opening angle β.

$$\tan(\beta/2) = - 12c_3 / (4c_2^2 + 1) \tag{8}.$$

The relation between the coefficients and the front angle θ_1 is obtained from applying Equation (1) at the lowest point of the bending curve.

$$(f''(\xi))^2 = [(f'(\pi))^2 + 1] \tan^2(\theta_1/2) \tag{9}.$$

Additional relations also apply. The first two of these ensure that the planar bending curve has its turning point at $\xi = 0$ and is concave downwards.

$$f'(\xi) = 0 \text{ and } f''(\xi) < 0 \text{ for } 0 \le \xi \le \pi \tag{10}.$$

A third relation follows from Inequality (2), which is the condition that there are no singularities in the collar surface.

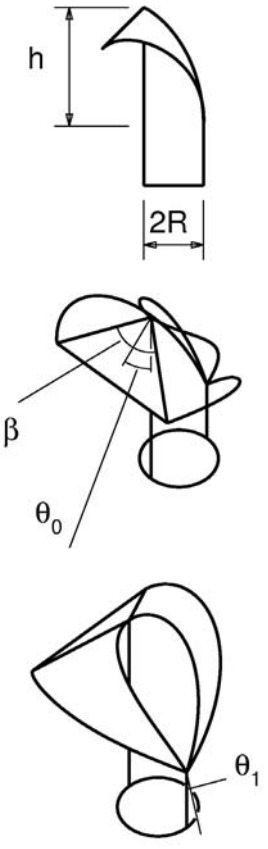

Fig. 5. *Parameters of a shoulder*

$$f''''(\xi) + f''() < 0 \text{ for } 0 \le \xi \le \pi \tag{11}.$$

For the given form of the bending curve, the left-hand side of this inequality is linear in ξ since the trigonometric terms involved in Equation (4) cancel out.

$$f''''(\xi) + f''(\xi) = (2c_2 + c_4) + (6c_3 + c_5)\xi \tag{12}.$$

Hence, Inequality (11) holds for the whole bending curve if and only if it holds at both $\xi = 0$ and $\xi = \pi$.

The method for finding a bending curve, given the four design parameters, is to start with Equations (5), (7), and (8) and determine c_0, c_2 and c_3. Equations (6) and (9) lead to a quadratic equation for c_4, which leads in turn to two values for c_4 and hence two values for c_5. Of these pairs of values, only one satisfies Relation (10) for $\xi = \pi$. Once the coefficients have been established,

Relations (10) and (11) need to be checked over the entire curve.

These additional inequality constraints mean that some configurations of design parameters generate coefficients that are not acceptable. Thus the class of shoulders that can be generated is restricted. It is beneficial at the design stage to have some understanding of what these restrictions are.

2 DESIGN LIMITATIONS

What emerges from studying industrial practice for designing forming shoulders is that there are several constraints involved. These limit what can be achieved.

The constraints fall into two classes. One class emerges from pure geometric considerations, centred around the shoulder geometry. As discussed in the Section 2, the geometry of the shoulder is critical and needs to be carefully defined to allow material to flow over it easily and without damage. In the design of the shoulder there is a small number of parameters that are at the designers disposal, but these are interrelated and this imposes limits on the designer's choice.

The other class of constraints arises from how the shoulder behaves in use and this involves the question of machine-material interaction. This includes frictional effects, which in turn helps to determine the (minimum) tension required in the web. If the tension is too large then damage to the material and to the shoulder itself may occur. Another important issue is tracking. This is the ability of the material to flow directly and symmetrically over the shoulder and not to veer away to one side. If tracking is poor, then the machine needs to be stopped and reset at frequent intervals and the quality of the packaging can be significantly reduced.

It is clear that the shoulder geometry is very dependent upon the shape of the bending curve. For example, Inequality (11) involves the fourth derivative of the curve. Only slight deviations in the curve due to manufacturing errors or to wear can easily result in this condition being violated. In practice, however, the compliance of the material is sufficient to ensure that some deviations do not have a significant effect, even if a theoretical constraint does not hold. However, this may lead to damage to the material itself.

Some of these limitations on the geometry of the shoulder are investigated in this section; particularly those associated with Relations (10) and (11). More details are given in [21].

The back angle θ_0 is one of the four design parameters. For given values of the other three, there is only a small range of allowable values for θ_0. The graphs in Figure 6 show the lower and upper bounds for θ_0 in a number of cases, in each of which the front angle $_1$ is 10^o. The graphs are for different values of the opening angle β. Each gives plots of the lower and upper limits of θ_0 against the height:radius ratio.

The plots show that there is a lower limit for the height:radius ratio, below which a shoulder is not possible. Just above this lower limit, the choices for θ_0 are bounded. The bounds on the interval of choice widen with the ratio and then the interval becomes roughly constant at around 17^o.

Figure 7 shows the corresponding graphs for the case when the front angle θ_1 is 30^o. These have the same form and again there is a lower limit on the height:radius ratio. This lower limit is slightly higher than in the previous case. However, the most obvious difference is that the curves have moved apart. The lower bound curves have moved significantly to the right and there is a smaller move of the upper bound curves. So there is now a greater choice for the back angle θ_0 for any given value of the height:radius ratio.

The effect that changing the bending curve has on the collar surface is now considered. Shoulders with a front angle θ_1 at 10^o and an opening angle β at 90^o (a common value in practice) are taken for a number of height:radius ratios. The bending curve is found for each when the back angle θ_0 is at the middle of its allowable range. The value of θ_0 is disturbed by a small amount up to 5^o either side of this mid-curve. The largest deviation in the bending curve is identified and plots of these against the change in the back angle are shown in Figure 8. The gradients of these curves provide a measure of the sensitivity of the bending curve to changes in the back angle. The sensitivity increases with the height:radius ratio. Arguing conversely, small changes in the bending curve (which leave it smooth) have the greatest effect on the surface when the height:radius ratio is large.

Now consider the effects of small localised changes to the bending curve. These might arise from wear or damage. In Equality (11) the conditions may become violated and cause the film to distort or buckle. Suppose the bending curve

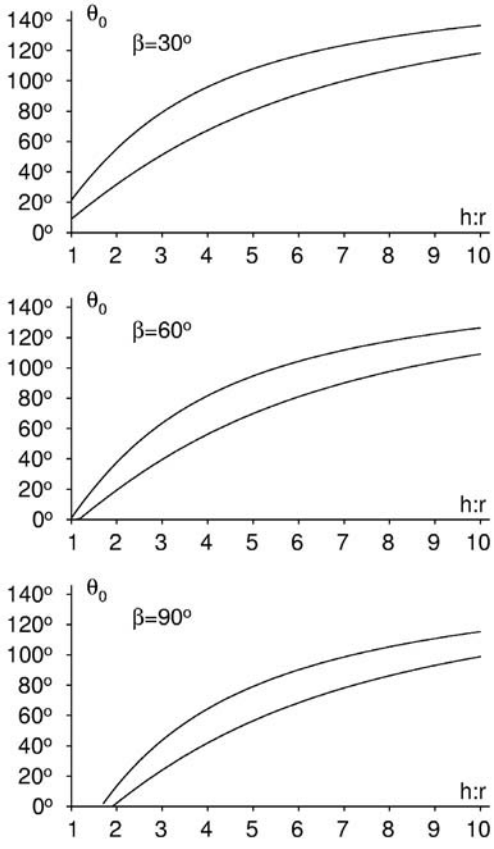

Fig. 6. *Upper and lower bounds of back angle θ_0 for front angle $\theta_1 = 10^o$ and various opening angles β*

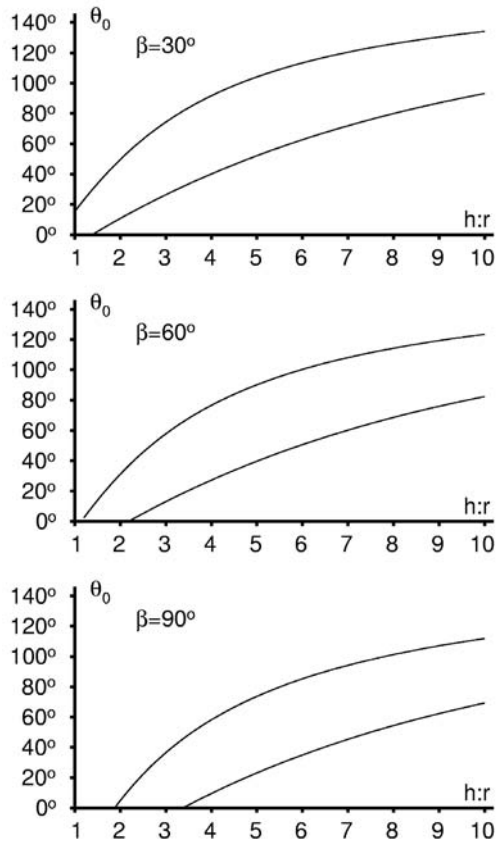

Fig. 7. *Upper and lower bounds of back angle θ_0 for front angle $\theta_1 = 30^o$ and various opening angles β*

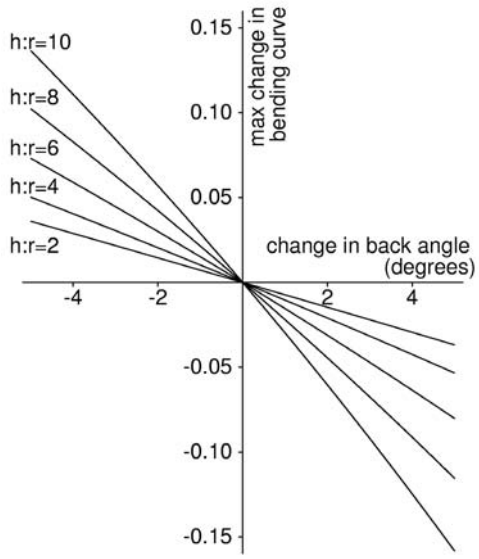

Fig. 8. *Sensitivity of bending curve to changes in back angle θ_0 when $\theta_1 = 10^o$ and $\beta = 90^o$*

becomes modified from $f(\xi)$ to $f(\xi) + e(\xi)$ where e (which may be zero for most values of ξ). The required inequality is the following:

$$| f''''(\xi) + f''(\xi) | + | e''''(\xi) + e''(\xi) | < 0$$

and using Equation (12) this is the same as:

$$[(2c_2 + c_4) + (6c_3 + c_5)\xi] + |e''''(\xi) + e''(\xi)| < 0$$

Figure 9 shows plots of the first term in square brackets, for ξ between 0^o and 180^o in a number of cases. These plots are all when the front angle θ_1 is 10^o and the opening angle β is 90^o. The cases are when the height:radius ratio is 2, 4, 6, 8 and 10, and, for each, the front angle is taken at its lower and upper bounds. It is clear that the value becomes more negative as the ratio increases. This suggests that for higher ratios, small (local) deviations in the bending curve are more likely to be accommodated.

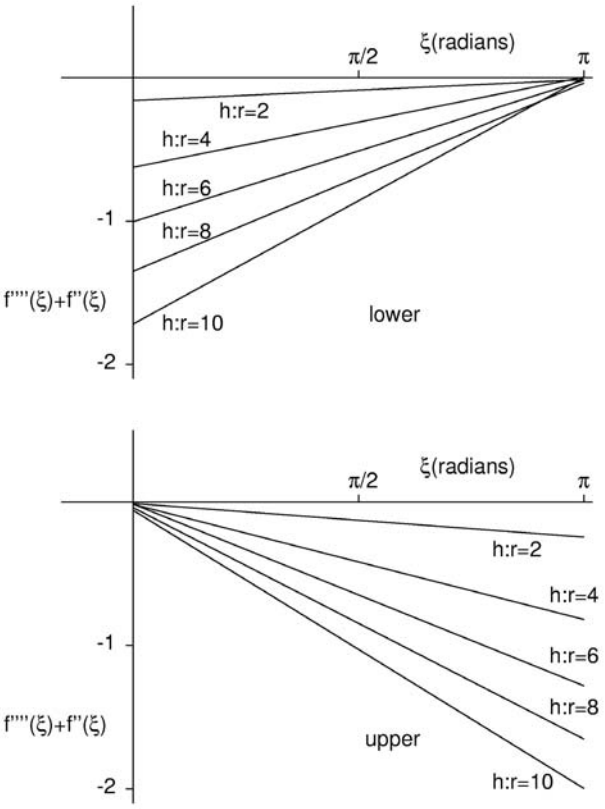

Fig. 9. *Graphs of f ””(ξ) + f ”(ξ) for various height:radius ratios and back angles θ_0 with $_1$ = 10° and β = 90°*

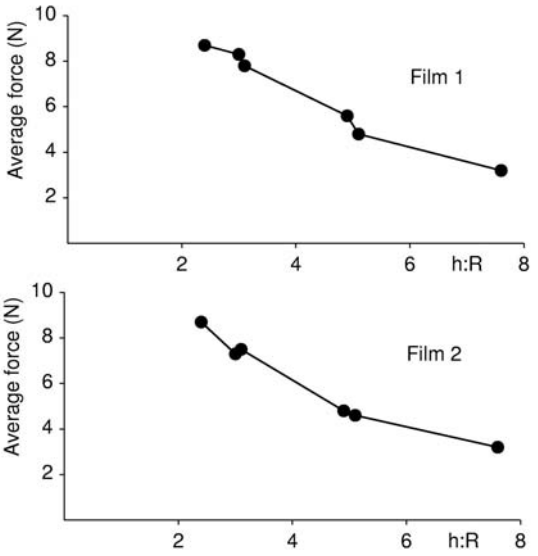

Fig. 10. *Forces required to pull films over shoulders*

3 PULLING FORCES

As well as the purely geometric properties of a shoulder, its interaction with the packaging material is important. This section discusses the force required to pull material over the shoulder surface. The higher the force that is needed, the more likely that damage occurs to the material.

Experiments have been conducted to investigate the force required to draw material over a range of forming shoulders. Two different films were tested across six forming shoulders. The shoulders were selected to represent the continuum of feasible height:radius ratios for a particular bag width.

To perform the tests, a strip of material was used, whose width was slightly less than the corresponding bag width. This helped in setting up the experiment and took account of the fact that the industrial shoulders used were not designed for precisely the same bag width.

The strip was centred around the highest point of the shoulder and drawn over the shoulder at a constant speed. The free end of the strip was loaded with a range of weights to represent the pre-tension in the web.

The graphs in Figure 10 are for the two films. In fact, the results for both are very similar. What is clear is that the pulling force required is significantly less for shoulders with higher height:radius ratios. As the ratio doubles between 3 and 6, so the force halves from (approximately) 8N to 4N.

This suggests that if a material is susceptible to damage from being stretched, then a shoulder with a high height:radius is required.

4 USE OF EXACT SHOULDERS

Section 1 discusses the geometry of a shoulder that is isomorphic to a plane. Such a

geometry ensures that material can pass over it without wrinkling or stretching. It is common in current industrial practice for a modified form of such a surface to be used. The modification is to reduce slightly the height of the shoulder around the highest point of the bending curve. This is felt to improve the tracking of the film. In particular, it gives the material the ability to self-centre, so if it starts moving asymmetrically then out-of-balance forces encourage it to return to the centre.

The downside of such a modification is that some deformation of the material must occur. Indeed to ensure that the material is in contact with the entire shoulder, including the area of modification, the tension in the material is deliberately increased. This causes it to stretch and so counteract the imprecision in the geometry of the shoulder. The tension is increased by creating a pre-tension in the web by adding weights or springs to the moving rollers in the material feed (to the left in Figure 2) or retardation to the motion of the reel.

To investigate the differences in behaviour between the exact and modified shoulders, a number of exact shoulders were manufactured with dimensions similar to those for some standard modified ones. The exact shoulders can be made by milling from a solid block using machining instructions generated from the geometric model.

Testing revealed that the exact shoulders required significantly less pre-tension to run successfully. As an example, Figure 11 shows results for exact and modified shoulders with a 60° back angle. The bars correspond to three different materials: a metalised film, a polypropylene film, and a paper material that is coated to make it heat sealable. The unhatched parts of the bars show the minimum pre-tension required to run the material over a modified shoulder. This part is missing for the paper since no pre-tension was found that allowed operation and did not tear the web. In contrast all three materials ran successfully with a pre-tension of 5N, which is the minimum that is allowable under normal operation for the machine used in the tests. This is the single hatched area in the bars. To reduce the pre-tension still further, the material was detached from the input reel and allowed to flow freely into the machine. The shoulder still performed correctly, and tracking was good provided that the web fed in straight. The doubly hatched part of the bars represents the pre-tension of 2N that was estimated for this test.

It is clear that the exact shoulder offers a considerable reduction in the required tension in the web over the form of modified shoulder often used in practice.

It is less clear whether the exact shoulders could experience tracking problems during extended used. No problems were observed during testing. This may be because care was taken to ensure that the feed rollers were correctly aligned with respect to the back of the collar surface. Such an exact set-up is not always possible in an industrial context: for example, the shoulder or related parts may need to be changed from one material to another. However, it seems that the exact shoulder may be more tolerant to variations in the material. So it may be possible to design vertical form, fill and seal machines with a single shoulder to cope with a range of materials. This would eliminate one or more of the major change parts

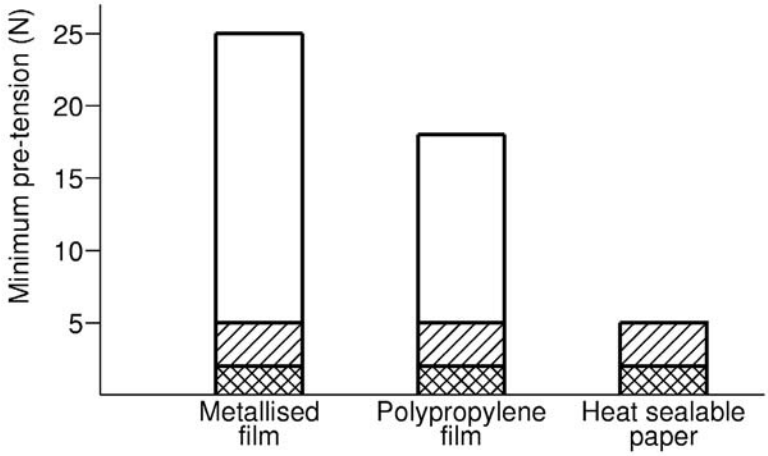

Fig. 11. *Minimum pre-tensions for successful operation*

for this class of machine. If so, care can be taken during manufacture to ensure correct alignment of the rollers and the shoulder.

5 DISCUSSION

A number of design implications can be drawn from the previous work. Four design parameters are identified and the key one is the height:radius ratio. Once this is chosen, strict limitations are imposed upon the values of the other three by the requirements of the geometry. So the following discussion is in terms of this ratio.

In practice, designers often try to use small values for the height:radius ratio. Typical values are around 2 or 3. This ensures that the shoulder itself is more compact. This means that it is easier to manufacture and easier to handle as a change part. The material tension needs to be high simply to pull the web over the shoulder and this may lead to damage to the material. However, a high tension seems to improve tracking during operation.

The graphs in Figures 6 and 7 indicate that a small value for the height:radius ratio means a low back angle is required and there is a narrow range of choice for it. A low back angle means that the web needs to approach the shoulder from below. However, considered as a whole, the overall machine is compact.

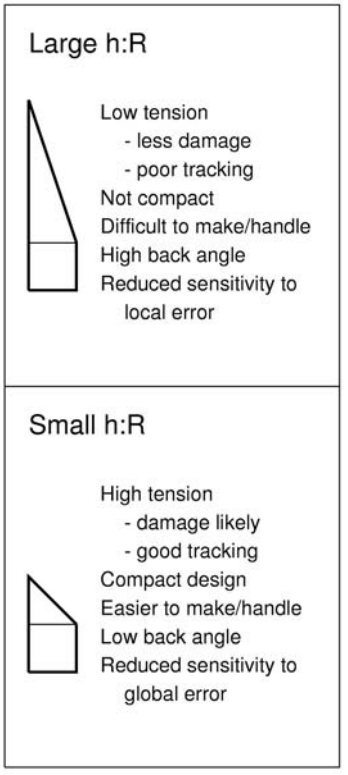

Fig. 12. *Design implications of the choice of height:radius ratio*

Figure 8 suggests that a low ratio means that there is reduced sensitivity to global errors in the manufacture of the shoulder. The length of the bending curve is low and so there is less opportunity for error in manufacture.

Conversely, consider the case of a high height:radius ratio. Values of 6 or 7 (or greater) occur in practice. This has the advantage of requiring a lower tension in the web and hence less likelihood of damage to it. However, reducing the tension may lead to problems with tracking. A high ratio means the shoulder is less compact and so it is more difficult to manufacture and set up on the machine. The choices for the other design parameters are still bounded, but the interval of choice has widened, giving greater scope to the designer. In particular, the back angle can be chosen to be around 90°, meaning that the web can be fed horizontally to the shoulder, which is more convenient for the operator. In addition, there is less sensitivity to local errors, possibly due to wear; and the wear itself is reduced by the lower web tension.

These considerations are summarised in Figure 12.

The current design practice is to use shoulders with modified geometry to improve tracking. The basic design strategy is to form a compromise between a low web tension to prevent damage to the material and a high tension to guarantee tracking. The critical tension that would cause damage needs to be estimated. This involves some understanding of the frictional forces involved. The smallest height:radius ratio that does not cause a tension in excess of this critical value is often a good choice.

It seems possible that the modified shoulder geometry is used to allow for misalignment in the feed system that comes about through operational use of the machine. Experience with shoulders of the exact geometry suggests that they can be operated successfully with low tensions on a wide range of material types. However, their performance in extended industrial trials still needs to be assessed. These need to investigate questions of tracking and whether the overall machine can be set up so that the intrinsic self-centring of the modified geometry is not required.

If these questions can be answered positively, then there are two significant implications. The first is a simplified approach to the design of forming shoulders, particularly to the design of shoulders to handle a given film (or range of films). If tracking can be made less of an issue, then there is scope to consider the design initially in terms of obtaining an appropriate (low) tension. This means selecting a suitable height:radius ratio to keep the tension as small as possible (as in Section 4) without making the size unwieldy. The other three parameters for the shoulder are then fairly closely defined by the limitations discussed in Section 3. The second implication is the possibility for using a much reduced range of shoulders (perhaps even a single one) to handle existing ranges of materials. This means that there is less of a requirement to change parts for different production runs, and it reduces the need to design specific shoulders for specific applications.

6 CONCLUSIONS

This paper has considered the effects of machine-material interaction and the parameters of the design that influence these. Issues involved in the design of vertical form, fill and seal machines have been investigated. One of the critical elements is the forming shoulder. Current industrial practice is based on only a limited understanding of the process. This means that often many prototype shoulders have to be designed, tested and modified before a suitable shoulder is configured for the particular application. This process can be time-consuming and costly.

To address some of these issues a mathematical model of the forming shoulder has been examined. This starts with the definition of the bending curve and leads to the construction of the collar surface. This includes a planar triangular region which allows film to be taken from a cylindrical roll.

Four main design parameters have been identified. These are: the height:radius ratio h/R; the front and back angles θ_0 and θ_1 ; and the opening angle of the triangular insert. The limitations which exist upon these have been discussed. It is noted that very small changes in these parameters may corrupt the good surface definition. In practice the material web may deform to alleviate some of the errors but this is often considered undesirable as it leads to damage to the material.

As well as purely geometric considerations, issues about performance need to be addressed. The force required to pull the web over the shoulder has been considered experimentally and shown to reduce as the height:radius ratio increases.

One of the other practical issues is tracking. To address this, manufacturers often use a modified form of geometry. To compensate for the modification, the web tension needs to be raised, which increases the possibility of damage to the material (and the shoulder). Experimental work with shoulders that have the exact geometry suggests that they can operate over a wider range of material types and with lower tensions. This has implications for the approach used to design shoulders for particular films. Consideration can initially be given to limiting the tension, and effects due to tracking can be considered later on. It also means that it may be possible to use a smaller range of shoulders (perhaps just one) to handle a number of different materials and thus improve the machine design by reducing the amount of change-over required.

Acknowledgements

The work reported in this paper arose from a research project sponsored by the EPSRC via the Innovative Manufacturing Research Centre at the University of Bath. Additional support has been provided by DEFRA, the Food Processing Faraday, the Process and Packaging Machinery Association, Pira International, and other collaborators. The authors gratefully express their thanks for the advice and support of all concerned.

7 REFERENCES

[1] Hanlon, J. F., Kelsey, R. J. and Forcinio, H. E. (1998). Handbook of package engineering. *Technomic Publishing Company Inc*., Penn.

[2] Twede, D. and Goddard, R. (1998). Packaging materials. *Pira International*, Leatherhead.

[3] PMMI (2001) 7th Annual packaging machinery shipments and outlook study, the U.S. packaging machinery industry executive summary. *PMMI, Packaging Machinery and Manufacturers Institute*, Arlington, VA.
[4] Hicks, B. J., Medland, A. J. and Mullineux, G. (2001). A constraint based approach to the modelling and analysis of packaging machines. *Packaging Technology and Science*, 14(5), 209-226.
[5] Paine, F. A. and Paine, H. Y. (1992). A handbook of food packaging, second edition, Blackie, London.
[6] Mans, J. (2001). The A-B-Cs of f/f/s'. *Packaging Digest*, August 2001, 40-43.
[7] Packaging Digest. (2004). Vertical form-fill-seal machine runs almonds at 120 pouches per minute. *Packaging Digest*, September 2004, 49-55.
[8] Schmidt, T. and Leiking, L. (2005). Reliability of evaluations for the choice of system solutions at the example of automated order-picking systems for bagged goods. *Logistics Journal*, reviewed article, 2005, 1-13.
[9] Vercelino Alves, R. M., Garcia, E. E. C. and Bordin, M. R. (1999). Influence of packaging material/ sealing on the quality of biscuits. *Journal of Plastic Film and Sheeting*, 15, 57-71.
[10] Czerniawski, B. (1990). Flexible packaging of disposable medical devices: a review. *Packaging Technology and Science*, 3(4), 203-217.
[11] Lazarus, A. (2005). The milky way. *Canadian Packaging*, February 2005, 45-45.
[12] Zhou, Y.-J. and Wang, Z.-W. (2004). Study on rhomb shoulder in packaging machines. *Packaging Technology and Science*, 17(5), 287-294.
[13] McPherson, C. J., Mullineux, G., Berry, C., Hicks, B. J. and Medland, A. J. (2005). Design of forming shoulders with complex cross-sections. *Packaging Technology and Science*, 18, 199-206.
[14] Zhou, Y.-J. and Qian, X.-M. (2006). Non-centrosymetric section forming shoulders in packaging machines. *Packaging Technology and Science*, 19(2), 97-104.
[15] Clark, T. A. and Wagner, J. R. (2002). Film properties for good performance on vertical form-fill-seal packaging machines. *Journal of Plastic Film and Sheeting*, 18, 145-156.
[16] Boersma, J. and Molenaar, J. (1995). Geometry of the shoulder of a packaging machine. *SIAM Review*, 37(3), 406-422.
[17] Culpin, D. (1980). A metal-bending problem. *Mathematical Scientist*, 5,121-127.
[18] Mot, E. (1973). The forming shoulder problem on pouch form, fill and seal machinery. *Verpackungs-rundschau*, 5, 35-39.
[19] Forsyth, A. R. (1912). Lectures on the differential geometry of curves and surfaces, *Cambridge University Press*, Cambridge.
[20] Pressley, A. (2001). Elementary differential geometry. *Springer-Verlag*, London.
[21] McPherson, C. J., Mullineux, G., Berry, C., Hicks, B. J. and Medland, A. J. (2004). The performance envelope of forming shoulders and implications for design and manufacture. Proc. Instn Mech. Engrs - Part B: *Journal of Engineering Manufacture*, 218, 925-934.

Authors' Address:
Prof. Dr. G. Mullineux
C. J. McPherson
Dr. B. J. Hicks
C. Berry
Prof. Dr. A. J. Medland
University of Bath
Department of Mechanical Engineering
Bath BA2 7AY, United Kingdom

Prejeto: 2.5.2007
Received:
Sprejeto: 27.6.2007
Accepted:
Odprto za diskusijo: 1 leto
Open for discussion: 1 year

Strojniški vestnik - Journal of Mechanical Engineering 53(2007)7-8, 491-502
UDK - UDC 678.056:678.7
Izvirni znanstveni članek - Original scientific paper (1.01)

Ocena tlaka v kalupu za stroškovni model obstojnosti stroja za batno brizganje

Cavity-Pressure Estimation for a Piston-Moulding Life-Cycle Cost Model

Charl L. Goussard - Anton H. Basson
(Stellenbosch University, South Africa)

Pričujoči prispevek predstavlja in vrednoti postopek za hitro oceno tlakov v kalupu med batnim brizganjem termoplastičnih materialov. Postopek uvaja analitične rešitve v manjšem številu nadzornih prostornin. Rezultat je delno analitičen model, namenjen uporabi med optimizacijo konstrukcije strojev za batno brizganje, kar vodi do optimizacije stroškov v celotnem krogu obstojnosti izdelka. Model je prav tako mogoče prilagoditi primerom brizganja. S tem namenom so pojasnjene tudi nekatere prednosti in pomanjkljivosti batnega brizganja v primerjavi z injekcijskim. Glavna prednost delno analitičnega modela je hitrost, s katero je določena razmeroma točna ocena tlaka brizganja v kalup. Tak pristop pride še posebej v poštev, kadar bi bile numerične simulacije preobsežne in časovno potratne, na primer v primerih optimizacij s širokim razponom neodvisnih spremenljivk. Prav tako so obravnavani različni analitični tokovni modeli, ki jih je moč najti v literaturi, ter njihova možnost uporabe v področju injekcijskega brizganja. Sledi obravnava izpeljanega delno analitičnega modela z njegovimi pripadajočimi poenostavitvami. Njegovi rezultati so primerjani z numeričnimi rešitvami na treh primerih. Ti primeri so pokazali, da je model dovolj natančen za zasnovo konstrukcije naprave in za raziskave stroškovnih usmeritev obstojnosti naprave.

(Ključne besede: brizganje polimerov, batno brizganje, tlaki v kalupu, optimiranje stroškov)

In this paper we propose and evaluate an approach for quickly estimating the cavity pressures during the piston moulding of thermoplastics. The approach applies analytical solutions in a small number of control volumes. The resulting semi-analytical model is intended for use when optimising the design of piston moulding machines, leading to a life-cycle cost optimisation. The model is also applicable to similar injection-moulding cases. Some advantages and disadvantages of piston moulding, compared to injection moulding, are discussed. The main contribution of the semi-analytical model is the speed with which a reasonably accurate estimate of the cavity injection pressure is calculated. This approach is useful in cases when numerical simulations would be too cumbersome and time consuming, e.g., in optimisation studies where the independent variables could vary over a wide range. Different analytical flow models found in the literature and their applicability to injection moulding are discussed. This is followed by a discussion of the derived semi-analytical model, with its underlying simplifications. The results from the semi-analytical model are compared to numerical solutions for three case studies. These case studies show that the model is sufficiently accurate for machine-layout design purposes and for investigating life-cycle cost trends.

(Keywords: injection moulding, piston moulding, cavity pressure, cost modelling)

0 INTRODUCTION

Lomolding is a piston moulding process designed to make similar parts to injection moulding. Its main operational sequence (illustrated in Fig. 1) starts by measuring off in the metering cylinder the exact amount of molten thermoplastic required for a part, transferring the melt to the moulding cylinder and then pushing the melt into the moulding cavity with the moulding piston. During solidification, the moulding piston holds the cavity under pressure and the piston face forms part of the cavity wall.

The area where the melt enters the cavity is much larger than the typical sprue of injection moulding, which is anticipated to bring advantages,

such as the ability to mould long fibres, lower material shear rates, and lower clamping-force requirements.

A life-cycle cost model is being developed to optimise the designs of the lomolding machine and to investigate the range of products suitable for the profitable application of lomolding. This model is aimed at the part of the life-cycle cost of a lomolded product that is related to the processing (as opposed to that contributed by the material used, the distribution, disposal, etc). The processing's contribution to the life-cycle cost is largely determined by the design of the lomolding machine and the processing parameters. Typical issues that must be addressed, considering the life-cycle cost and the quality of a part, are the optimum ratio of the moulding-piston area to the part projected area, the choice between electric and hydraulic actuators, and the choice between a single piston and multiple piston arrays. The effect of design and process choices on the energy consumption must also be assessed.

These machine-design and processing parameters are strongly driven by the injection pressure needed to fill a mould cavity, as well as the clamping force needed to resist the cavity pressures to avoid material flashing. To investigate the processing's contribution to the life-cycle costs and to optimise the design for minimum cost, a method is therefore needed to quickly obtain the injection pressure and clamp force needed to produce a certain part for a range of operating parameters (i.e., cycle time, melt and mould temperatures, and material properties). As little as possible user intervention should be required in the early design phases to facilitate the automation of the optimisation process, but the dominant physical aspects, such as the effect of fill rate, solidification rate against the mould walls during mould filling, and the non-Newtonian character of the flow, must be accounted for.

In practice, numerical simulation programs (Cadmould, Mouldflow, etc.) are used to analyse the behaviour of the molten material before expensive moulds are manufactured. These programs require a large amount of user interaction (creating a mesh, setting large numbers of process and material parameters, cumbersome post-processing, etc.) to accurately simulate a specific part and are therefore not suitable for the cost modelling required to explore the overall machine-design decisions and optimisation. Numerical methods can, however, be used to obtain more accurate pressure predictions once the solution region is narrowed down with the use of other methods. This approach can be used when similar trends are predicted by the approximate and the more accurate methods.

Analytical solutions for non-Newtonian flow with solidification in simple geometries have been reported, e.g., the flow between parallel plates, the flow in round tubes and disc flow geometries (outlined in Section 3). Since the analytical solutions are only applicable to a limited range of geometries, they cannot be applied as such in the cost model. The approach described in the present paper is to subdivide the cavity into a small number of simple, large control volumes and to use the

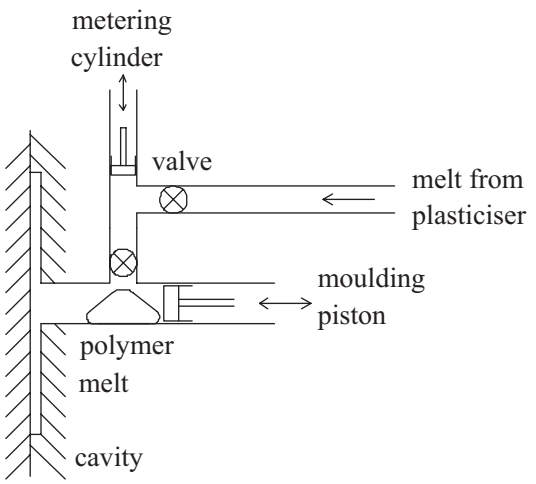

Fig. 1. *The lomolding process*

analytical solutions to approximate the flow in each control volume. The key factors in the success of the approach are formulating an equivalent flow pattern in each control volume and selecting the appropriate analytical solution for that control volume, such that the prediction of the solidification rate gives the correct overall results. Once the effective flow areas (h^*) are known, the pressure profiles can be calculated fairly easily.

The work presented in this paper was driven by the development of lomolding. However, most of the results are equally applicable to injection moulding. The paper's main contribution is an approach to reasonably accurately estimate the cavity pressures during mould filling, which is fast and simple enough to use for optimisation studies.

1 LITERATURE REVIEW

Researchers have shown an interest in theoretical and experimental studies involving fluid flow with solidification in circular tubes and on the walls of parallel-plate channels. The effect of this solidification layer on laminar flow heat transfer has been reported ([1] to [3]). Zerkle and Sunderland [1] and Lee and Zerkle [4] studied the steady solidification of fluid flow for Newtonian fluids with constant physical properties and no viscous heating. They cast the energy equation into a form which is similar to one that describes the classical Graetz problem. The solution is found by the method of the separation of variables and it takes the form of an infinite sum of eigenvalues.

Janeschitz-Kriegl [5] and Dietz et al. [6] proposed methods to calculate the thickness of the frozen layer that is formed on the cold cavity walls during the injection-moulding process. Janeschitz-Kriegl [5] used a steady-state heat-transfer coefficient, and the viscous heat generated was estimated from the average melt velocity and the pressure gradient under isothermal conditions. Dietz et al. [6] estimated the thickness of the frozen solid layer by applying the solution for an infinite solid slab. Janeschitz-Kriegl [7] showed in a later paper that a more detailed study with the aid of coupled motion and energy equations will not improve the accuracy of the solid-layer thickness estimation. Effects such as the glass transition or the crystallization kinetics at extreme rates of cooling and shearing have a strong influence on these results.

Richardson et al. [8] described the benefits of decomposing moulding networks into basic geometries and solving an analytical flow problem for each segment. This scheme aided mould-maker decisions regarding hot-runner, sprue and mould design. Richardson [9] extended the solution of Zerkle and Sunderland [1] and Lee and Zerkle [4] to non-Newtonian fluids with viscous heating. Again, the energy equation is transformed and the temperature and the frozen-layer thickness are expanded in a power series. The thickness of the frozen layer is then computed by substituting the first three terms of the power series into the energy equation. This solution is well suited for material flows with high Graetz (Gz) numbers, i.e., in the thermal-entrance region. The Graetz number is the ratio between the heat convection in the flow direction and the heat conduction in the direction perpendicular to the flow. In the work presented here, the solutions for flow between parallel plates were used. These solutions and how they are adapted to compute flows in discs, for instance, are described in more detail in Section 2.

Richardson also published three papers on flows with freezing of variable-viscosity fluids. The first [10] described developing flows with very high heat generation due to viscous dissipation that is large enough to cause significant variations in viscosity. However, the difference between the polymer temperature at the inlet to a specific part of the mould network and the melting temperature of the polymer is assumed not to cause significant variations in polymer viscosity.

The second paper [11] described developing flows with very low heat generation due to viscous dissipation. Furthermore, the difference between the temperature of the polymer at the entry to a specific part of the mould network and the melting temperature of the polymer is assumed to be sufficiently large so as to cause significant variations in polymer viscosity. Polymer flows in pipes, between discs and between parallel plates were considered.

These results compare reasonably well with the results obtained from Richardson's [9] previous paper, as long as the flow Graetz number is sufficiently large. However, combining the closed-form solutions for the three different geometry types, as will be required for the work presented in this paper, is not feasible.

In the third paper, Richardson [12] discussed solutions for cases where the polymer flow is fully developed.

The first models proposed by Richardson [10] did not produce good results for typical lomolding flows when compared to numerical simulation results. It could be argued that the variations in the shear rate are overshadowed by the large difference between the polymer inlet temperature and the polymer melt temperature (± 70°C) and therefore the second paper [11] produces more acceptable results. The third paper's flow solutions are not applicable to lomolding as the flows considered in the work presented here are generally undeveloped with regard to the temperature field.

All of the above papers consider polymer injection at a constant flow rate. This constant-flow-rate phase comprises approximately the first 90% of the polymer-injection stage and is followed by polymer injection at a constant pressure. Richardson published three more case studies involving cavity filling at a constant pressure: freezing off at polymer injection gates [13], freezing off in round and flat cavities [4] and freezing off in disc cavities [15]. As cavity filling occurs at a more or less constant polymer flow rate for such a large part of the injection stage, the focus in the work presented here was placed on filling at a constant flow rate.

Hill [16] proposed solutions to find the equilibrium height of the solidified polymer layer, where the polymer temperature increases due to viscous dissipation in equilibrium with the temperature drop due to heat conduction to the cold cavity wall. However, attention was restricted to the Newtonian case, for which numerical solutions are provided as well. Neither the equilibrium nor the Newtonian-flow assumptions are reasonable for the work presented here.

Today, far more complex cavities and flow geometries can be analyzed with numerical methods. Analytical models are often used to test numerical algorithms for simple case studies. Yang et al. [17] compared the results for the steady solidification of non-Newtonian fluids flowing in round tubes. Gao et al. [18] studied the effect of variable injection speed during injection-mould filling. They also tested their numerical algorithms against simple analytical solution case studies.

The scarcity of more recent papers reporting analytical solutions is probably due to the complexity of the physics involved, limiting analytical solutions to a very few simple geometries. In recent years, however, considerable effort has been invested in developing numerical simulations, mostly using finite-element modelling, that can handle the complex geometries commonly encountered when processing plastics.

2 SEMI-ANALYTICAL MODEL

This section describes Richardson's [9] analytical model briefly as well as the adaptation of the model to flows in channels of varying width. All the equations in this section come from [9].

Fig. 2 shows a schematic of the polymer flow between parallel plates. The flow is symmetrical with respect to the centreline and therefore only half of the cavity is shown. The half-height of the cavity is given by h, and the distance between the centreline and the solidified layer, by h^*. The solution is split into two regions, a thermal-entry region and a melt-front region. The melt-front region comprises most of the total flow length in typical cases.

The pressure drop (ΔP) over the entire flow length is given by Equation 1:

$$\Delta P = \mu^* \int_0^{x_f} \left(\frac{(m+2)Q}{2wh^{*m+2}} \right)^{1/m} dx \qquad (1).$$

The half-height of the polymer melt region (h^*) is found by introducing:

$$\delta = 1 - \frac{h^*}{h} \qquad (2).$$

For the thermal-entrance region, δ is given by:

$$\delta = 6\theta^* \Gamma(4/3) \left(\frac{\varepsilon}{6(m+2)Gz} \right)^{\frac{1}{3}} + 0\left(Gz^{\frac{-2}{3}} \right) \qquad (3)$$

and for the melt-front region, by:

$$\delta = 4w^* \left(\frac{\varepsilon_f - \varepsilon}{Gz} \right)^{\frac{1}{2}} \qquad (4),$$

where:

$$\theta^* = \frac{k_S (T_m - T_w)}{k_L (T_i - T_m)} \qquad (5)$$

$$\Gamma(4/3) \approx 0.893 \qquad (6)$$

$$\varepsilon = \frac{x}{L} \qquad (7)$$

$$\varepsilon_f = \frac{x_f}{L} \qquad (8)$$

$$\omega^* = (S_f / 2\kappa)^{0.5} \qquad (9)$$

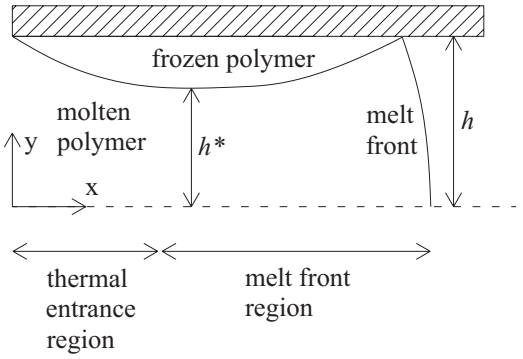

Fig. 2. *Polymer flow in a channel*

$$\kappa = \frac{k_L/(\rho_L c_L)}{k_S/(\rho_S c_S)} \qquad (10).$$

The Stefan number (S_f) is the ratio of the heat required to raise the polymer temperature from the cavity wall temperature to the polymer melting point, and the heat required to melt the polymer solid.

Once the half-height of the polymer-melt region is found for a control volume, the pressure drop can be calculated. These equations were derived for cases where the flow-channel width remains constant and the flow front enters the cavity evenly over the whole channel width.

Consider a typical moulding case: a rectangular cavity with constant thickness is filled through a sprue in the centre of the cavity. Fig. 3 shows a quarter of such a cavity.

Clearly, the longest flow path is given by the diagonal line *D* running from the injection point to one corner. This longest flow path is divided into a number of control volumes. To calculate h^* for a specific control volume at a certain time, it is necessary to know the flow-front position along *D*, the start point of the control volume with respect to *D*, the length of this control volume along *D* and the average width of the control volume.

To place a particular control volume at an equivalent *x*-position in the analytic model, assumptions have to be made about the upstream and downstream conditions:

- The upstream flow-path length in the semi-analytical model is taken to be the same as the true (geometric) length.
- The upstream and downstream flow-path width is taken to be equal to the average width of the control volume under consideration.
- Once the melt front has passed through the control volume, its position is calculated using the above flow-channel width (even though this will, in general, not coincide with the true flow-front position).

Case studies, as shown here, have confirmed that the approximated upstream geometry gives reasonable results, even though any upstream variation in flow area will influence the time that the flow front takes to reach a control volume. The approximated downstream geometry can deviate from the true geometry without affecting the solidified layer thickness in the control volume under consideration since, for these cases where the flow rate is constant, the only upstream effect is in the pressure gradient.

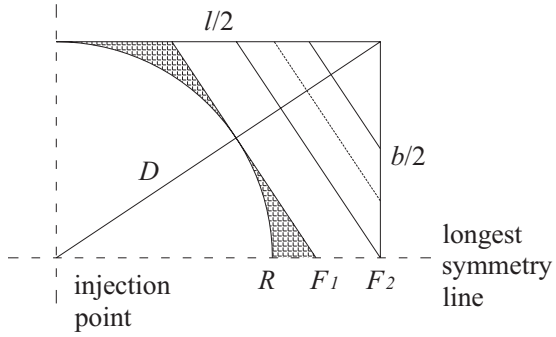

Fig. 3. *Schematic of the polymer flow front in a rectangular cavity (quarter segment shown)*

The pressure drop and the height of the solid layer are calculated for this control volume in a straightforward manner, as described above. It is necessary, in order to solve Equation 1 correctly, to check if a control volume is positioned entirely in the thermal-entrance region, entirely in the melt-front region or contains both.

Therefore, it is necessary to calculate the equivalent width, volume and start position along *D* for each control volume. From Fig. 3 it is clear that the flow front will be circular until the nearest side of the rectangle (*b/2)* is met. Therefore, the radius of the largest circular flow front is given by Equation 11:

$$R = \frac{b}{2} \tag{11}.$$

Up to this point, the equivalent control-volume width is given by Equation 12:

$$w_i = 2\pi R_i \tag{12}.$$

From F_1 to F_2 (Fig. 3, note F_2 is where the longest symmetry line meets the edge of the cavity) the equivalent flow widths are set equal to four times (note Fig. 3 shows a quarter of the cavity) the length of a line perpendicular to *D*, extending from the side of the cavity to the longest symmetry line. Note that these flow control volumes fall away when working with a square cavity (see Fig. 4). From position F_2 onwards the control-volume width is calculated as four times the length of a line perpendicular to *D*, extending from side to side.

Fig. 5 shows that the assumptions made for the equivalent widths of the control volumes approximate the true flow case numerically calculated by Cadmould.

It now remains to calculate the position of the melt-flow front as closely as possible to the true flow phenomenon. As is clear from Fig. 3, the hatched area is the only area not accounted for in the control volumes. To preserve the filling time, the volume associated with the hatched area is added to all the control volumes on a per-volume basis, except for the round control volumes. Once this correction has been applied, it is easy to calculate the position of the flow front.

The semi-analytical model is validated in the next section using different case studies.

3 CASE STUDIES

The semi-analytical model was implemented in software by the authors. This section shows some

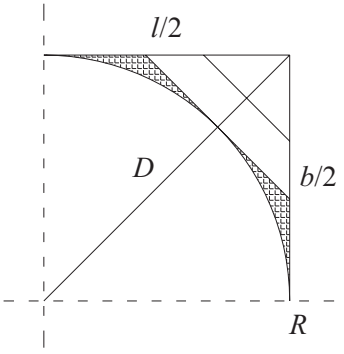

Fig. 4. *Schematic of the polymer flow front in a square cavity*

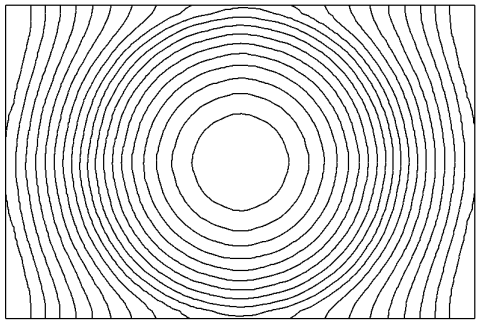

Fig. 5. *Flow lines for a rectangular cavity filled in the centre as calculated with Cadmould*

results to verify the semi-analytical model. The most restrictive requirement of the analysis presented above is that the flow Graetz number must be sufficiently high, which is explored later in this section.

The results of the semi-analytical model are compared with those of Cadmould. Although it would have been preferable to compare the results directly with experimental data, Cadmould is a widely accepted simulation tool in industry and therefore its results have considerable credibility. Furthermore, numerical simulations can give details that are extremely difficult to measure, such as the thickness of the solidified layer.

Two polymer materials suited for lomolding were selected for the case studies, i.e., Novolen 1100 N (a homogeneous polypropolene) and Celstran PP GF30 (a polypropolene with 30% glass-fibre component). The material properties for these materials given by Cadmould [19] and Osswald and Menges [20] were used and are summarised in Table 1. Cadmould [19] provides a Carreau viscosity model for these two materials. The unit shear-rate viscosity (μ^*) and the viscosity shear-rate coefficient (m) are found by fitting a power-law model to the Carreau model. The power-law viscosity model is given in Equation 13:

$$\mu = \mu^* \left| \frac{\partial u_x}{\partial y} \right|^{\frac{1}{m}-1} \qquad (13).$$

The figures in this section showing the results use the following abbreviations: AM for the semi-analytical model result; CM for the Cadmould numerical result; Cel for the Celstran material; and Nov for the Novolen material.

The first case study is the filling of a 500-mm-diameter disc, 3 mm thick, with the injection occurring along the circumference of an 80-mm-diameter piston into the cavity. Therefore, the flow-path length is shown in Fig. 6 as 210 mm. The disc is filled in one second at a constant flow rate. Fig. 6 shows that the growth of the solid layer along the flow path (a radial line) is underestimated, relative to Cadmould, for both materials. The pressure drop along the flow path relates well to the results obtained with Cadmould (Fig. 7). The lowest calculated Graetz number was 209 for the Celstran material and 230 for Novolen.

The second case study involves a square cavity with a length and breadth of 200 mm and a thickness of 2 mm. The injection point is in the centre and the longest flow path D is equal to $100\sqrt{2}$ mm. The cavity is filled in 0.5 seconds. As can be seen from Fig. 8, the semi-analytical model overestimates the growth of the solid layer in this case, especially near the end of the flow path. This leads to higher predicted pressure drops for both materials, as is clear from Fig. 9. The lowest calculated Graetz number was 134 for the Celstran material and 143 for Novolen. Note the sudden rise near the end due to the narrowing flow area.

The last case study is that of a rectangular cavity, 300 mm x 200 mm, with a thickness of 3 mm. The longest flow path D is equal to 180.28 mm. The cavity is filled in one second. Fig. 10 shows that the height of the solid layer is reasonably well predicted for both materials. As a result of this, Fig. 11 shows good agreement for the pressure drop across the rectangular cavity. The lowest calculated Graetz number was 191 for the Celstran material and 209 for Novolen.

In some situations a cavity will be filled in a time that will minimize the pressure drop experienced during filling. However, if this filling time is too long, a larger injection-pressure-capacity machine may be used, since this will save costs

Table 1. *Material properties*

Property	Novolen 1100 N	Celstran PP GF30	Unit
Unit shear-rate viscosity (μ^*)	5655	6958	N.s/m^2
Viscosity shear-rate exponent (m)	2.63	3.31	
Melt inlet temperature (T_i)	220	260	°C
Polymer melting temperature (T_m)	154	170	°C
Cavity-wall temperature (T_w)	40	55	°C
Polymer-melt thermal conductivity (k_L)	0.236	0.150	W/mK
Polymer-melt density (ρ_L)	910	994	kg/m^3
Polymer thermal diffusivity (α)	0.1043	0.0685	10^{-6} m^2/s

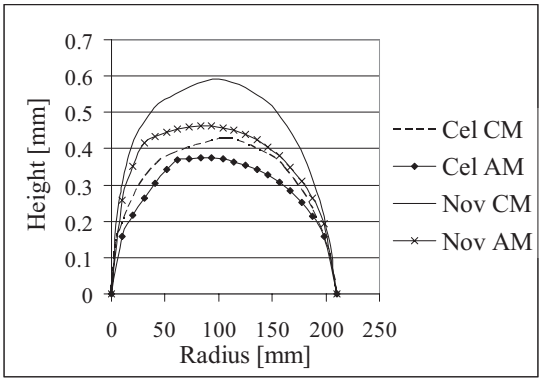

Fig. 6. *Growth of the solid layer in a disc cavity*

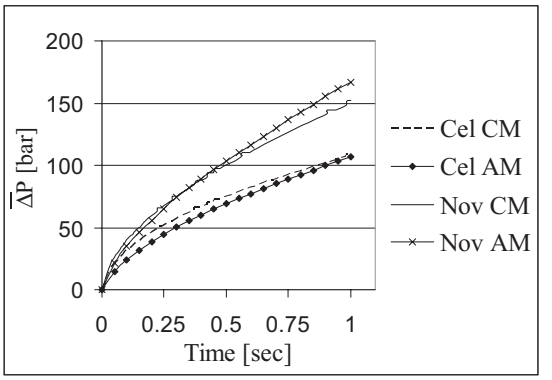

Fig. 7. *Pressure drop occurring in a disc cavity*

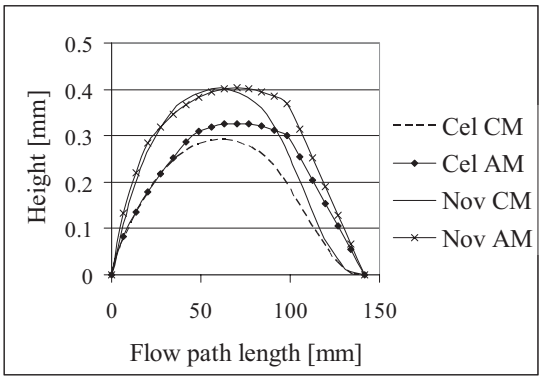

Fig. 8. *Growth of the solid layer in a square cavity*

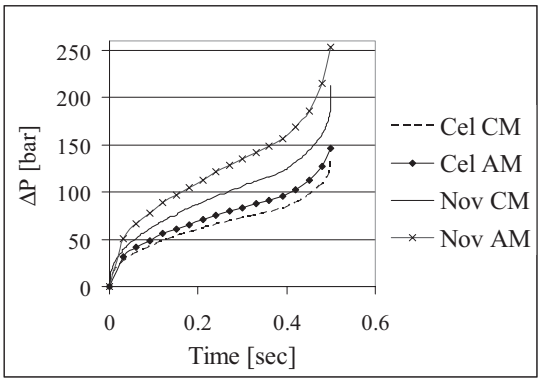

Fig. 9. *Pressure drop occurring in a square cavity*

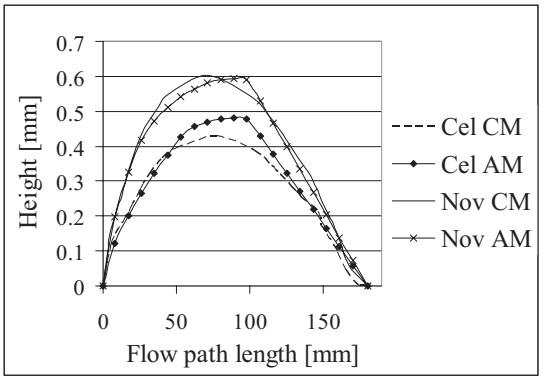

Fig. 10. *Growth of the solid layer in a rectangular cavity*

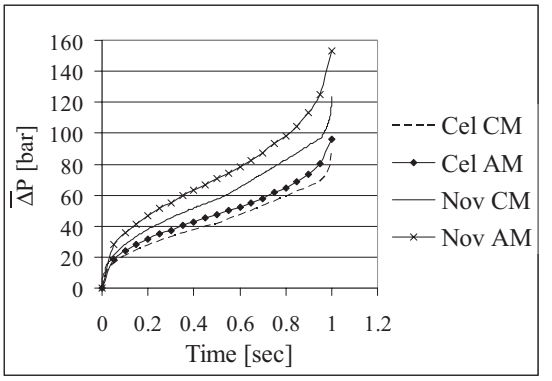

Fig. 11. *Pressure drop occurring in a rectangular cavity*

during the machine's lifetime as the part cycle time will be reduced. The fill rate directly influences the Graetz number, but the analytical model is only applicable to "large" Graetz numbers. It is therefore worth investigating what the influence is of the Graetz number on the accuracy of the semi-analytical model and what acceptable numerical values for the Graetz number would be.

Figures 12 to 15 show the influence of the Graetz number on the results obtained with the semi-analytical model for the same case studies used above. It is compared to numerical results obtained from Cadmould [19]. The Graetz numbers reported in the figures are the smallest calculated at the end of the filling stage under a constant flow rate. The objective was to find the filling time for

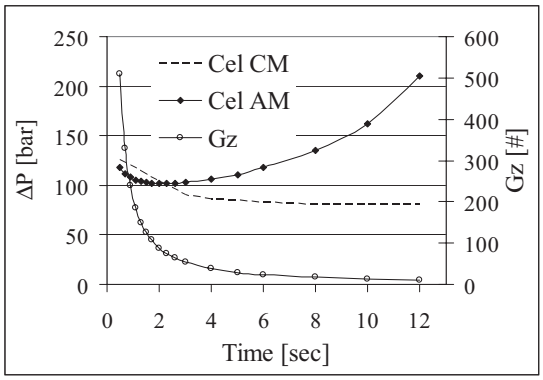

Fig. 12. *Pressure drop for different filling times in a disc cavity for Celstran material*

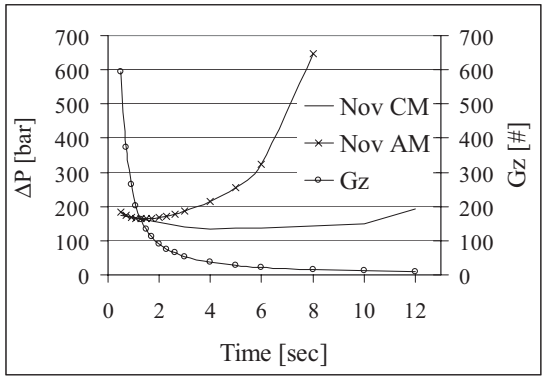

Fig. 13. *Pressure drop for different filling times in a disc cavity for Novolen material*

which the pressure drop across the cavity would be a minimum. These pressure drops are then compared to those found using the analytical model. It is also checked to see if this local minimum occurs at more or less the same filling time for both the analytical and numerical results.

Figures 12 and 13 show that for the disc cavity the pressure-drop results differ significantly for the two models when the Graetz number drops below 100. The analytical model estimates the lowest pressure drop around a 2-seconds filling time. However, Cadmould estimates these minima at around 4 seconds for both materials. At 2 seconds the error for the semi-analytical model is 6% in the case of the Novolen material and less in the case of Celstran. At 4 seconds this error grows to 59% in the worst case, which is again for the Novolen material. At this point the Graetz number is 37, well below 100.

In the case of the square cavity shown in Figures 14 and 15, the analytical model predicts the smallest pressure drop at around a filling time of 1 second for both materials. This compares well to the filling times found by Cadmould, especially in the case of the Novolen material. The minimum pressure drop varies very little across a filling time of 1 to 10 seconds in the case of the Celstran material. The error of the semi-analytical model is at most 33% for the Novolen case at a filling time of 1 second. At this point the Graetz number is equal to 57.

In the case of the rectangular cavity (Figures 16 and 17), both models predict a minimum pressure drop at around a 2-seconds cavity-fill time. In the case of the Novolen material it is noted that the analytical model calculates a slightly smaller filling time. The semi-analytical model's error is 49%, at most, for the Novolen case at a filling time of 2 seconds. At this point the Graetz number is equal to 83.

It is clear from these results that the semi-analytical model is reasonably well suited to finding

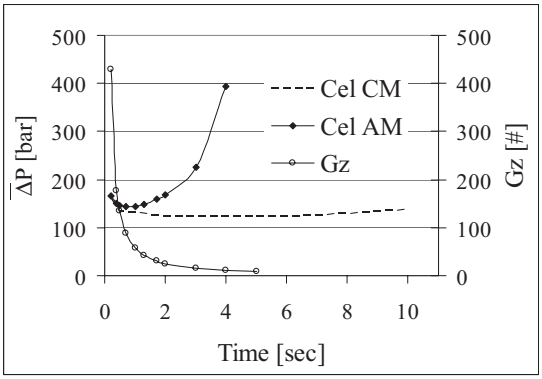

Fig. 14. *Pressure drop for different filling times in a square cavity for Celstran material*

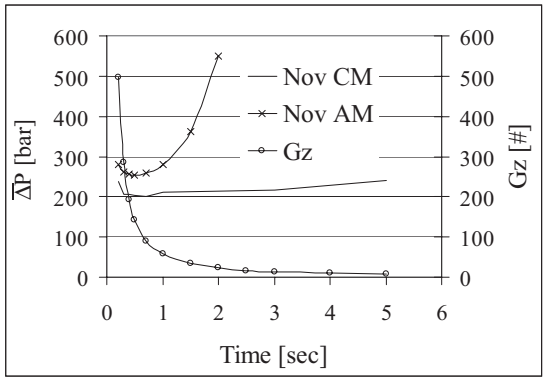

Fig. 15. *Pressure drop for different filling times in a square cavity for Novolen material*

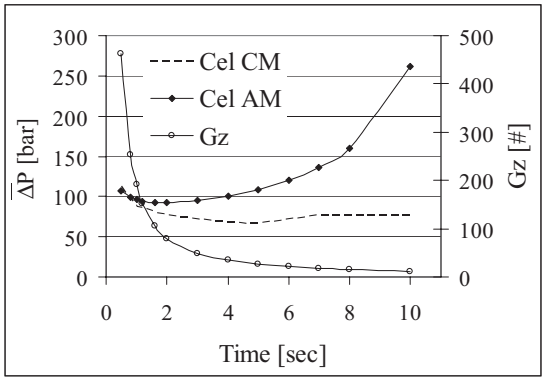

Fig. 16. *Pressure drop for different filling times in a rectangular cavity for Celstran material*

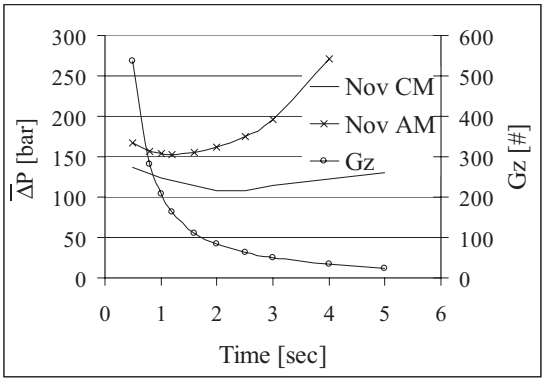

Fig. 17. *Pressure drop for different filling times in a rectangular cavity for Novolen material*

the filling time that will correspond to a minimal pressure drop across the cavity as long as the Graetz number stays above 100. Numerical simulations can then be carried out around this approximate optimum filling time and a better estimate for the pressure drop can be calculated. It is noted that the pressure drop computed by the semi-analytical model is higher than the pressure drop computed by Cadmould. This would mean that machines designed from these values will be slightly over designed and may be able to manufacture either slightly larger parts in the same time or produce the same part in a quicker cycle time.

4 CONCLUSION

The results presented above show that the semi-analytical model gives reasonable results for the pressure drop across the cavity when compared with the numerical results obtained with Cadmould. The main restriction of the model is that too high pressure drops are predicted when the Graetz number drops below 100. The reason for that is the overestimation of the solid-layer thickness due to higher conduction between the molten material and the solid layer to the cavity wall. Due to the associated smaller flow area, the overestimated solid-layer growth leads to a higher pressure drop than calculated with Cadmould. Otherwise, the model can be used for cavities with a flow-path-length to cavity-thickness aspect ratio in the range of the case studies presented here. The model provides a quick way of estimating the pressure drop across the cavity during filling, where numerical solutions would have been too cumbersome and time consuming.

The geometry-creation and computation times for the models presented here are modest to insignificant. Whether the results are accurate enough for machine-layout calculations is not easy to answer. However, the largest pressure errors occur towards the end of the filling phase. In practice a constant-pressure control strategy is used for the last part of the filling phase. The machine-sizing calculations are therefore based on the pressures encountered somewhat before the end of the filling phase. This filling method is shown in Fig. 18. The case (a) shows a constant flow rate throughout the filling phase. In case (b) the flow rate is kept constant up to a certain time and it is

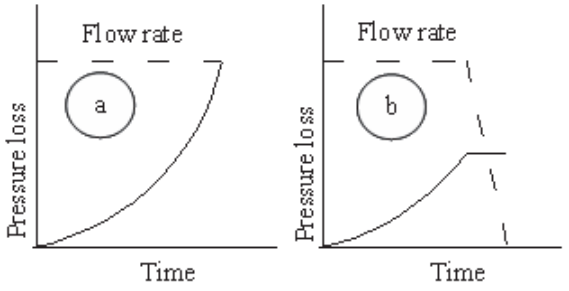

Fig. 18. *Cavity pressure loss and material flow rate during mould filling*

followed then by filling under constant pressure until the cavity is completely filled.

Since the pressures encountered during mould filling are related to the filling rate, the filling rate can in practice be reduced if the pressures exceed the design values for a given machine size. Also, the filling phase is normally much shorter than the cooling phase and the potential effects of the under/over prediction of pressure is restricted to a small part of the filling phase. Therefore, the influence of the largest pressure errors (i.e., those at the end of the filling phase) on the machine-size and cycle-time estimation is small. These pressure errors will have a small influence on the life-cycle cost, and the semi-analytical model can be expected to give useful results for machine-sizing studies and life-cycle cost assessment.

The computing times for the analytical model are insignificant on a 3-GHz computer. The computation time for the numerical results is sensitive to the finite mesh density used to model the cavities. The case studies presented here involved relatively coarse meshes to keep the computation time reasonably low, as many simulations were carried out. The computation time varied between 30 seconds and 3 minutes. The semi-analytical model will therefore yield substantially faster optimisation calculations, in addition to shorter pre- and post-processing times. Once a layout design has been selected, using the semi-analytical model presented here, final optimisation and design refinement can be done by using a numerical flow simulation package, such as Cadmould.

5 NOMENCLATURE

b	shortest side of rectangle
c_L	polymer melt specific heat capacity
c_S	frozen polymer specific heat capacity
Gz	Graetz number = $\rho_L c_L Q 2h / w k_L x$
h	half-height of cavity
h^*	half-height of the polymer-melt region
k_L	thermal conductivity of polymer melt
k_S	thermal conductivity of frozen polymer
l	longest side of rectangle
L	length of thermal entrance region
m	viscosity shear-rate coefficient
ΔP	pressure drop
Q	constant material volume flow rate
R	radius
R_i	average radius of control volume i
S_f	Stefan number = $c_S (T_m - T_w)/\Lambda$
T_i	polymer inlet melt temperature
T_m	polymer melting temperature
T_w	uniform cavity-wall temperature
u_x	polymer velocity in the flow direction
w	width of flow channel
w_i	width of flow channel of control volume i
x	axial coordinate in channel
x_f	melt-front position in channel
y	coordinate in h-direction
$\Gamma( )$	gamma function
δ	dimensionless thickness of frozen polymer
θ^*	dimensionless wall temperature
ε	dimensionless axial coordinate in channel
ε_f	dimensionless melt-front position in channel
Λ	latent heat of fusion
ρ_L	polymer melt density
ρ_S	frozen melt density
μ^*	material unit shear-rate viscosity

6 REFERENCES

[1] Zerkle, R.D., Sunderland, J.E. (1968) The effect of liquid solidification in a tube upon laminar flow heat transfer and pressure drop, *ASME Journal of Heat Transfer*, 90, pp. 183-190.

[2] Hsing-Lung, L., Hwang, G.J. (1977) An experiment on liquid solidification in thermal entrance region of a circular tube, *Letters in Heat Mass Transfer*, 4, pp. 437-444.

[3] Weigand, B., Beer, H. (1991) Heat transfer and solidification of a laminar liquid flow in a cooled parallel plate channel: The stationary case, *Wärme- und Stoffübertragung*, 19, pp. 233-240.

[4] Lee, D.G., Zerkle, R.D. (1969) The effect of liquid solidification in a parallel-plate channel upon laminar flow heat transfer and pressure drop, *ASME Journal of Heat Transfer*, 91, pp. 583-585.

[5] Janeschitz-Kriegl, H. (1977) Injection moulding of of plastics: Some ideas about the relationship between mould filling and birefringence, *Rheol. Acta*, 16, pp. 327-339.

[6] Dietz, W., White, J.L., Clark, E.S., (1978), Orientation development and relaxation in injection molding of amorphous polymers, *Polymer Engineering and Science*, 18:4, pp. 273-281.
[7] Janeschitz-Kriegl, H. (1979) Injection moulding of plastics: II. Analytical solution of heat transfer problem, *Rheol. Acta*, 18, pp. 693-701.
[8] Richardson, S.M., Pearson, H.J., Pearson, J.R.A. (1980) Simulation of injection moulding, *Plastic and Rubber: Processing*, 5, pp. 55-60.
[9] Richardson, S.M. (1983) Injection moulding of thermoplastics: Freezing during mould filling, *Rheol. Acta*, 22, pp. 223-236.
[10] Richardson, S.M. (1986a) Injection moulding of thermoplastics: Freezing of variable-viscosity fluids: Developing flows with very high heat generation, *Rheol. Acta*, 25, pp. 180-190.
[11] Richardson, S.M. (1986b) Injection moulding of thermoplastics: Freezing of variable-viscosity fluids: Developing flows with very low heat generation, *Rheol. Acta*, 25, pp. 308-318.
[12] Richardson, S.M., (1986c), Injection moulding of thermoplastics: Freezing of variable-viscosity fluids. Fully-developed flows, *Rheol. Acta*, 25, pp. 372-379.
[13] Richardson, S.M. (1985a) Injection moulding of thermoplastics. I. Freezing-off at gates, *Rheol. Acta*, 24, pp. 497-508.
[14] Richardson, S.M. (1985b) Injection moulding of thermoplastics. II. Freezing-off in cavities", *Rheol. Acta*, 24, pp. 509-518.
[15] Richardson, S.M. (1987) Freezing-off in disc cavities, *Rheol. Acta*, 26, pp. 102-105.
[16] Hill, D. (1996) Further studies of the injection moulding process, *Applied Math Modelling*, 20, pp. 719-730.
[17] Yang, L.C., Chen, S.J., Charmchi, M. (1991) Steady solidification of non-Newtonian fluid flowing in a round tube, *Polymer Engineering and Science*, 31, Nr. 3, pp. 191-196.
[18] Gao, D.M., Nguyen, K.T., Girard, P., Salloum, G. (1994) Effect of variable injection speed in injection mould filling, *Proceedings of the 52nd Annual Technical Conference*, Society of Plastic Engineers, Brookfield, CT, USA, pp. 712-715.
[19] Cadmould v6 (2002) Simcon kunststofftechnische Software GmbH, Germany, (www.simcon-worldwide.com).
[20] Osswald, T.A., Menges, G. (1995) Materials Science of Polymers for Engineers, chapters 3-4, *Hanser*, Munich, Vienna, New York.

Authors' Address: Charl L. Goussard
Prof. Dr. Anton H. Basson
Stellenbosch University
Department of Mechanical and
Mechatronic Engineering
Private Bag X1
Matieland 7602
Stellenbosch
South Africa
ahb@sun.ac.za

Prejeto: 2.5.2007
Received:
Sprejeto: 27.6.2007
Accepted:
Odprto za diskusijo: 1 leto
Open for discussion: 1 year

Strojniški vestnik - Journal of Mechanical Engineering 53(2007)7-8, 503-518
UDK - UDC 678.056:678.7
Izvirni znanstveni članek - Original scientific paper (1.01)

Optimiranje debeline brizganih plastičnih delov na podlagi simulacije Moldflow

Minimizing the Thicknesses of Injection-Molded Plastic Parts Based on a Moldflow Simulation

Yimin Deng - Di Zheng
(Ningbo University, P. R. China)

Določitev debeline izdelka je pomembna naloga pri konstruiranju brizganih plastičnih izdelkov. Praviloma želimo čim tanjše debeline izdelkov, s čimer se prihrani material, toda pri tem mora izdelek še vedno zadostiti vsem zahtevam po kakovosti. Obstaja že množica metod za optimizacijo debeline na podlagi strukturne optimizacije, torej metode, ki temeljijo na trdnosti, stabilnosti, deformaciji itn. V nasprotju s tem pa je bilo narejenih zelo malo raziskav s področja optimizacije debeline izdelkov na podlagi brizganja ter drugih kakovostnih zahtev s področja brizganja. Konstruiranje plastičnih izdelkov brez optimizacije debeline, ki temelji na kakovosti brizganja vodi bodisi k odvečni uporabi materiala, bodisi k slabši kakovosti brizganja. Kot prvi korak k problemu je v prispevku prikazan poskus zmanjšanja debeline izdelka z uporabo simulacijske metode znotraj programskega paketa Moldflow®. V grobem je postopek sestavljen iz avtomatiziranega iterativnega postopka, ki spreminja debelino izdelka ter izvaja simulacijo brizganja plastike Moldflow, ter zajema rezultatov simulacije za oceno kakovosti brizganja, vse dokler niso dosežene postavljene zahteve konstrukcije. Predlagan je postopek za spreminjanje debeline izdelkov, ki je pod različnimi pogoji voden z omenjeno metodo. Predlagani so trije konvergenčni kriteriji za optimizacijo, prav tako pa je razvit in predstavljen prototip programske opreme, ki vključuje predstavljeno metodo. Z namenom predstavitve metode in izdelane programske opreme je v prispevku prikazan konstrukcijski študijski primer. Opisano delo je potrdilo, da je predlagana metoda primerna za minimalizacijo debeline izdelkov na podlagi kakovosti brizganja.

(Ključne besede: brizganje polimerov, optimiranje debeline, simuliranje, programski paketi, MOLDFLOW)

Determining the thickness of parts is an important task in injection-molded plastic-part design. In general, the thicknesses of parts should be minimized so that less material is used and at the same time the relevant quality requirements are also met. There are already a number of methods for thickness optimization in the area of structural optimization, where strength, stability, deformation, etc., are the primary concerns. In contrast to this, very little work has been done on thickness optimization that is oriented to part moldability and other molding-quality requirements. Without molding-quality-oriented thickness optimization, the plastic-part design will result in either a waste of material or poor molding qualities. As a first step to tackle this problem, this paper attempts to seek minimized part thicknesses by employing a Moldflow® simulation-based method. Briefly, it consists of an automated, iterative process of changing the part thicknesses, conducting a Moldflow simulation, retrieving the simulation results to assess the specified molding-quality criteria, until the design objectives are met. A route for part-thickness change is proposed, which is governed by the respective methods under several different situations. Three convergence criteria are proposed. A software prototype implementing the methodology was developed and presented. To illustrate the methodology as well as the software, a design case is also studied. The paper shows that the proposed methods are applicable to the molding-quality-oriented part-thickness minimization.

(Keywords: injection moulding, thickness optimization, simulations, software packages, MOLDFLOW)

0 INTRODUCTION

In injection-molded plastic-part design a number of requirements have to be taken into account, such as functionality, economy, moldability, ease of use, ease of service, and so on. Among other design tasks, the determination of the thicknesses of a plastic part has significant influences on the fulfillment of these requirements. In general, part thicknesses should be minimized so that less material is needed for the part, thus reducing its cost. This, however, is constrained not only by the requirements for mechanical, thermal and/or other aspects of performance of the part, such as strength and stiffness, but also the requirements on moldability and other molding-quality measures. A part that is too thin may cause defects in the molding process; or it may experience early failure in its usage. Hence, it is necessary to develop strategies and methods to minimize part thicknesses without violating any of these constraints.

There has been considerable work on thickness optimization from the perspective of structural optimization, concerning functional and performance requirements. However, the work on thickness optimization concerning molding-quality requirements is scarce. This has led to the problem that the parts are either unnecessarily thick or too thin to satisfy all the molding-quality requirements. As an initial step in achieving the molding-quality-oriented part-thickness optimization, this paper proposes a simulation-based method using the well-known injection-molding simulation software "Moldflow". By "thickness minimization", we mean that the target of optimality is fixed as the part thicknesses; and the molding qualities are not taken as the optimization objectives, but rather as the constraints of the problem. The method is based on the assumption that the preliminary design of a plastic part has already taken structural requirements into account, that is to say, the design problem may be initialized as consisting of a part structure (the geometry) and the relevant structural constraints relating to the part thicknesses. This initial structure and the constraints ensure that the design satisfies the functional and performance requirements. As a result, one of the subsequent design tasks, to be addressed in this paper, would be to determine the minimized part thicknesses, with which the part can further achieve the goal of moldability and satisfy other specified molding-quality requirements.

In the next section, a brief literature review will be given to further clarify the problem. Section 2 discusses the method in enabling the integration between injection-molding CAD and CAE, which works as a basis for the proposed simulation-based thickness minimization. Section 3 elaborates the relevant thickness-minimization methods, such as the iterative procedure, the thickness-change route, and so on. Section 4 studies a design case, whose results are discussed in Section 5. Section 6 concludes the study.

1 LITERATURE REVIEW

Thickness optimization has been well researched from the perspective of structural optimization. For example, McClung *et al.* [1] discussed the non-linear structural optimization of thickness in plastic-part design. Lam *et al.* [2] discussed the thickness optimization of plate and shell structures, where stress and stiffness are the optimality criteria. Rietz & Petersson [3] have studied the simultaneous optimization of both shape (topological structure) and thickness, where again the performance requirements are the objectives of the optimization.

As can be seen, all of the above work focuses on satisfying various functional and performance requirements. None has targeted the molding-quality requirements.

Among the few reports on molding-quality-oriented thickness optimization, Lee & Kim [4] studied the optimization of part thickness by employing a "Modified Complex Method" for its optimization algorithm, where a simulation-based approach was adopted using C-Mold software (which is now incorporated in the Moldflow package). Their work, however, is specifically for reducing warping, which is only one of the many molding quality measures. In another article of theirs, thickness optimization for a robust design against process variability was studied, where warping was once again selected as the target of optimization. By using FEM/ANN/GA (finite-element method, artificial neural network, genetic algorithms), Huang & Huang [5] discussed a thickness optimization method for blow-molded parts, yet the work was focused on a uniform part thickness after blow molding, without taking into account various other molding-quality requirements.

In fact, simulation software such as Moldflow has now been widely used in industry. There are also many reports on injection-molding optimization, adopting a simulation-based approach. For example, Pandelidis & Zou ([6] and [7]) have proposed an optimization method based on Moldflow simulation by using an objective function to characterize a quality measure of the molded part, which was based on the criteria of temperature difference, overpacking and frictional heating. Both the gate location and the molding conditions were optimized.

Due to concern about the computation time incurred in the simulation-based approach, some AI (artificial intelligence) techniques have been attempted for injection-molding optimization, such as neural networks ([8] to [10]); fuzzy logic [11]; and case-based reasoning ([12] to [14]).

However, even these AI-based approaches are not completely free from simulation – many of them rely on simulation for knowledge acquisition and/or verification of the design outcome. Furthermore, with the rapid advances in computer technology and in the functionality of simulation packages, the simulation-based approach is becoming increasingly viable and affordable.

As such, it is legitimate to consider using a simulation approach in achieving the molding-quality-oriented part-thickness optimization.

However, to implement the Moldflow simulation-based approach, a problem must be solved first: Moldflow cannot be used to improve a design such as part-thicknesses minimization directly; it is just meant to provide a designer with an intuitive result, regarding whether a specific part and/or molding-process design is good or not. The designer has to find a suitable part thickness by trial-and-error, i.e., the designer must modify the part thicknesses after each execution of the simulation and evaluation of the simulation results. This is not only time consuming and error prone; more importantly, it is by no means possible to guarantee an optimized result with a finite number of trials.

To enable an iterative process of part-thickness change, Moldflow simulation, simulation-result retrieval and objective-function calculation to be carried out automatically using a computer program, so that a simulation-based thickness minimization can be implemented, the technology of the *injection-molding CAD-CAE integration model* may be leveraged. This is an object-oriented feature-based model that incorporates both design and analysis information about an injection-molded part [15]. The model consists of a number of hierarchically organized features, such as part feature, wall feature, hole feature, rib feature, boss feature and treatment feature. The part feature holds the overall information about the part, while all the other features are constituent components of the part.

These features are defined by both their geometrical and topological information from the part's CAD model, as well as the relevant CAE analysis data. They are thus referred to as the *CAD-CAE features*. For example, the part material, the boundary conditions, the processing conditions, *etc*., are the overall CAE analysis information, and thus are stored in the part feature. Suppressibility is a measure of whether or not a feature should be suppressed, so as to prevent it from being incorporated into the CAE analysis model. It is used to simplify the CAE model and thus applies to the features such as rib, boss, hole and treatment. Wall, rib and boss features all have an attribute of thickness, relevant to the topic of this paper.

The CAD-CAE features also hold constraints on their respective relevant attributes. For example, the desired molding quality criteria may be defined as a constraint of the part feature, while the constraint on the gate location on a wall feature may be defined as the constraint of the corresponding wall feature. For thickness minimization, the constraint on the thickness of a certain feature can be specified on that particular feature.

The model uses a CAD and a CAE system as its underlying platforms [16]. The part-geometry data is stored in the part CAD database, which is established by the CAD platform. ActiveX automation from the CAD system (*e.g.,* Solid Edge®) is employed for the model to access the part geometry data as well as the operations on these data. The model exploits the exposed functionalities of the CAD system through its automation server. Given that such an integration model is created and fully specified, the relevant routines of the underlying CAE system (*e.g.,* Moldflow) can then be activated to generate an analysis model (the mesh), which in turn can be used for the CAE analysis. As such, the integration model enables the automatic execution of part-geometry change and retrieval, such as the assignment of gate location

on the part geometry (on the CAD side); and the execution of the relevant Moldflow modules and the retrieval of simulation results (on the CAE side), hence enabling an injection-molding CAD-CAE integration [17].

To conclude, the work on molding-quality-oriented part-thickness optimization is scarce and not comprehensive in terms of the number of molding qualities addressed. A simulation-based approach may be employed when addressing the problem of thickness minimization, for which the technology of the injection-molding CAD-CAE integration model may be leveraged.

2 CAD-CAE INTEGRATION FOR PART-THICKNESS MINIMIZATION

Before exploiting the existing CAD-CAE integration model in the part-thickness minimization, some enhancements to the integration model should be made first. These enhancements are used to enable the specification of the features whose thicknesses need be minimized, as well as the specification of molding-quality criteria to formulate the objective function.

2.1 Step variable for thickness change

A new attribute, i.e., a list of shape modification variables, is introduced for the CAD-CAE features. This is used to change the part geometry, including the part thicknesses. By specifying shape-modification variables, different types of shape modification problems, either positional or sizing of an individual feature, or modification to different features, can be handled in a unified manner. Hence, it benefits both model consistency and software-development efforts. In this paper, the shape-modification variable is used specifically for the step value of changing the part thicknesses, which is thus called the *step variable*, denoted as a "Step".

The part thicknesses may be changed by increasing or decreasing a step value from the thicknesses of the relevant features bearing a thickness attribute, such as the wall feature (*e.g.,* the thin-wall feature and the extrusion feature in Solid Edge), and the rib feature (*e.g.* the rib and web-network feature in Solid Edge). By following the route of thickness change to be elaborated later, with the help of this step variable, the minimized part thicknesses can then be derived. (This is elaborated in Section 3.)

2.2 Formulation of the objective function

The designer should also specify the molding-quality measuring criteria, to be used for the formulation of the objective function for the intended thickness minimization. Some of these criteria are as follows [18]:

- The shear stress should not exceed the maximum recommended for the material type;
- The shear rate should not exceed the maximum recommended for the material type;
- The flow-front temperature should not be more than 20°C below the melt temperature;
- The cooling time should be uniform and minimized;
- The melt flow should be uniform, that is, the designer should try to make sure that all extremities are filled at the same time and at the same pressure.
- The designer may also have some specific quality requirements, such as minimizing the maximum shear stress, minimizing the maximum cavity pressure, uniform end-of-fill temperature, uniform volumetric shrinkage, and uniform warping. Some of these requirements may be imposed on a particular location or area of the plastic part, such as the shear stress requirement at the vicinity of snap fits, screw holes, occasional thin areas and where frequent bending may be necessary.

To enable the designer to specify these criteria rather than hardwire them in a computer program, the part feature is extended to include an attribute for storing a list of criteria construction variables, from which the objective function can be formulated. Some of these variables (the units are put inside the brackets) include the melt temperature (°C), the mold temperature (°C), the specified injection time (s), the actual injection time (s), the maximum shear stress (MPa), the maximum shear rate (1/s), the maximum pressure (MPa), the maximum flow-front temperature (°C), the minimum flow-front temperature (°C), the maximum end-of-fill temperature (°C), the minimum end-of-fill temperature (°C), the maximum cooling time (s), the minimum cooling time (s), the maximum volumetric shrinkage (%), the minimum volumetric shrinkage (%), the maximum clamp tonnage (tons), etc.

With these variables, the designer may select the relevant variables and then formulate the molding-quality criteria and objective function for the part-thickness minimization. For example, if the designer wishes to specify a constraint relating to the maximum shear stress, *e.g.,* the maximum shear stress should not exceed 0.2 MPa, he or she can select this variable (assuming it is denoted as "v1") and formulate the constrained objective function as follows:

$$\begin{cases} \text{Minimize:} & x = f(v1) \\ \text{Subject to:} & v1 < 0.2 \end{cases} \quad (1),$$

where the variable x is the number of times of the "Step" is used to increase the minimized part thicknesses, *e.g.,* x = -1.5 means that the minimized part thicknesses would be the original thicknesses reduced by "1.5 Step" (the value of "Step" is previously specified by the designer). The relationship between the variable x and the variable v1, *i.e.,* the function f (v1), is implicitly determined by the Moldflow simulation results. Given a specified value for the variable x, which determines the part geometry, there would be the value for the variable v1 from the Moldflow simulation results. Since there is no explicit mathematical relationship between x and v1, the usual optimization procedure is not applicable. This is addressed in the next section.

It is worth noting that the optimization result should be examined against the requirements on thicknesses from the part's structural design, to ensure that the part can function properly in its application.

3 PROCEDURE FOR PART-THICKNESS MINIMIZATION

By not taking the usual steps of optimization, this paper proposes a specific way for part-thickness minimization, in that the minimization is achieved by directly changing the part thicknesses until an optimality is eventually arrived at. To make the elaboration of the methodology easy and clear, we will be introducing a software prototype first. This software was developed to implement the proposed thickness-minimization approach. It was developed using Microsoft Visual C++® as the programming language, where Solid Edge is used as the underlying CAD system, and Moldflow is used as the underlying CAE system. Fig. 1 shows the graphical user interface (GUI) of the software, where the Solid Edge environment is shown, while

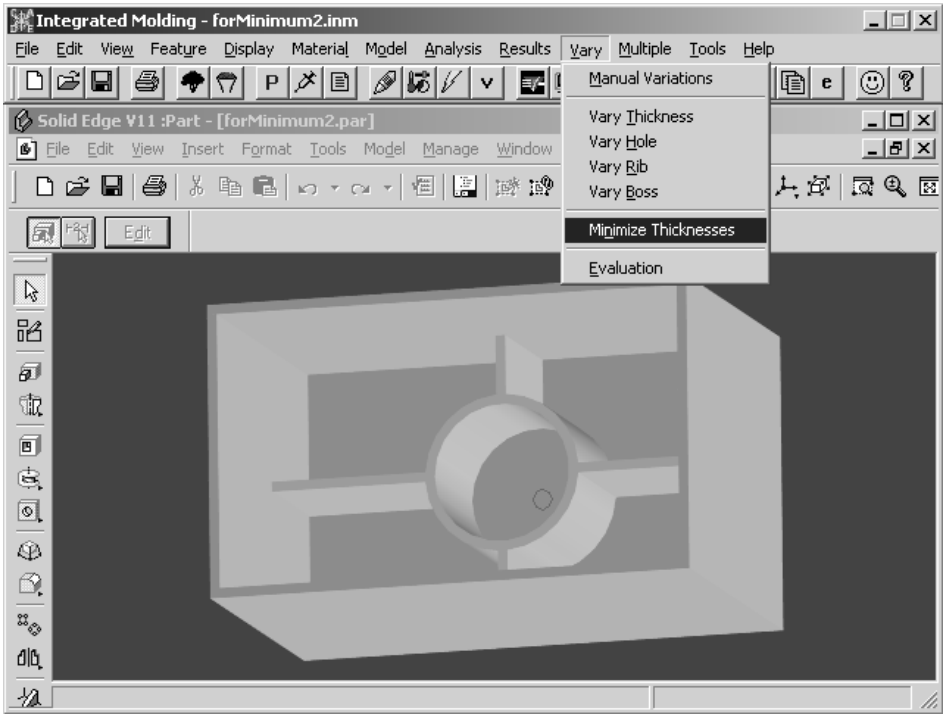

Fig. 1. *User interface of the developed software for minimizing part thicknesses*

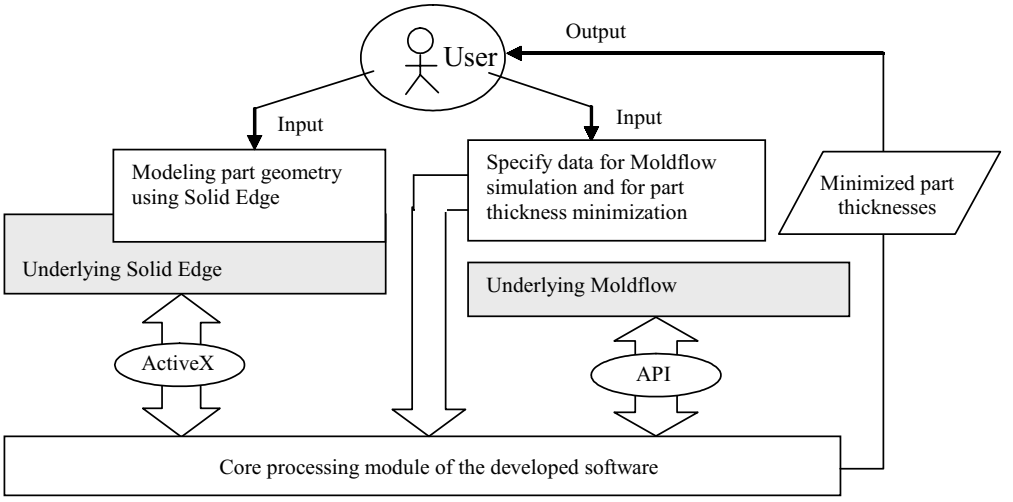

Fig. 2. *System framework of the developed software*

the Moldflow module is not shown because it only appears when its relevant routines are activated by the software. The screen snapshot also captured a part geometry, which will be used later as the case study.

It should be noted that the software has been developed over the past several years, addressing a number of injection-molding optimization problems. This paper only deals with the newly added function module of part-thickness minimization, which can be activated by using the highlighted (mouse-selected) menu item: "Minimize Thicknesses". The system framework of the developed software is shown in Fig. 2. Basically, it consists of two input modules, a core processing module and an output module, in addition to the two underlying systems (*i.e.,* Solid Edge and Moldflow). The communication between the core processing module and Solid Edge is through the ActiveX automation of Solid Edge. By ActiveX automation, Solid Edge exposes its functionalities to the outside world (*i.e.*, the other applications). The communication between the core processing module and Moldflow is through the APIs (Application Program Interfaces) provided by Moldflow. The following sections will introduce these modules, which form the proposed procedure for minimizing the part thicknesses.

3.1 Step 1: to create the initial integration model using the first input module

According to the existing CAD-CAE integration model, the designer first creates a part geometric model by using the underlying CAD system, *i.e.,* Solid Edge. After that the Moldflow simulation analysis information should be specified, including the part material, the gate location (as a boundary condition), the melt temperature, the mold temperature, the injection time, *etc.* (See references [15] to [17] for details.) For the mesh generation, the designer should also specify the mesh-density data, such as the number of elements or the number of divisions of unit length. Fig. 3 shows a screen snapshot, where the upper section is the user interface for specifying such information.

The specified data are used for the Moldflow simulation, which in turn is used for calculating the molding-quality criteria. As such, the designer should also specify or formulate quality criteria by first selecting criteria-construction variables. The lower section of Fig. 3 shows the user interface for selecting the relevant variables, as well as for formulating the quality criteria. For the variable selection, as is shown in the lower left corner, the combo-box stored all the aforementioned variables. By clicking the "Use" button, the selected variables will be listed in the list-box below the combo-box. For the criteria formulation, as is shown in the lower-right corner, the designer can use the "Add" button to put the formulated criteria into the lower list-box. For brevity, the use of the other buttons ("Edit", "Delete", "Extremity") is not elaborated. The detailed procedure for formulating the quality criteria from the criteria construction variables can be found in [17].

By using this input module, the initial integration model will be created, which contains all the data shown in Fig. 3.

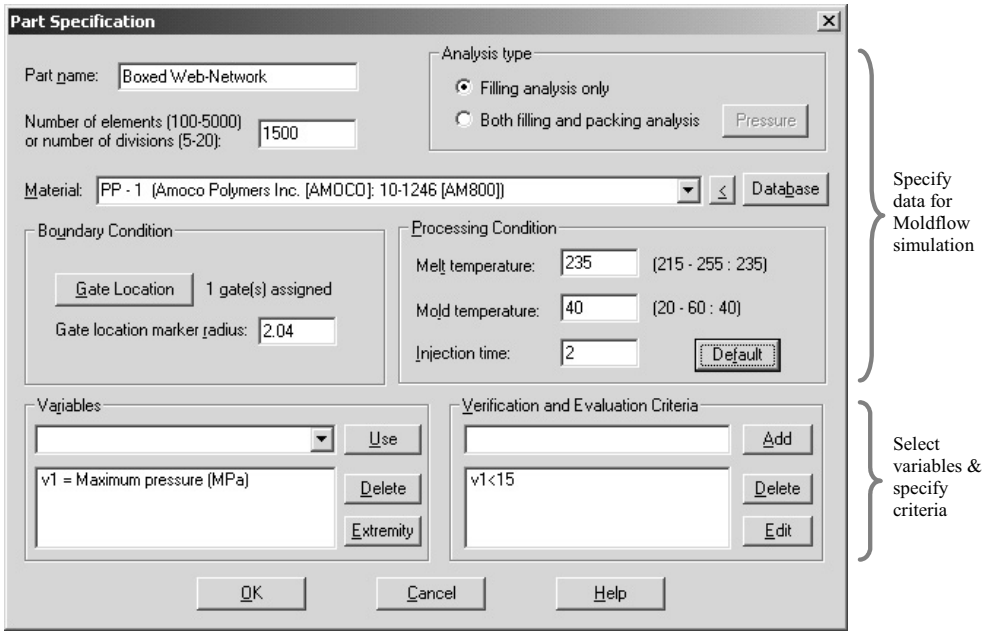

Fig. 3. *Specify the data for the Moldflow simulation and the quality criteria*

3.2 Step 2: to specify the features whose thicknesses need be minimized by using the second input module

By exploiting the ActiveX automation of Solid Edge, the software automatically examines all the features of the part geometry, and lists those features bearing thickness attributes. The designer can then select which of these features will be used for the thickness minimization. Fig. 4 shows the user interface for selecting these features, as well as other relevant data for the part-thickness minimization. This is the second input module of the software.

The upper list-box lists the features and their corresponding initial thicknesses. The designer also needs to specify the step value of the thickness

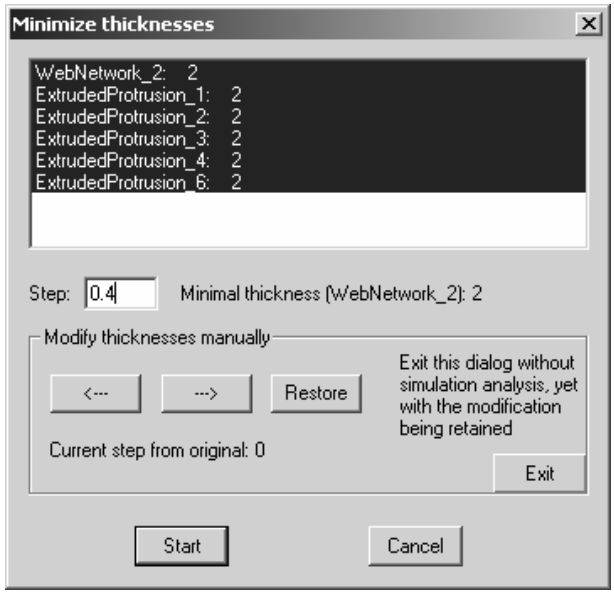

Fig. 4. *User interface for specifying the features whose thicknesses should be minimized*

change with which the thicknesses of the selected features will increase or decrease each time the part geometry is modified during the iterative part-thickness minimization process. The user interface also shows the minimal thickness of the selected features, which is used to help the designer in specifying the step value.

There is an additional functionality within this user interface, in that the designer can also manually change the initial thicknesses of the selected features. The user can dynamically reduce or increase the selected feature thicknesses by pushing the buttons "←" and "→" respectively, with each push changing the step value.

After all the intended features are selected and the step value is assigned, the designer can push the "Start" button to start the thickness minimization process.

3.3 Step 3: an iterative process following a route of thickness change by using the core processing module

Generally, for a thin-walled plastic part, increasing the part thicknesses will enhance the molding-quality results. (These should of course be within certain limits, because if the thicknesses are too large, the part will not be thin-walled, and then even the Moldflow simulation results will not be trustworthy.) The thickness minimization process is in effect a process of how the part thicknesses should be changed, *i.e.,* a route of thickness change should be identified. At first, the initial part (without thickness change) should be used to conduct a Moldflow simulation analysis. This is denoted as the first simulation. The implementation software will make use of the specified data discussed in Section 3.1 to activate the necessary Moldflow routines to fulfill the task. Upon completion, the software will extract relevant data from the simulation results and calculate the specified quality-measuring criteria to determine whether any of them is violated. Depending on the results from the first simulation, there will be two situations for the next step of action (*i.e.,* how the thicknesses should be changed):

(1) If all the criteria are met (we say the simulation has "passed"), the part thicknesses may be reduced. Hence the thicknesses of all the selected features will be reduced by a step value, denoted as "- Step".

(2) If one or more of the criteria are not met (we say the simulation has "failed"), the part thicknesses will have to be increased. Hence, the thicknesses will be increased by a step value, denoted as "+ Step".

The changed part geometry will then be used to activate another round of Moldflow simulation and criteria calculations; this is called the second simulation.

After the first two simulations, there will be four situations for the next step of action (*i.e.,* how the third simulation is going to be activated), depending on their results:

(1) If the first simulation passed and the second simulation passed again, then the next step will be reducing the thicknesses by another step value, *i.e.,* "- Step".

(2) If the first simulation failed, and the second simulation failed again, then the next step will be increasing the thicknesses by another step value, *i.e.,* "+ Step".

(3) If the first simulation passed, while the second simulation failed, then the next step will be increasing the thicknesses for ½ Step, denoted as "+ ½ Step". This is because, from the first to the second simulation, see Fig. 5 (a), the change

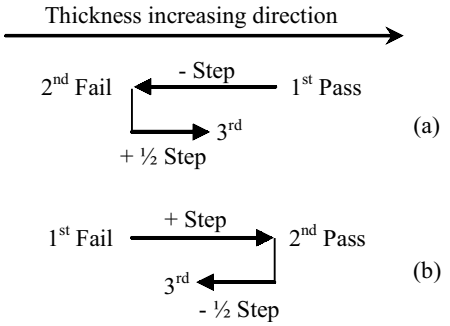

Fig. 5. *Situations involving "± ½ Step" of thickness change: (a) "+ ½ Step"; (b) "- ½ Step"*

of thickness was "- Step"; now from the second to the third, the part thickness increase should obviously be less than one "Step". As such, "+ ½ Step" is used.

(4) If the first simulation failed, while the second simulation passed, then the next step will be reducing the thicknesses by ½ Step, denoted as "- ½ Step". The reason for this situation is the same as situation No.3. See Fig. 5 (b) for an illustration.

The fourth simulation will depend on the results from the second and the third simulations. Like with the above four situations, the change in the part thicknesses will be "± Step", or "± ½ Step", or "± ¼ Step". The first two are easy to understand. The situations of "± ¼ Step" occur when "± ½ Step" were used from the second to the third simulation, and there were Pass/Fail swaps between these two proceeding simulations. For example, in Fig. 5 (a), there was "+ ½ Step" thickness change from the second (Failed) to the third (assuming Passed). Since the third simulation has passed, the next step will be changing the thicknesses by "- ¼ Step". In Fig. 5 (b), there was "- ½ Step" thickness change from the second (Passed) to the third (assuming Failed). Since the third simulation has failed, the next step will be changing the thicknesses by "+ ¼ Step".

However, if there was no Pass/Fail swap, the next step will arrive at a part geometry that has thicknesses already encountered before. For example, in Fig. 5 (a), from the second simulation (Failed) to the third simulation (assuming Failed again), the change of "+ ½ Step" again will lead to the part geometry for the fourth simulation be the same as that for the first simulation. In Fig. 5 (b), from the second simulation (Passed) to the third simulation (assuming Passed again), the change of "- ½ Step" again will lead to the part geometry for the fourth simulation also being the same as that for the first simulation. To avoid repetition of the same Moldflow simulation, thus saving computation time and other resources, the implementation software stores the results of each simulation and automatically retrieves them once a past record is encountered.

The subsequent steps will follow the above route of the thickness-minimization process. The process stops once any of the following situations occur (called the convergence criteria):

(1) If the thickness change from the previous simulation to the current is in between "± ¼ Step" and "± 1/16 Step" inclusive, and the current simulation has passed the specified criteria, the process will stop and the part thicknesses corresponding to the current simulation will be the thickness minimization result. If the thickness change has already arrived at "± 1/16 Step" and the simulation has always failed since after the thickness change of "± ¼ Step", then there is no need for the process to proceed further, and the part thickness corresponding to the last passed simulation (which should be before the "± ¼ Step" was encountered) will be the thickness minimization result. The latter is necessary because there is no practical usefulness in getting an extremely small thickness change.

(2) If the total number of simulations has exceeded 30, the process stops, and the part thicknesses corresponding to the last passed simulation will be the thickness minimization result. If, however, there has been no successful simulation, then the work for thickness minimization is considered unsuccessful. In such a case the designer may consider increasing the specified step value, and executing the implementation software again. For example, if the specified "Step" value is 0.01mm, then after 30 times of "± Step" thickness change, the total thickness change is only 0.3 mm, which may not be significant enough to affect the simulation results effectively.

(3) If the minimal thickness was less than 0.1 mm, which is too small to be practically applicable, then the process stops, and the part thicknesses corresponding to the last passed simulation will be the thickness minimization result. The work for thickness minimization is considered unsuccessful if there was no successful simulation previously. Of course, this situation is very unlikely to occur, unless the specified criteria are extremely loose. This is because such small thicknesses shall definitely lead to a very low level of molding quality.

4 CASE STUDY

4.1 Problem assignment

The design case is a plastic box with a web-network inside (a cylinder and four plates), as shown

in Fig. 6. It consists of several wall features (called extruded protrusions in Solid Edge), and a web-network feature. This part structure was chosen because it comprises most commonly used features where the thicknesses of the features might be changed. The web-network feature is representative of rib features because they are all used for the enforcement of the part strength. The initial thicknesses are all 2 mm. The part geometric model was created interactively by using the modeling tools provided by Solid Edge. A circle sketch was also created, which is used by the CAD-CAE integration model to indicate the gate location. The analysis information specified includes:

- Part material:
  Type: PP (Polypropylene);
  Manufacturer: Amoco Polymers Inc. [AMOCO];
  Trade name: 10-1246 [AM800].
- Boundary condition: the gate location is defined by the centre of the circle sketch, which is at the outer side of the part's bottom surface, as is shown in Fig. 6;
- Molding conditions (the melt temperature and mold temperature are suggested by the Moldflow material database):
  Melt temperature: 235°C;
  Mold temperature: 40°C;
  Injection time: 2 s.
- Criteria construction variable:
  v1 = maximum cavity pressure (MPa).
- The molding quality criterion for the thickness minimization:
  $v1 < 15$.

The goal of the current design problem is to seek the minimized part thicknesses, including the thicknesses of the wall features and the web-network feature, on the condition that the specified criterion can be met. The objective function is thus formulated as:

$$\begin{cases} \text{Minimize:} & x = f(v1) \\ \text{Subject to:} & v1 < 15 \end{cases} \quad (2),$$

where the variable x has the same meaning as in Equation (1), mentioned in Section 2.2. Fig. 4 shows the selected features and the specified step value (0.4 mm).

4.2 Solution

After the specification of the above data, the software will automatically generate a mesh model from the part geometry, conduct the Moldflow simulation, extract the analysis results, evaluate the molding-quality criteria, and then change the part thicknesses, following the route of the thickness change. The process is iterative, until one of the convergence criteria is met. Fig. 7 shows a screen snapshot of the final results of this design case.

A close look at the results summary (Fig. 7) will reveal the route of the thickness change, as is illustrated in Fig. 8. The first two simulations all

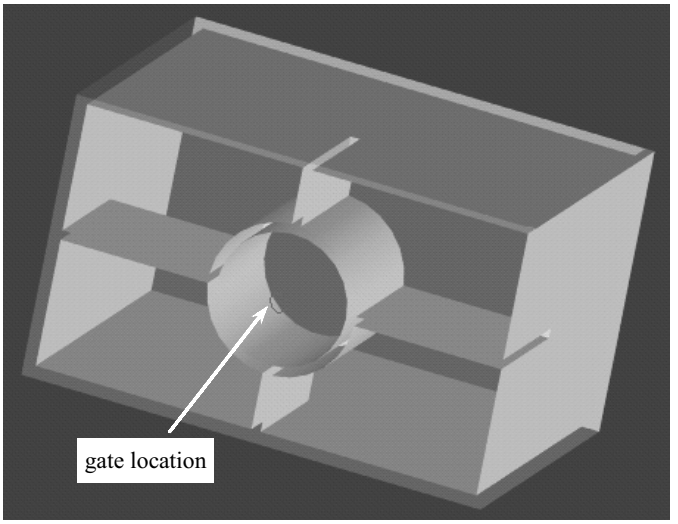

Fig. 6. *Initial part geometry (the small circle in the sketch indicates the gate location). Remarks: (1) the box and the interior web-network feature were displayed in different colors just for viewing purposes; (2) the wall with the circle sketch, i.e., the bottom wall of the box, was intentionally displayed in a transparent color to allow its inside to be seen.*

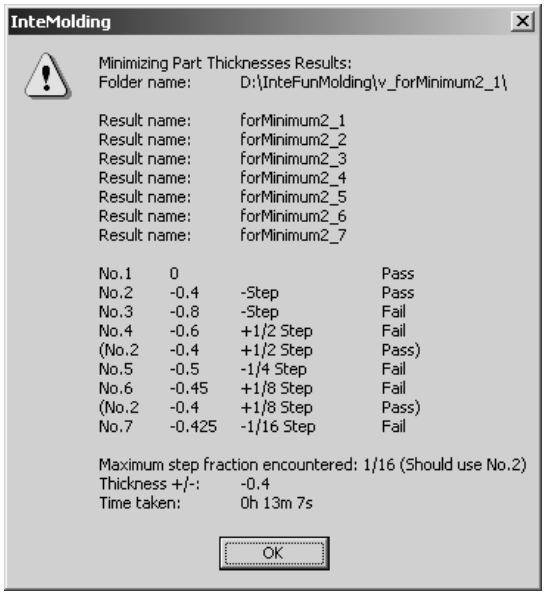

Fig. 7. *Thickness-minimization results for the studied design case*

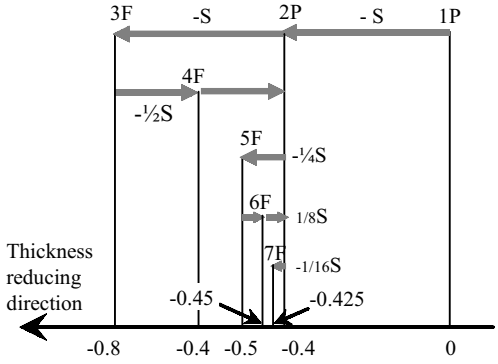

Fig. 8. *Route of thickness change for the design case. Remarks: P-Pass, F-Fail, S-Step, e.g., "1P" means simulation No.1 passed, "3F" means simulation No.3 failed*

result with "Pass", that is, No. 1 (using the initial part geometry without the thickness change) and No.2. The thickness change after each of the two simulations was "- Step", trying to reduce the part thicknesses. Simulation No. 3 failed, hence a "+ ½ Step" change of thickness was applied to generate the part geometry for simulation No. 4. Simulation No. 4 failed again, hence a continuous change of thickness, *i.e.,* "+ ½ Step" was applied. Now, the part geometry coincided with that of simulation No. 2, thus there was no need to conduct the Moldflow simulation again. Since simulation No.2 passed, the thickness change for the next simulation (No. 5) will be "- ¼ Step". This procedure went on until the convergence criterion No.1 was triggered (*i.e.,* the thickness change is between "¼ Step" and "1/16 Step" inclusive, and there is no simulation that passed the molding-quality criteria within this range. In this situation the last simulation with "Pass" will be retrieved as the final result). The simulation No.2 was the immediate last one with a "Pass", thus its thickness change corresponds to the thickness-minimization result.

Hence, for this design case, the sought x = -1, and the total change of thicknesses is -Step = -0.4 mm. The results can be summarized as:

- The sought: x = -1;
- Thickness change: -Step = -0.4 mm; (from 2.0 mm to 1.6 mm)
- Thickness reduction percentage: 0.4/2 = 20%.

Fig. 9 shows the part from the thickness minimization, with the Moldflow simulation results

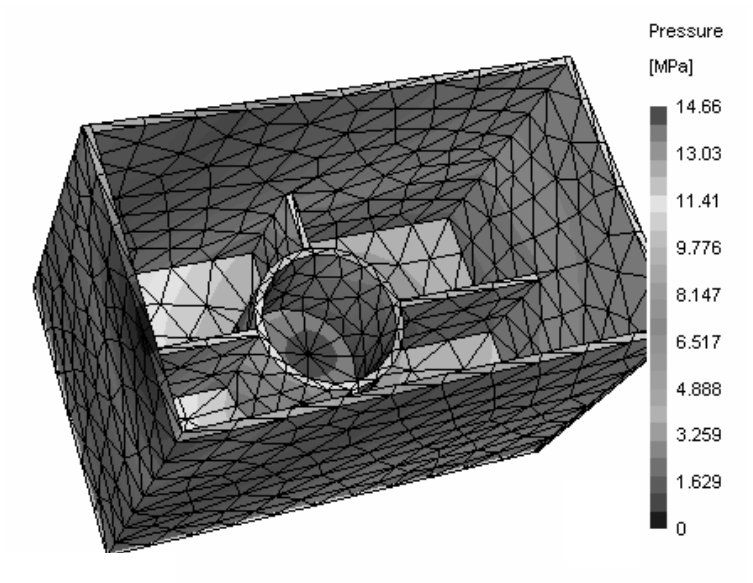

Fig. 9. *Pressure distribution for the design case at the end of the fill*

showing the pressure distribution at the end of the fill.

The above example shows that the part thicknesses were indeed reduced after the thickness minimization. However, if the molding criteria were set tighter, the minimization results might be quite different. For example, if we change the criterion to the following:

$$v1 < 5$$

The minimization result based on this new criterion is shown in Fig. 10.

As can be seen, for the modified molding criteria:

- the sought: x = 3 –1/2 +1/4 = 2.75;
- thicknesses change: 2.75 Step = 1.1 mm; (from 2 mm to 3.1 mm)
- thickness increase percentage: 1.1/2 = 55%.

This time the route of the thickness change is quite clear. The first convergence criterion was again triggered (*i.e.,* the thickness change is between the "¼ Step" and the "1/16 Step" inclusive, and there is one simulation that passed the molding-quality criteria. In this situation, this one will be

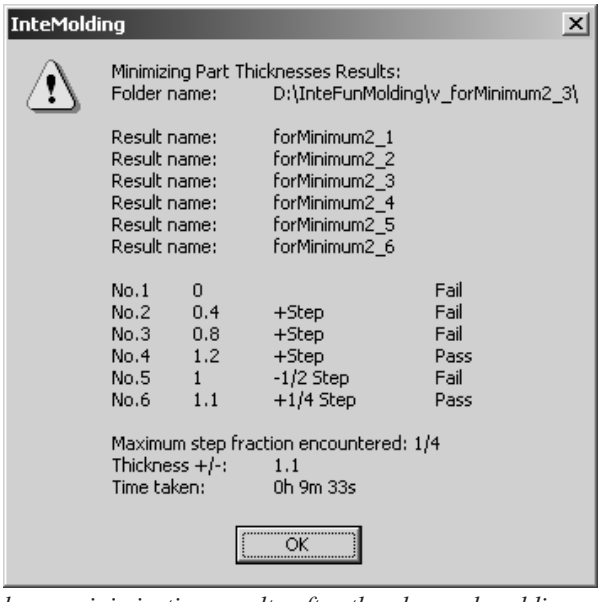

Fig. 10. *Thickness minimization results after the changed molding-quality criteria*

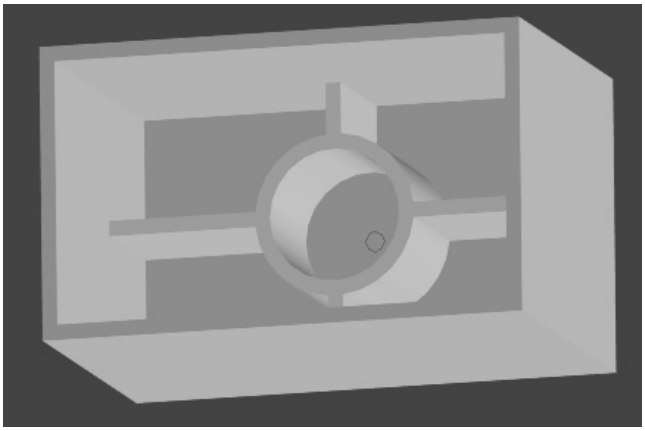

Fig. 11. *Part geometry as a result of the thickness minimization after the changed molding-quality criteria*

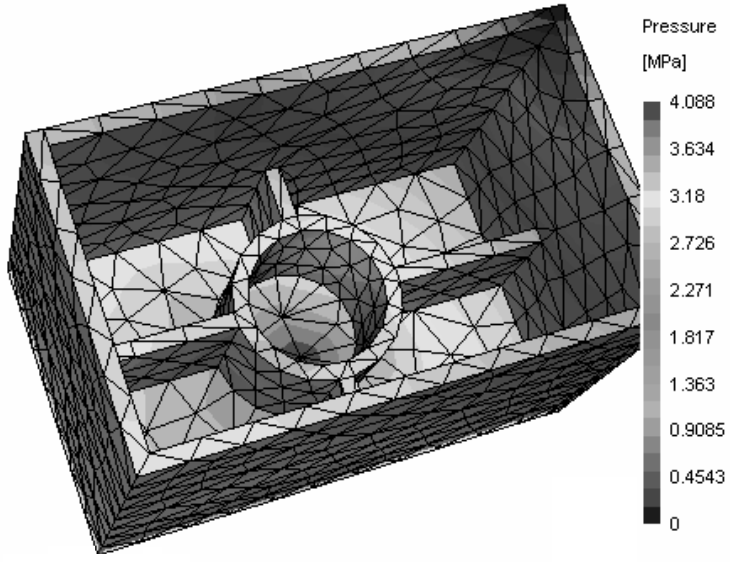

Fig. 12. *Pressure distribution after the changed molding-quality criteria*

regarded as the final result, i.e., simulation No. 6). Fig. 11 shows the part geometry as a result of the thickness minimization, and Fig. 12 shows the corresponding pressure distribution from the Moldflow simulation. By comparing Fig. 11 and 12 with Fig. 6, it is easy to see the difference resulting from the different molding-quality requirements.

Now let us change the design case by using multiple quality criteria. Assume that this time the designer is more concerned about the clamp tonnage and maximum shear rate. He or she can then specify the following two criteria:

- Criteria construction variables:
  v1 = maximum clamp tonnages (tonne),
  v2 = maximum shear rate (1/s).
- The corresponding molding-quality criteria for the thickness minimization:
  $v1 < 10$,
  $v2 < 50000$.

The requirement on clamp tonnage is easy to understand. The second quality criterion is actually a more stringent material requirement that was mentioned previously: “Shear rate should not exceed the maximum recommended for the material type”, which, for the current material, is 10^5 (1/s).

All the other molding conditions remain unchanged. The minimization results were shown in Fig. 13, which show that the total change of thicknesses is –0.6 mm. Hence, the part thicknesses can be reduced by 0.6/2 = 30%.

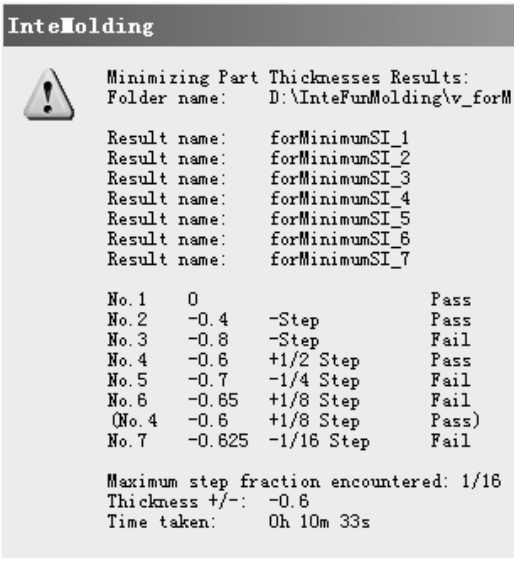

Fig. 13. *Thickness-minimization results when multiple molding-quality criteria are used*

5 DISCUSSION

The results from the above case study show that, apart from the initial part geometry and molding conditions (gate location, melt temperature, mold temperature, injection time, *etc.*), the part-thickness-minimization results are predominantly determined by the specified molding-quality requirements. Different molding-quality requirements for the same design problem might result in quite opposite results: the part thicknesses may be reduced or they may have to be increased.

In the studied design case the pressure distribution is selected as a molding-quality measure. As discussed in Section 2.2, there are many molding qualities that may be used as the injection-molding optimization criteria. Among these criteria, some are more sensitive to part thicknesses, such as pressure, shear stress, clamp tonnage, and volumetric shrinkage. For the case of the pressure distribution, the "maximum end-of-fill pressure" may be used to characterize the molding quality partially. This variable should generally not exceed a certain value, because the maximum hydraulic pressure of an injection-molding machine ram is determined by the injection-molding machine, which is related to the maximum pressure at the nozzle, which in turn is related to the pressure in the molding cavity. Setting a threshold for the maximum end-of-fill cavity pressure will ensure that the injection molding machine can provide the necessary ram pressure for the molding process, reducing the possibility of molding defects caused by flow hesitation and short-shot.

The case study shows that if the threshold for the cavity pressure is set high (15 MPa), the part thicknesses may be reduced; if it is set low (5 MPa), the part thicknesses may have to be increased. This is true because if the part walls are too thin, the melt flow will face more resistance in the cavity, leading to a higher cavity pressure. In contrast, if the wall thicknesses are large, the plastic melt will flow more easily in the cavity, hence the cavity pressure will be lower. However, regarding how much the part thicknesses can be reduced or increased, there has to be a certain algorithm and some calculation. This is where the work described in this paper has made its contribution.

The case was then further explored when multiple molding-quality criteria were used. The results show that multiple quality criteria can be specified and used for the thickness minimization as well.

6 CONCLUSIONS

The design of an injection-molded plastic part should take both functional and performance requirements, as well as injection-molding requirements into account. Optimization of part thicknesses is an important design task. One of the problems in part-thickness optimization is that most of the existing works are only oriented to the functional and

performance requirements. To tackle this problem, the above sections have presented a simulation-based methodology for minimizing the part thicknesses. This is basically an iterative process of changing the thicknesses of the selected part features, executing a Moldflow simulation, assessing the molding-quality criteria, and based on the results, determining the next change (following the route of the change) of part thicknesses. The thickness change can be in both directions, *i.e.,* "+/-" the specified step value; and it can be a full step value, or a fraction of a step value, including 1/2, 1/4, 1/8, 1/16 step values.

The methodology was implemented in a software prototype, with which the part-thickness change and the Moldflow simulation can be made automatically by the computer programs. The design case study has further demonstrated the usefulness of the proposed methodology.

The presented paper provides a novel method for injection-molding designers to obtain minimized part thicknesses related to the part-molding quality requirements. The innovation has three aspects: first, a route of thickness change towards meeting the specified quality criteria was proposed; second, the existing injection-molding CAD-CAE integration model was enhanced to allow a part-thickness change to be specified and executed; and third, several convergence criteria were proposed for the thickness-minimization search process.

However, the problem of part-thickness optimization is complex, due to the complex nature of the injection molding process itself. This paper has only addressed the problem of "thickness minimization", where the objective for optimality is the thicknesses, while the molding-quality requirements are only treated as the constraints; rather than that of "thickness optimization", where both the thicknesses and the molding qualities should be the optimization objectives. Hence, it was only an initial effort in tackling the problem thoroughly. Future work will involve taking the molding qualities as part of the optimization objectives, so that the part thicknesses can be optimized in such a way that, not only the plastic material requirement is low, but also the part molding-qualities are high.

Acknowledgments

This paper is based on work funded by Zhejiang Provincial Natural Science Foundation of China under Grant No. R104247 (the talent-nurturing program).

7 REFERENCES

[1] McClung, R. A., Rudolph, K. G., LeMonds, J. (1996), Thickness optimization in the structural design of engineering thermoplastic parts, in the *Proceedings of the 54th Annual Technical Conference*, Vol. 3, pp. 3201-3205.

[2] Lam, Y. C., Manickarajah, D., Bertolini, A. (2000), Performance characteristics of resizing algorithms for thickness optimization of plate structures; *Finite Elements in Analysis and Design*, Vol. 34, pp.159-174.

[3] Rietz, A., Petersson, J. (2001), Simultaneous shape and thickness optimization, *Structural and Multidisciplinary Optimization*, Vol. 23, No. 1, pp. 14-23.

[4] Lee, B. H., Kim, B. H. (1996), Optimization of part wall thickness to reduce warpage in injection molded part based on the modified complex method, in *SPE Annual Technical Conference*, pp. 692-697.

[5] Huang, G.-Q., Huang, H.-X. (2005), Thickness optimization of blow molded parts using FEM/ANN/GA methods, in the *Proceedings of the Annual Technical Conference - ANTEC*, Vol. 1, pp. 24-27.

[6] Pandelidis, I., Zou, Q. (1990a), Optimization of injection molding design. Part 1: Gate location optimization, *Polymer Engineering and Science*, Vol. 30, No. 15, pp. 873-882.

[7] Pandelidis, I., Zou, Q. (1990b), Optimization of injection molding design. Part 2: Molding conditions optimization, *Polymer Engineering and Science*, Vol. 30, No. 15, pp. 883-892.

[8] Choi, G. H., Lee, K. D., Chang N., Kim, S. G. (1994), Optimization of process parameters of injection molding with neural network application in a process simulation environment, *Annals of the CIRP*, Vol. 43, pp. 449-452.

[9] He, W., Zhang, Y. F., Lee, K. S., Fuh, J. Y. H., Nee, A. Y. C. (1998), Automated process parameter resetting for injection molding: a fuzzy-neuron approach, *Journal of Intelligent Manufacturing*, Vol. 9, pp. 17-27.
[10] Yarlagadda, P. K. D. V. (2001), Prediction of processing parameters for injection molding by using a hybrid neural network, *Proc Instn Mech Engrs*, Vol. 215, Part B, pp. 1465-1470.
[11] Tan, K. H., Yuen, M. M. F. (1996), Computer-aided system for the initial setting of injection molding machine, *Proceedings of SPIE - The International Society for Optical Engineering*. Vol. 2644, Society of Photo-Optical Instrumentation Engineers, Bellingham, WA, USA, pp. 657-664.
[12] Shelesh-Nezhad, K., Siores, E. (1997), An intelligent system for plastic molding process design, *Journal of Material Processing Technology*, Vol. 63, pp. 458-462.
[13] Kwong, C. K., Smith, G. F. (1998), A computational system for process design of injection molding: combining blackboard-based expert system and case-based reasoning approach, *International Journal of Advanced Manufacturing Technology*, Vol. 14, pp. 239-246.
[14] Mok, S. L., Kwong, C. K., Lau, W. S. (2000), An intelligent hybrid system for initial process parameter setting of injection molding, *International Journal of Production Research*, Vol. 38, No. 17, pp. 4565-4576.
[15] Deng, Y.-M., Britton, G. A., Lam, Y. C., Tor, S. B., Ma, Y. S. (2002a), A feature-based CAD-CAE integration model for injection molded product design, *International Journal of Production Research*, Vol. 40, No. 15, pp. 3737-3750.
[16] Deng, Y.-M., Lam, Y. C., Tor, S. B., Britton, G. A. (2002b), A CAD-CAE integrated injection molding design system, *Engineering with Computers*, Vol. 18, No. 1, pp. 80-92.
[17] Deng, Y.-M., Lam, Y. C., Britton, G. A. (2004), Optimization of injection molding conditions with user-definable objective functions based on genetic algorithm, *International Journal of Production Research*, Vol. 42, No. 7, pp. 1365-1390.
[18] Moldflow Corporation (2002). Moldflow plastic insight release 4.0 online documentation.

Authors' Address: Dr. Yimin Deng
Dr. Di Zheng
Faculty of Engineering
Ningbo University
P. R. China
dengyimin@nbu.edu.cn
zhengdi@nbu.edu.cn

Prejeto: 2.5.2007
Received:
Sprejeto: 27.6.2007
Accepted:
Odprto za diskusijo: 1 leto
Open for discussion: 1 year

Strokovna literatura - Professional Literature

Nova knjiga - New Book

Miodrag Lazić
Alati, metode i tehnike unapređenja kvaliteta
Zal.: Mašinski fakultet - Kragujevac, Centar za kvalitet, 2006
200 strani, 154 slik, 2 prilogi
format 170 x 241 cm

Nenehno izboljševanje kakovosti je ena izmed osrednjih zahtev standarda kakovosti ISO 9000:2000. Orodja, metode in tehnike kakovosti pa predstavljajo združeno znanje o zbiranju, urejanju, analizi, razlaganju, prikazovanju in nadzoru dejanskih podatkov z namenom zadovoljiti želje, potrebe in zahteve uporabnikov izdelkov ali storitev. V svetu se dandanes uporablja prek 300 orodij, metod in tehnik kakovosti, ki se med seboj bolj ali manj razlikujejo. Vendar podjetja običajno redno uporabljajo le od 10 do 30 različnih tehnik (orodij) kakovosti. Pri tem je treba poudariti, da med orodji in tehnikami ni jasno definirane razmejitve, kar pogosto povzroča zmedo pri praktični uporabi.

Pričujoča knjiga, ki je zasnovana kot učbenik pri predmetu *Metode in orodja za izboljševanje kakovosti,* po učnem načrtu Fakultete za strojništvo v Kragujevcu, je razdeljena na 5 glavnih poglavij, katerim sta dodani dve prilogi:

1. *Izboljševanje kakovosti* – osnove metod za izboljševanje kakovosti, zahteve standarda QMS ter pregled orodij in tehnik kakovosti.
2. *Statistični nadzor kakovosti* – osnove statističnih metod za preverjanje kakovosti, specificirane meje in naravne meje postopka, nadzorne karte, statistični prevzem na podlagi načrtov vzorčenja.
3. *Orodja, metode in tehnike kakovosti* – sedem osnovnih orodij kakovosti, dopolnilna orodja in tehnike kakovosti, najpogosteje uporabljane metode in tehnike kakovosti.
4. *Napredna orodja in tehnike izboljševanja kakovosti* – benchmarking, zmožnost postopka, metoda sedmih korakov izboljševanja kakovosti, šest sigma, Taguchijeva funkcija izgub.
5. *Načrtovanje preizkusov (DoE)* – modeliranje pojava, postopka in sistema, načrtovanje preizkusov, izvedba načrta preizkusov, načrtovanje preizkusov po Taguchi-ju.

   Priloga 1 - preglednice za statistični nadzor postopka (SPC).

   Priloga 2 - primeri in naloge s področij: statistični nadzor postopka, nadzorne karte, zmožnost postopka.

Vsebina knjige je napisana zelo zgoščeno, vendar v razumljivem strokovnem jeziku, s številnimi izvirnimi in zanimivimi slikami, strokovno in didaktično pravilno. Dolgoletne izkušnje avtorja, kot predavatelja na različnih seminarjih, izobraževanjih in v šolah kakovosti, ki jih organizira Center za kakovost pri Fakulteti za strojništvo v Kragujevcu, se kažejo v primernem razmerju med posredovano teorijo in izbranimi praktičnimi primeri iz vsakdanje prakse. Knjigo priporočamo kot primerno gradivo tako študentom tehničnih fakultet, ki se prvič neposredno srečujejo s problematiko kakovosti, kakor tudi nadzornikom kakovosti ali inženirjem kakovosti iz neposrednega proizvodnega okolja.

Prof. dr. Mirko Soković

Osebne vesti - Personal Events

Doktorati, magisteriji in diplome - Doctor's, Master's and Diploma Degrees

MAGISTERIJ

Na Fakulteti za strojništvo Univerze v Maroboru je z uspehom zagovarjal svoje magistrsko delo:

dne *19. junija 2007*: **Ambrož Rožman**, z naslovom: "Optimizacija vzdrževanja v kartonažni industriji" (mentor: prof. dr. Boris Aberšek).

S tem je navedeni kandidat dosegel akademsko stopnjo magistra znanosti.

DIPLOMIRALI SO

Na Fakulteti za strojništvo Univerze v Mariboru so pridobili naziv univerzitetni diplomirani inženir strojništva:

dne *21. junija 2007*: Simon KLANČNIK, Marko TOMŠIĆ;

dne *27. junija 2007*: Aleš MEDVED;

dne *28. junija 2007*: Janez AŽNOH, Branko STVARNIK.

*

Na Fakulteti za strojništvo Univerze v Mariboru so pridobili naziv diplomirani inženir strojništva:

dne *21. junija 2007*: Janez FRELIH, Matej HRIBAR, Marjan VRTAČNIK, Cvetka ZRIMŠEK;

dne *27. junija 2007*: Robertino RIBIČ;

dne *28. junija 2007*: Zdenko KLEMENČIČ, David KOS, Milan PETRAK, Tadej POČIVAVŠEK, Robo POGOREVC, Tadej SEKAVČNIK, Gregor URBANČIČ.

Navodila avtorjem - Instructions for Authors

Članki morajo vsebovati:
- naslov, povzetek, besedilo članka in podnaslove slik v slovenskem in angleškem jeziku,
- dvojezične preglednice in slike (diagrami, risbe ali fotografije),
- seznam literature in
- podatke o avtorjih.

Strojniški vestnik izhaja od leta 1992 v dveh jezikih, tj. v slovenščini in angleščini, zato je obvezen prevod v angleščino. Obe besedili morata biti strokovno in jezikovno med seboj usklajeni. Članki naj bodo kratki in naj obsegajo približno 8 strani. Izjemoma so strokovni članki, na željo avtorja, lahko tudi samo v slovenščini, vsebovati pa morajo angleški povzetek.

Za članke iz tujine (v primeru, da so vsi avtorji tujci) morajo prevod v slovenščino priskrbeti avtorji. Prevajanje lahko proti plačilu organizira uredništvo. Če je članek ocenjen kot znanstveni, je lahko objavljen tudi samo v angleščini s slovenskim povzetkom, ki ga pripravi uredništvo.

VSEBINA ČLANKA

Članek naj bo napisan v naslednji obliki:
- Naslov, ki primerno opisuje vsebino članka.
- Povzetek, ki naj bo skrajšana oblika članka in naj ne presega 250 besed. Povzetek mora vsebovati osnove, jedro in cilje raziskave, uporabljeno metodologijo dela,povzetek rezulatov in osnovne sklepe.
- Uvod, v katerem naj bo pregled novejšega stanja in zadostne informacije za razumevanje ter pregled rezultatov dela, predstavljenih v članku.
- Teorija.
- Eksperimentalni del, ki naj vsebuje podatke o postavitvi preskusa in metode, uporabljene pri pridobitvi rezultatov.
- Rezultati, ki naj bodo jasno prikazani, po potrebi v obliki slik in preglednic.
- Razprava, v kateri naj bodo prikazane povezave in posplošitve, uporabljene za pridobitev rezultatov. Prikazana naj bo tudi pomembnost rezultatov in primerjava s poprej objavljenimi deli. (Zaradi narave posameznih raziskav so lahko rezultati in razprava, za jasnost in preprostejše bralčevo razumevanje, združeni v eno poglavje.)
- Sklepi, v katerih naj bo prikazan en ali več sklepov, ki izhajajo iz rezultatov in razprave.
- Literatura, ki mora biti v besedilu oštevilčena zaporedno in označena z oglatimi oklepaji [1] ter na koncu članka zbrana v seznamu literature. Vse opombe naj bodo označene z uporabo dvignjene številke[1].

OBLIKA ČLANKA

Besedilo članka naj bo pripravljeno v urejevalnilku Microsoft Word. Članek nam dostavite v elektronski obliki.

Ne uporabljajte urejevalnika LaTeX, saj program, s katerim pripravljamo Strojniški vestnik, ne uporablja njegovega formata.

Enačbe naj bodo v besedilu postavljene v ločene vrstice in na desnem robu označene s tekočo številko v okroglih oklepajih

Papers submitted for publication should comprise:
- Title, Abstract, Main Body of Text and Figure Captions in Slovene and English,
- Bilingual Tables and Figures (graphs, drawings or photographs),
- List of references and
- Information about the authors.

Since 1992, the Journal of Mechanical Engineering has been published bilingually, in Slovenian and English. The two texts must be compatible both in terms of technical content and language. Papers should be as short as possible and should on average comprise 8 pages. In exceptional cases, at the request of the authors, speciality papers may be written only in Slovene, but must include an English abstract.

For papers from abroad (in case that none of authors is Slovene) authors should provide Slovenian translation. Translation could be organised by editorial, but the authors have to pay for it. If the paper is reviewed as scientific, it can be published only in English language with Slovenian abstract, that is prepared by the editorial board.

THE FORMAT OF THE PAPER

The paper should be written in the following format:
- A Title, which adequately describes the content of the paper.
- An Abstract, which should be viewed as a mini version of the paper and should not exceed 250 words. The Abstract should state the principal objectives and the scope of the investigation, the methodology employed, summarize the results and state the principal conclusions.
- An Introduction, which should provide a review of recent literature and sufficient background information to allow the results of the paper to be understood and evaluated.
- A Theory
- An Experimental section, which should provide details of the experimental set-up and the methods used for obtaining the results.
- A Results section, which should clearly and concisely present the data using figures and tables where appropriate.
- A Discussion section, which should describe the relationships and generalisations shown by the results and discuss the significance of the results making comparisons with previously published work. (Because of the nature of some studies it may be appropriate to combine the Results and Discussion sections into a single section to improve the clarity and make it easier for the reader.)
- Conclusions, which should present one or more conclusions that have been drawn from the results and subsequent discussion.
- References, which must be numbered consecutively in the text using square brackets [1] and collected together in a reference list at the end of the paper. Any footnotes should be indicated by the use of a superscript[1].

THE LAYOUT OF THE TEXT

Texts should be written in Microsoft Word format. Paper must be submitted in electronic version.

Do not use a LaTeX text editor, since this is not compatible with the publishing procedure of the Journal of Mechanical Engineering.

Equations should be on a separate line in the main body of the text and marked on the right-hand side of the page with numbers in round brackets.

Enote in okrajšave

V besedilu, preglednicah in slikah uporabljajte le standardne označbe in okrajšave SI. Simbole fizikalnih veličin v besedilu pišite poševno (kurzivno), (npr. *v, T, n* itn.). Simbole enot, ki sestojijo iz črk, pa pokončno (npr. ms^{-1}, K, min, mm itn.).

Vse okrajšave naj bodo, ko se prvič pojavijo, napisane v celoti v slovenskem jeziku, npr. časovno spremenljiva geometrija (ČSG).

Slike

Slike morajo biti zaporedno oštevilčene in označene, v besedilu in podnaslovu, kot sl. 1, sl. 2 itn. Posnete naj bodo v ločljivosti, primerni za tisk, v kateremkoli od razširjenih formatov, npr. BMP, JPG, GIF. Diagrami in risbe morajo biti pripravljeni v vektorskem formatu, npr. CDR, AI.

Pri označevanju osi v diagramih, kadar je le mogoče, uporabite označbe veličin (npr. *t, v, m* itn.), da ni potrebno dvojezično označevanje. V diagramih z več krivuljami, mora biti vsaka krivulja označena. Pomen oznake mora biti pojasnjen v podnapisu slike.

Vse označbe na slikah morajo biti dvojezične.

Preglednice

Preglednice morajo biti zaporedno oštevilčene in označene, v besedilu in podnaslovu, kot preglednica 1, preglednica 2 itn. V preglednicah ne uporabljajte izpisanih imen veličin, ampak samo ustrezne simbole, da se izognemo dvojezični podvojitvi imen. K fizikalnim veličinam, npr. *t* (pisano poševno), pripišite enote (pisano pokončno) v novo vrsto brez oklepajev.

Vsi podnaslovi preglednic morajo biti dvojezični.

Seznam literature

Vsa literatura mora biti navedena v seznamu na koncu članka v prikazani obliki po vrsti za revije, zbornike in knjige:

[1] A. Wagner, I. Bajsić, M. Fajdiga (2004) Measurement of the surface-temperature field in a fog lamp using resistance-based temperature detectors, *Stroj. vestn.* 2(2004), pp. 72-79.
[2] Vesenjak, M., Ren Z. (2003) Dinamična simulacija deformiranja cestne varnostne ograje pri naletu vozila. *Kuhljevi dnevi '03*, Zreče, 25.-26. september 2003.
[3] Muhs, D. et al. (2003) Roloff/Matek Maschinenelemente – Tabellen, 16. Auflage. *Vieweg Verlag*, Wiesbaden.

SPREJEM ČLANKOV IN AVTORSKE PRAVICE

Uredništvo Strojniškega vestnika si pridržuje pravico do odločanja o sprejemu članka za objavo, strokovno oceno recenzentov in morebitnem predlogu za krajšanje ali izpopolnitev ter terminološke in jezikovne korekture.

Avtor mora predložiti pisno izjavo, da je besedilo njegovo izvirno delo in ni bilo v dani obliki še nikjer objavljeno. Z objavo preidejo avtorske pravice na Strojniški vestnik. Pri morebitnih kasnejših objavah mora biti SV naveden kot vir.

PLAČILO OBJAVE

Avtorji vseh prispevkov morajo za objavo plačati prispevek v višini 20,00 EUR na stiskano stran prispevka. Prispevek se zaračuna po sprejemu članka za objavo na seji Uredniškega odbora.

Units and abbreviations

Only standard SI symbols and abbreviations should be used in the text, tables and figures. Symbols for physical quantities in the text should be written in italics (e.g. *v, T, n,* etc.). Symbols for units that consist of letters should be in plain text (e.g. ms^{-1}, K, min, mm, etc.).

All abbreviations should be spelt out in full on first appearance, e.g., variable time geometry (VTG).

Figures

Figures must be cited in consecutive numerical order in the text and referred to in both the text and the caption as Fig. 1, Fig. 2, etc. Pictures may be saved in resolution good enough for printing in any common format, e.g. BMP, GIF, JPG. However, graphs and line drawings sholud be prepared as vector images, e.g. CDR, AI.

When labelling axes, physical quantities, e.g. *t, v, m,* etc. should be used whenever possible to minimise the need to label the axes in two languages. Multi-curve graphs should have individual curves marked with a symbol, the meaning of the symbol should be explained in the figure caption.

All figure captions must be bilingual.

Tables

Tables must be cited in consecutive numerical order in the text and referred to in both the text and the caption as Table 1, Table 2, etc. The use of names for quantities in tables should be avoided if possible: corresponding symbols are preferred to minimise the need to use both Slovenian and English names. In addition to the physical quantity, e.g. *t* (in italics), units (normal text), should be added in new line without brackets.

All table captions must be bilingual.

The list of references

References should be collected at the end of the paper in the following styles for journals, proceedings and books, respectively:

[1] A. Wagner, I. Bajsić, M. Fajdiga (2004) Measurement of the surface-temperature field in a fog lamp using resistance-based temperature detectors, *Stroj. vestn.* 2(2004), pp. 72-79.
[2] Vesenjak, M., Ren Z. (2003) Dinamična simulacija deformiranja cestne varnostne ograje pri naletu vozila. *Kuhljevi dnevi '03*, Zreče, 25.-26. september 2003.
[3] Muhs, D. et al. (2003) Roloff/Matek Maschinenelemente – Tabellen, 16. Auflage. *Vieweg Verlag*, Wiesbaden.

ACCEPTANCE OF PAPERS AND COPYRIGHT

The Editorial Committee of the Journal of Mechanical Engineering reserves the right to decide whether a paper is acceptable for publication, obtain professional reviews for submitted papers, and if necessary, require changes to the content, length or language.

Authors must also enclose a written statement that the paper is original unpublished work, and not under consideration for publication elsewhere. On publication, copyright for the paper shall pass to the Journal of Mechanical Engineering. The JME must be stated as a source in all later publications.

PUBLICATION FEE

For all papers authors will be asked to pay a publication fee prior to the paper appearing in the journal. However, this fee only needs to be paid after the paper is accepted by the Editorial Board. The fee is €20.00 per printed paper page.